SNAP: Low-Latency Test-Time Adaptation with Sparse Updates

Hyeongheon Cha¹ Dong Min Kim¹ Hye Won Chung¹ Taesik Gong²* Sung-Ju Lee¹*

¹School of Electrical Engineering, KAIST, Daejeon, Republic of Korea ²Department of Computer Science and Engineering, UNIST, Ulsan, Republic of Korea

Abstract

Test-Time Adaptation (TTA) adjusts models using unlabeled test data to handle dynamic distribution shifts. However, existing methods rely on frequent adaptation and high computational cost, making them unsuitable for resource-constrained edge environments. To address this, we propose SNAP, a sparse TTA framework that reduces adaptation frequency and data usage while preserving accuracy. SNAP maintains competitive accuracy even when adapting based on only 1% of the incoming data stream, demonstrating its robustness under infrequent updates. Our method introduces two key components: (i) Class and Domain Representative Memory (CnDRM), which identifies and stores a small set of samples that are representative of both class and domain characteristics to support efficient adaptation with limited data; and (ii) Inference-only Batch-aware Memory Normalization (IoBMN), which dynamically adjusts normalization statistics at inference time by leveraging these representative samples, enabling efficient alignment to shifting target domains. Integrated with five state-of-the-art TTA algorithms, SNAP reduces latency by up to 93.12%, while keeping the accuracy drop below 3.3%, even across adaptation rates ranging from 1% to 50%. This demonstrates its strong potential for practical use on edge devices serving latency-sensitive applications. The source code is available at https://github.com/chahh9808/SNAP.

1 Introduction

Deep learning models often suffer performance degradation under domain shifts caused by environmental changes or noise [37]. Test-Time Adaptation (TTA) offers a promising solution for domain shifts by utilizing only unlabeled test data without requiring source data. While TTA algorithms have advanced in complexity to improve accuracy in data streams [48, 30, 50, 53, 31, 43], they are typically designed for resource-rich servers, overlooking the computational limitations crucial for real-world deployment. Operations such as backpropagation, data augmentation, and model ensembling [50, 53, 55] result in substantial latency and memory consumption, making state-of-the-art (SOTA) TTA methods inefficient for practical use.

For edge devices with limited computational power, such as mobile devices or IoT sensors, the adaptation latency from TTA methods becomes a critical bottleneck, particularly in delay-sensitive applications such as autonomous driving and real-time health monitoring. Moreover, the model must keep up with the data stream in those applications, but high computational overhead could cause it to miss critical samples, resulting in inference lags and reduced accuracy. This issue is exacerbated with fast data streams, such as high-frame-rate videos or high-performance sensors. For example, even a

^{*}Corresponding authors.

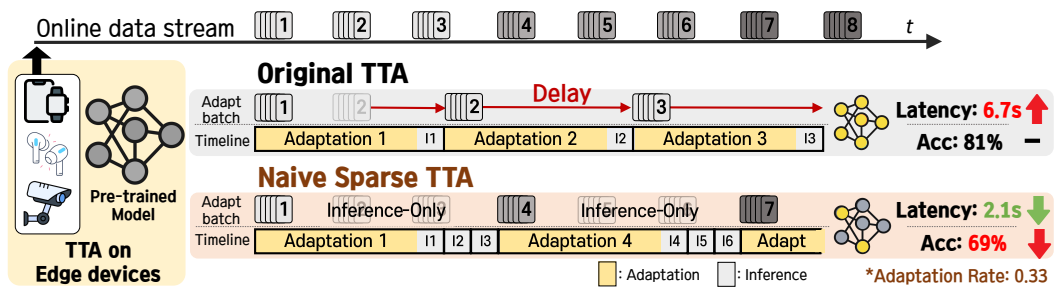


Figure 1: Comparison of average latency per batch and accuracy between the Original and Naïve Sparse TTA approaches on edge devices processing an online data stream. With an adaptation rate of 0.33, adaptation occurs once every three batches, reducing latency proportional to the rate but leading to a significant accuracy drop compared with fully adapting Original TTA.

slight delay in processing sensor data can lead to dangerous situations in autonomous driving. A high adaptation latency accumulating with each batch not only undermines real-time performance but also limits the potential of TTA algorithms in latency-sensitive applications (Section 3). In response to this challenge, forward-only TTA methods [13, 29] propose adjusting lightweight components such as prototypes or prompts during inference. While these mechanisms improve efficiency, their reliance on fixed model parameters fails to adapt to dynamic distribution shifts [7, 53, 29]. Consequently, a robust performance of backpropagation-based approaches across diverse conditions (Appendix B.10) underscores the necessity of efficient model updates.

In online TTA scenarios where rapid response is required under strict resource constraints, *Sparse TTA (STTA)* offers a practical compromise by reducing the frequency of adaptation rather than eliminating it entirely. By adapting intermittently instead of at every batch, STTA significantly reduces computational overhead and latency. However, naïvely reducing update frequency degrades performance since only a limited data portion is utilized (Figure 1). Thus, the success of STTA hinges on strategically selecting representative stream samples to enable effective adaptation under sparse update schedules (detailed analysis in Section 5).

Existing sampling-based TTA methods are especially designed for handling dynamic data stream such as non-i.i.d. [6, 31, 53] or noisy data [7]. However, they are not optimized for data efficiency and continue to utilize a large proportion of samples. For example, EATA [30] reduces sample usage by filtering out unreliable samples but experiences performance degradation when reductions become too aggressive. Meanwhile, research in data-efficient deep learning has shown that selecting easy, class-representative samples is effective at low sampling rates (e.g., below 0.4) [51, 2]. However, these approaches depend on ground-truth labels, which are not available in TTA.

We propose **SNAP**: Sparse Network Adaptation for Practical Test-Time Adaptation, a low-latency unsupervised domain adaptation framework for resource-constrained devices. SNAP balances adaptation accuracy with computational efficiency through two key components: Class and Domain Representative Memory (CnDRM) and Inference-only Batch-aware Memory Normalization (IoBMN). CnDRM stores a pool of *class-representative* samples (high pseudo-label confidence, balanced across predictions) and *domain-representative* samples (closest to the target domain centroid in feature space). This approach enables the model to adapt effectively to domain shifts with minimal data (Section 4.1). Meanwhile, IoBMN dynamically refines the normalization layers during inference by utilizing CnDRM's class-domain representative statistics to correct skewed feature distributions at each inference step. This keeps the model aligned with the evolving data distribution, enabling effective batch-wise adaptation without backpropagation (Section 4.2).

SNAP is a lightweight module that reduces latency while seamlessly integrating with existing TTA methods, preserving their adaptation behavior. To assess its effectiveness, we integrated SNAP with five SOTA TTA algorithms: Tent [48], EATA [30], SAR [31], CoTTA [50], and RoTTA [53]. We tested it on three widely-used TTA benchmarks (CIFAR10-C, CIFAR100-C, and ImageNet-C [10]) across various adaptation rates (Section 5). We also validate SNAP on ImageNet-R [9] and ImageNet-Sketch [49] to assess generalization (Appendix B.11).

In addition, we measured SNAP's latency and memory usage on three popular edge devices—Raspberry Pi 4 [38], Raspberry Pi Zero 2 W [39], and NVIDIA Jetson Nano [32]—to assess its real-world applicability. SNAP significantly reduces latency while minimizing performance degradation from existing TTA methods. On a Raspberry Pi 4 testbed, it reduced CoTTA's latency by

up to 93.12% at an adaptation rate of 0.1 in CIFAR10-C, with no loss in performance. Moreover, SNAP maintained performance comparable to original TTA methods across adaptation rates from 0.01 to 0.5, achieving 77.12%–81.74% for Tent, close to the full adaptation accuracy of 80.43%. SNAP also operates efficiently under memory constraints, with low memory overhead and seamless integration with a memory-efficient TTA module [12], as detailed in Appendices B.7 and B.8.

2 Related work

Test-time adaptation. Test-time adaptation aims to improve model performance on out-of-distribution data by using only the unlabeled test data stream to adapt the model. Test-time normalization [28, 40] adjusts the batch normalization (BN) statistics using test data to improve performance. Other works mainly involve updating the parameters of the model during test time. Tent [48] adapts the affine parameters of the BN layers to minimize the entropy of its predictions. EATA [30] builds upon Tent, sampling reliable and non-redundant samples and utilizing an anti-forgetting regularizer for efficiency. Other works introduce more complex schemes, primarily to improve robustness against more practical test-time scenarios. CoTTA [50] addresses a continually changing test-time environment by using weight-averaged and augmentation-averaged predictions with stochastic restoring. SAR [31] filters samples with large and noisy gradients to stabilize the model during wilder test-time scenarios. RoTTA [53] targets a practical test-time setting of changing distributions and correlative sampling by introducing a memory bank and a teacher-student model. We further analyze how prior TTA methods perform under sparse-update regimes and how our approach differs in Appendix B.3.

TEST-time adaptation on edge devices. TTA on edge devices primarily inherit the challenges of on-device learning:, including limited memory and reduced computational efficiency [21]. Several memory-efficient TTA works have been proposed in this regard. MECTA [12] aims to reduce the memory consumption of gradient-based TTA, proposing an adaptive normalization layer to reduce the intermediate caches for backpropagation. EcoTTA [43] proposes memory-efficient continual TTA by adapting lightweight meta networks instead of the originals to reduce the size of intermediate activations. Despite works to promote memory-efficiency, the latency of TTA, especially on resource-constrained edge devices, has been generally overlooked. While many adaptation-based TTA [48, 30, 31, 53] update only the affine parameters for general time and memory concerns, they still involve computationally-heavy operations every batch, which can lead to high latency on edge devices. A recent work [1] introduces a more practical TTA evaluation protocol that penalizes slow TTA methods by providing them with fewer samples for adaptation.

Data-efficient deep learning. Data-efficient deep learning methods enable deep learning models to achieve competitive performance with less data. Among these methods, data selection, or data sampling, involves utilizing a small subset of the training data in an attempt to match that of full-dataset training. A branch of data-selection is score-based selection, which scores each sample based on some predefined metric, such as a sample's influence [16], difficulty [46, 34], prediction confidence [35], or consistency [14], and selects samples with scores in a certain range. Another set of data-selection methods involves optimization-based selection, which formulates an optimization problem to find an optimal subset that can best approximate full-dataset training [26, 52, 36]. While these approaches work well in their preconceived settings, they generally suffer performance drop as their settings change, such as a change in sampling rates. More recent studies such as Moderate Coreset [51] propose a more robust selection approach by using the distance of a sample to the class center as a score criterion, for an effective representation of the dataset.

3 Preliminaries

Our work addresses the challenge of test-time adaptation latency on edge devices, where efficient, low-latency inference must be achieved despite limited resources.

Test-time adaptation and its latency challenge on edge devices. In unsupervised domain adaptation, the source domain data $\mathcal{D}_{\mathcal{S}} = \mathcal{X}^{\mathcal{S}}, \mathcal{Y}$ is drawn from the distribution $P_{\mathcal{S}}(\mathbf{x}, y)$, while the target domain data $\mathcal{D}_{\mathcal{T}} = \mathcal{X}^{\mathcal{T}}, \mathcal{Y}$ follows $P_{\mathcal{T}}(\mathbf{x}, y)$, typically without known labels y_j . Given a pre-trained model $f(\cdot; \Theta)$ on the source domain $\mathcal{D}_{\mathcal{S}}$, TTA adjusts the model to the target distribution $P_{\mathcal{T}}$ using only target instances \mathbf{x}_j , updating the parameters Θ to reduce domain discrepancy [48].

On resource-constrained edge devices, frequent adaptation poses a significant bottleneck. Our experiments on a Raspberry Pi 4 [38] revealed that existing TTA methods incur a minimum latency of 3.83 seconds per batch (Figure 2), severely limiting real-time inference for fast data streams (e.g., autonomous driving [45, 22]). Additional latency tracking for other devices is reported in Appendix B.6. Even lightweight TTA algorithms suffer from considerable backpropagation overhead, creating bottlenecks on resource-constrained devices without GPU-level computation. More computationally intensive methods like CoTTA, which depend on data augmentation and ensembles, require over 70 seconds per adaptation step, rendering them impractical for edge devices (Figure 2).

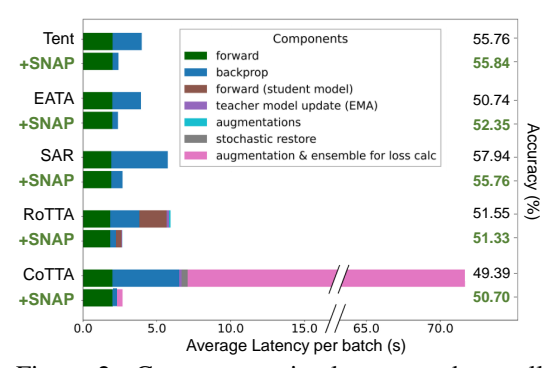


Figure 2: Component-wise latency and overall accuracy comparison between full SOTA TTA and SNAP (sparse update with frequency 0.1) on CIFAR100-C, measured on Raspberry Pi 4. SNAP matches accuracy with significantly lower cost.

A recent work [1] recognized latency as a crucial problem and proposed a TTA evaluation protocol that penalizes methods slower than the data stream rate. Instead of penalizing a model for being slow, we propose *Sparse TTA*, where the model adapts at sparse intervals to sustain real-time throughput. As real deployments involve devices with different computational capabilities and data streams of varying speeds, we believe a framework that effectively maintains various TTA methods' performance across different latency requirements is crucial.

Sparse test-time adaptation and adaptation rates. Sparse Test-Time Adaptation (STTA) lowers the frequency of model updates, a key factor in reducing adaptation latency on resource-constrained devices. Unlike conventional TTA methods that process full batches and incur significant overhead, STTA updates the model using only a subset of batches (Figure 1). The core parameter of STTA, the *Adaptation Rate (AR)*, determines the proportion of batches or samples used for adaptation compared to the Original TTA. By tuning the AR, STTA balances the performance and computational latency. Furthermore, STTA's periodic adaptation can be optimized by strategically distributing sparse model updates across selected intervals during inference. This approach helps distribute the adaptation overhead, smooths latency fluctuations across inference batches, and preserves overall performance.

4 Methodology

SNAP framework resolves the high latency and inefficiency issue of existing TTA methods. By introducing a Sparse TTA (STTA) strategy combined with a novel sampling method, SNAP minimizes adaptation delays while maintaining accuracy. The overall system, illustrated in Figure 3, consists of two primary components: (i) Class and Domain Representative Memory (CnDRM) for efficient sampling and (ii) Inference-only Batch-aware Memory Normalization (IoBMN) to correct feature distribution shifts during inference. Together, these components enable effective STTA with minimal computational overhead.

4.1 Class and Domain Representative Memory

CnDRM is a core component of SNAP that addresses the challenges of efficient data sampling for STTA. As the adaptation rate directly impacts the number of samples used for adaptation, this necessitates a careful sampling strategy to optimize performance with minimal data. Given this limited sampling rate, CnDRM selects both class and domain-representative samples to maintain model performance while minimizing adaptation overhead.

Motivation. Effective data sampling is essential for data-efficient deep learning, particularly when only a few samples are available. While score-based methods that prioritize difficult samples perform well at high sampling rates, selecting easy, class-representative samples is more effective at lower rates [2]. Moderate Coreset [51] also demonstrates that selecting samples near the class center improves performance in noisy-label settings, a principle that aligns with the STTA scenario where ground truth is unavailable.

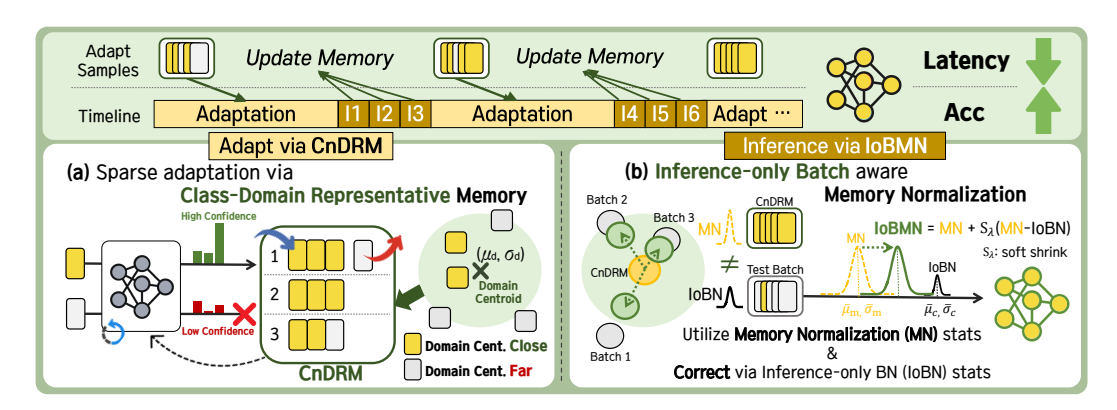


Figure 3: Design overview of SNAP. The framework consists of two primary components: (a) Class and Domain Representative Memory (CnDRM), which efficiently selects representative samples to minimize adaptation overhead, and (b) Inference-only Batch-aware Memory Normalization (IoBMN), which corrects feature distribution shifts during inference. Together, these components implement the Sparse TTA (STTA) strategy, reducing latency while maintaining model accuracy.

In addition, on real-world deployments, latency constraints often limit adaptation frequency, requiring models to function at low adaptation rates (e.g., 0.1). At such low rates, class-representative sampling alone is insufficient (Table 2), as it fails to capture distributional shifts between source and target domains. To overcome this limitation, we propose selecting both **class- and domain-representative samples** to enhance adaptation efficiency in low-data environments. Detailed theoretical analysis on the proposed efficient sampling strategy is in Appendix B.1.

Criteria 1: class representation. To ensure stable adaptation without ground truth labels, CnDRM selects high-confidence samples, avoiding low-confidence samples that often lie near decision boundaries and carry incorrect pseudo-labels. This ensures stable learning signals and reduces error propagation from incorrect pseudo-labels, supporting more effective and stable adaptation (Details in Appendix B.5). The confidence score $C(\mathbf{x})$ for each sample \mathbf{x} is calculated as: $C(\mathbf{x}) = \max_{y \in \mathcal{Y}} p(y|\mathbf{x};\Theta)$ where $p(y|\mathbf{x};\Theta)$ is the softmax probability for class y. Only samples with confidence above a threshold τ_{conf} are retained. For a balanced representation across diverse classes, CnDRM selects these high-confidence samples in a prediction-balanced manner. This helps maintain the model's overall classification capability by preventing bias towards certain classes when only a low sample rate is available for adaptation. By leveraging both high confidence and prediction balance, CnDRM effectively selects class-representative samples that are diverse and reliable, even without access to ground-truth labels.

Criteria 2: domain representation. In addition to class-representative sampling, Cn-DRM selects domain-representative samples to facilitate adaptation to new domain conditions. Building on the efficient class-representative sampling criteria, we argue that *selecting samples close to the domain centroid* would enhance performance in STTA. Our preliminary experiment results validate improved performance when selecting samples near the centroid (Figure 4). For ImageNet-C Gaussian noise, TTA with the closest 20% of samples achieved 26.65% accuracy, whereas the farthest 20% showed a lower accuracy of 18.52%.

As early layers in deep learning models tend to retain domain-specific features [54, 19, 42], we utilize the hidden features of early layers to identify domain-representative samples (Appendix B.4). Specifically, CnDRM uses the feature statistics (mean and variance) of the first normalization layer to assess domain representation, since domain discrepancies can be effectively mitigated through normaliza-

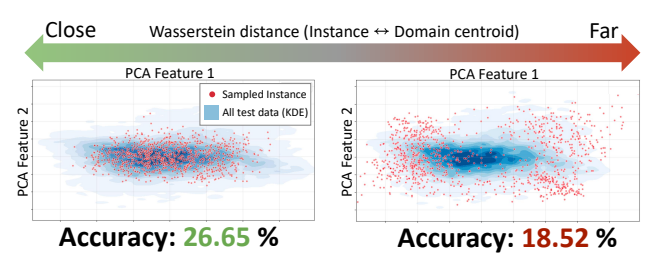


Figure 4: Sampling visualization and accuracy comparison between the closest 20% and farthest 20% samples from the domain centroid on ImageNet-C Gaussian noise.

tion adjustments using these statistics [28, 40]. Domain discrepancies in hidden features are substantially reduced after passing through a single normalization layer, significantly minimizing domain shift [20]. While deeper layers provide detailed information, using the first layer balances capturing domain-specific information and maintaining computational efficiency.

The domain centroid \mathbf{c}_d is computed using a momentum-based update of batch statistics from the normalization layer: $\mu_{domain} \leftarrow (1-\beta)\mu_{domain} + \beta\mu_t$ and $\sigma_{domain}^2 \leftarrow (1-\beta)\sigma_{domain}^2 + \beta\sigma_t^2$, where μ_t and σ_t^2 are the mean and variance of the current batch t, and β is the momentum parameter. In our preliminary study, we found that using only the mean and standard deviation values before the first normalization was sufficient to calculate the domain centroid. The sampled instances effectively represented the domain and were correctly positioned in the embedding space for each criterion (Figure 4).

We formally define a *domain-representative sample* as one whose early-layer feature statistics are closest to the domain centroid, as measured by the Wasserstein distance [47]. The Wasserstein distance quantifies the similarity between two distributions by considering their mean and variance, evaluating how well a sample represents the domain. It is useful for capturing domain characteristics, thus widely used in domain generalization [42]. Following common practice in domain adaptation [20, 27], we approximate channel-wise feature distributions as independent univariate Gaussians (i.e., with diagonal covariance) to efficiently estimate mean/variance-level domain shifts, which yields the following closed-form expression:

$$W(\mathbf{x_t}, \mathbf{c}_{domain}) = \sqrt{(\mu_{\mathbf{x_t}} - \mu_{domain})^2 + (\sigma_{\mathbf{x_t}} - \sigma_{domain})^2}.$$
 (1)

For each sample $\mathbf{x_t}$, the feature statistics $(\mu_{\mathbf{x_t}}, \sigma_{\mathbf{x_t}})$ are taken from the input to the normalization layer. Further clarification and assumption details are provided in Appendix B.2.

Algorithm 1 Class and Domain Representative Memory (CnDRM) Management

```
Require: test data stream x_t, memory M with capacity N, confidence threshold \tau_{conf}, adaptation
     rate 1/k
 1: for batch b \in \{1, \dots, B\} do
           \hat{Y}_b \leftarrow f(b; \Theta)
 2:
           for each sample x_t in batch b do
 3:
 4:
                \hat{y}_t \leftarrow \hat{Y}_b[t]
                confidence \leftarrow C(x_t; \Theta)
 5:
                 \mathbf{c}_t(\mu_{\mathbf{x_t}}, \sigma_{\mathbf{x_t}}) \leftarrow \text{mean \& variance of early feature}
 6:
 7:
                w_{x_t} \leftarrow W(x_t, \mathbf{c}_{domain})
                if confidence > 	au_{conf} then
 8:
 9:
                      Add \mathbf{s}_t(x_t, \hat{y}_t, c_t, w_{x_t}) to M
                                                                                           ▶ Add class-representative samples
                      if |M| > N then
10:
                           L^* \leftarrow class with most samples in M
11:
                           if \hat{y}_t \notin L^* then
                                                                                ▶ Remove domain-centroid farthest sample
12:
13:
                                \mathbf{s}_{farthest} \leftarrow \arg\max_{\mathbf{s}_i \in M \land \hat{y}_i \in L^*} w_{x_i}
14:
                           else
15:
                                \mathbf{s}_{farthest} \leftarrow \arg\max_{\mathbf{s}_i \in M \land \hat{y}_i = \hat{y}_t} w_{x_i}
                           Remove s_{farthest} from M
16:
17:
                                                                                                        ▶ Update domain-centroid
           \mathbf{c}_{domain} \leftarrow (1 - \beta)\mathbf{c}_{domain} + \beta\mathbf{c}_t
18:
           Recalculate w_{s_i} for all s_i in M
           if b \mod k == 0 then
                                                                                          \triangleright Adaptation occurs every k batches
19:
20:
                Update model \Theta using samples in M
```

Memory management algorithm. CnDRM maintains a compact yet adaptive memory that jointly preserves class balance and domain representativeness while keeping computational overhead minimal. To achieve this, the memory size is fixed to match the batch size for efficiency. Within this limited capacity, samples are managed so that each class remains well-represented while the overall memory distribution stays close to the domain centroid. Specifically, when the memory reaches its capacity, the farthest samples from the domain centroid (those with the largest Wasserstein distance) are replaced by new, high-confidence samples that better align with both class balance and domain characteristics. This joint management ensures that the memory continually retains the most class-and domain-representative samples under dynamic distribution shifts.

Algorithm 1 implements these procedures: lines $8{\sim}16$ handle both *class balancing* and the *remove domain-centroid farthest sample* operation, where the least representative sample (i.e., the one with the largest Wasserstein distance within an overrepresented class) is discarded. Lines $17{\sim}20$ perform the *update domain-centroid* operation using a momentum-based moving average (with $\beta=0.9$) that enables the centroid to smoothly adapt to the evolving feature distribution. This linkage clarifies how CnDRM maintains a unified class-domain representative memory throughout continuous adaptation on edge devices.

4.2 Inference-only Batch-aware Memory Normalization

Motivation. Sparse Test-Time Adaptation (STTA) requires models to adapt to domain shifts with limited update opportunities. Consequently, stored adaptation batch statistics may become misaligned with subsequent inference data when updates are skipped. Traditional normalization methods, relying solely on test batch statistics, also struggle with such shifts. To address this, we propose Inference-only Batch-aware Memory Normalization (IoBMN), which stabilizes adaptation by leveraging representative memory statistics while selectively adjusting for distributional mismatches. This approach ensures both robustness and adaptability in STTA, significantly improving model stability, as demonstrated in our ablation study (Section 5).

Approach. Given a feature map $f \in \mathbb{R}^{B \times C \times L}$, where B is the batch size, C is the number of channels, and L is the number of spatial locations, the batch-wise statistics $\bar{\mu}_c$ and $\bar{\sigma}_c^2$ for the c-th channel are calculated as follows:

$$\bar{\mu}_c = \frac{1}{B \times L} \sum_{b=1}^{B} \sum_{l=1}^{L} f_{b,c,l}, \quad \bar{\sigma}_c^2 = \frac{1}{B \times L} \sum_{b=1}^{B} \sum_{l=1}^{L} (f_{b,c,l} - \mu_{b,c}), \tag{2}$$

where $\bar{\mu}_m$ and $\bar{\sigma}_m^2$ are calculated from the most recent adapted CnDRM samples in the same way with Equation 2, using the memory capacity M with m representing the memory. We assume that μ_m and σ_m^2 follow the *sampling distribution* of the feature map size L and memory capacity M. The corresponding variances for the memory mean μ_m and variance σ_m^2 are calculated as:

$$s_{\mu_m}^2 := \frac{\bar{\sigma}_m^2}{L \times M}, \quad s_{\sigma_m^2}^2 := \frac{2\bar{\sigma}_m^4}{L \times M - 1}.$$
 (3)

For the normalization process to adapt efficiently to the current inference batch statistics, IoBMN corrects $(\bar{\mu}_m, \bar{\sigma}_m^2)$ only when $\bar{\mu}_c$ (and $\bar{\sigma}_c^2$) significantly differ from $\bar{\mu}_m$ (and $\bar{\sigma}_m^2$) through soft shrinkage function:

$$\mu_m^{\text{IoBMN}} = \bar{\mu}_m + S_{\lambda}(\bar{\mu}_c - \bar{\mu}_m; \alpha s_{\mu_m}), \quad (\sigma_m^{\text{IoBMN}})^2 = \bar{\sigma}_m^2 + S_{\lambda}(\bar{\sigma}_c^2 - \bar{\sigma}_m^2; \alpha s_{\sigma_m^2}), \tag{4}$$

where $\alpha \geq 0$ in IoBMN controls the reliance on the normalization layer statistics. A larger α gives more weight to the last adapted memory normalization statistics, whereas a smaller α emphasizes the current inference batch normalization statistics. The soft shrinkage function $S_{\lambda}(x;\lambda)$ is defined as:

$$S_{\lambda}(x;\lambda) = \operatorname{sign}(x) \cdot \max(|x| - \lambda, 0), \tag{5}$$

where λ is the threshold and x is the input. The function allows for proportional adjustments based on the magnitude of the values, where smaller values are adjusted less and larger values more, preserving the critical information inherent in the adapted memory normalization statistics.

Finally, the output of the IoBMN for each feature $f_{b,c,l}$ is computed as

$$IoBMN(f_{b,c,l}; \bar{\mu}_m, \bar{\sigma}_m^2, \mu_m^{IoBMN}, (\sigma_m^{IoBMN})^2) := \gamma \cdot \frac{f_{b,c,l} - \mu_m^{IoBMN}}{\sqrt{(\sigma_m^{IoBMN})^2 + \epsilon}} + \beta, \tag{6}$$

where γ and β are learnable affine parameters of normalization layer, and ϵ is a small constant added for numerical stability. In our experiments, we chose α as 4 to handle various out-of-distribution scenarios effectively. The parameter s is a hyperparameter that determines the degree of adjustment desired and can be tuned based on specific requirements.

IoBMN utilizes CnDRM's class-domain representative statistics and adjusts them based on the current inferencing batch statistics. This dual-statistic approach allows IoBMN to correct the outdated and skewed distribution of the memory, ensuring alignment with the data distribution at each inference point. By leveraging the statistics of the data used during model update points, IoBMN adapts effectively without significant computational overhead. Additionally, this method mitigates the performance degradation caused by the prolonged intervals between adaptations so that the model remains well-aligned with the evolving data distribution.

Table 1: Classification accuracy (%) and latency per batch (s) measured on a Raspberry Pi 4, comparing with and without SNAP (AR=0.1) on CIFAR100-C (ResNet18) and ImageNet-C (ResNet50). **Bold** numbers indicate the highest accuracy on the sparse setting. Extended results for CIFAR10-C and other ARs (0.01, 0.03, 0.05, 0.3, and 0.5) are in Appendix C.

Methods	Gau.	Shot	Imp.	Def.	Gla.	Mot.	Zoom	Snow	Fro.	Fog	Brit.	Cont.	Elas.	Pix.	JPEG	Avg.	Δ(Acc.)	Lat.
									CIFA	AR100-C								
Tent	46.71	48.06	40.98	65.19	44.10	62.78	63.95	55.43	55.46	59.32	67.43	63.83	53.89	59.40	49.91	55.76	-	4.54
+ STTA	43.55	44.25	37.95	62.56	41.80	59.45	62.13	53.04	51.60	56.76	64.60	61.19	51.01	56.42	46.28	52.84	(-2.92)	3.34
+ SNAP	46.51	47.68	39.92	65.39	44.14	63.29	64.53	55.20	55.55	59.71	68.05	64.90	53.91	59.28	49.58	55.84	(+0.08)	3.67
CoTTA	42.14	42.92	37.92	55.40	41.01	55.18	55.39	49.46	50.61	50.86	61.35	47.44	48.69	54.38	48.11	49.39	-	74.77
+ STTA	28.53	29.53	26.45	42.19	30.34	44.69	41.88	34.44	33.93	39.03	45.49	31.17	37.25	36.17	36.84	35.86	(-13.53)	4.94
+ SNAP	41.72	42.62	37.46	58.43	41.24	57.33	57.96	50.34	51.17	52.29	63.59	51.32	49.68	54.78	47.89	50.52	(+1.13)	4.95
EATA	38.42	39.96	32.64	62.35	38.73	59.93	61.07	50.50	50.79	55.30	64.38	60.63	49.66	53.63	43.02	50.74	-	4.25
+ STTA	38.41	39.03	32.29	61.07	38.45	58.21	60.62	49.59	49.19	54.23	62.88	57.39	49.00	53.01	42.05	49.70	(-1.04)	3.13
+ SNAP	40.62	41.53	34.31	64.08	40.29	61.32	63.04	52.00	51.77	56.85	65.98	61.96	51.05	55.67	44.80	52.35	(+1.61)	3.51
SAR	50.75	52.00	43.87	65.44	46.30	63.60	64.68	58.41	58.26	61.34	68.03	67.68	54.53	61.52	52.72	57.94		6.68
+ STTA	43.92	45.28	38.64	63.36	42.58	60.36	62.78	53.39	52.23	57.54	65.41	60.88	52.07	56.80	47.16	53.49	(-4.45)	2.95
+ SNAP RoTTA	46.29 38.54	47.60 39.85	39.95 33.73	65.26 63.45	44.00 40.74	63.09 60.54	64.97 62.03	55.08 51.61	55.17 51.75	59.73 56.20	68.13 65.14	64.72 61.55	53.84 51.22	58.98 54.42	49.54 42.50	55.76 51.55	(-2.18)	3.09 6.71
+ STTA	36.28	37.12	31.38	61.20	38.36	58.26	60.30	49.20	48.21	53.54	62.80	56.78	49.61	52.28	41.26	49.11	(-2,44)	2.96
+ SI IA + SNAP	37.83	38.42	32.38	63.73	39.72	61.32	62.58	51.38	51.18	55.61	65.70	61.39	51.36	54.51	42.85	51.33	(-0.22)	2.96
TOMAI	37.03	30.42	32.30	03.73	37.12	01.52	02.50	31.30			03.70	01.57	31.30	34.31	42.03	31.33	(-0.22)	2.99
										geNet-C								
Tent	27.03	28.98	28.64	24.66	23.63	38.70	45.77	44.82	38.06	54.59	64.61	16.84	51.64	55.54	49.38	39.53		38.33
+ STTA	22.00	23.51	23.07	19.38	18.86	32.15	42.29	39.70	34.33	51.62	63.70	15.79	47.74	52.35	45.54	35.47	(-4.06)	18.01
+ SNAP	26.21	27.85	27.50	23.62	22.73	36.01	44.11	42.19	38.15	52.95	64.57	30.23	48.56	53.71	47.09	39.03	(-0.50)	18.76
CoTTA	13.12	13.98	13.94	12.44	12.18	23.74	35.22	31.78	30.26	44.40	62.40	15.13	40.42	45.26	36.53	28.72	(0.01)	300.23
+ STTA + SNAP	10.97 15.13	11.92	11.98 15.91	11.45 13.86	11.38 14.02	22.39 24.90	34.96 36.51	30.88	29.89 31.81	44.09	61.96	13.08	40.20 41.94	45.27 46.78	36.71 38.03	27.81 30.19	(-0.91)	161.98
EATA	29.62	16.03 31.79	31.17	26.89	26.30	40.65	47.44	32.56 46.29	40.78	46.02 55.57	63.60 64.97	15.69 38.02	52.66	56.03	50.26	42.56	(+1.47)	163.24 31.98
+ STTA	22.43	23.78	23.26	19.38	19.42	32.18	43.22	40.65	36.64	52.38	63.87	24.59	48.13	52.89	46.33	36.61	(-5.95)	16.00
+ SNAP	26.10	27.29	27.13	22.38	22.15	33.45	43.92	40.03	36.68	52.71	63.77	27.93	48.47	53.23	47.46	38.24	(-4.32)	17.45
SAR	29.23	31.14	29.88	29.29	27.39	39.76	44.13	45.98	29.39	55.13	63.71	17.34	52.31	56.09	49.35	39.34	(-4.32)	78.15
+ STTA	26.12	27.56	26.93	22.51	23.35	36.03	44.48	43.19	37.26	53.82	64.15	19.87	50.78	54.78	48.43	38.62	(-0.72)	21.39
+ SNAP	30.28	31.97	31.30	26.67	26.31	39.66	46.08	45.43	40.26	54.76	64.62	36.12	51.26	55.42	49.63	41.99	(+2.65)	23.99
RoTTA	20,60	22.83	19.81	10.46	10.10	21.31	31.83	39.66	32.09	46.08	62.22	20.27	42.54	47.47	40.67	31.20	- (12.05)	87.00
+ STTA	14.77	15.59	15.33	13.17	13.19	23.85	35.38	32.73	30.77	45.22	63.08	15.62	41.05	46.15	37.19	29.54	(-1.66)	45.98
+ SNAP	15.35	16.20	16.01	13.67	13.66	24.27	35.62	33.04	31.02	45.38	62.95	15.96	41.06	46.17	37.44	29.85	(-1.36)	47.47

5 Experiments

This section outlines our experimental setup and presents the results obtained under various STTA settings. Refer to Appendix A for further details.

Scenario. We varied the **Adaptation Rates** (**AR**) to examine how different update frequencies affect both model accuracy and latency under latency-constrained scenarios. In our setup, AR controls how frequently the model is adapted and also corresponds to the memory sampling rate, as the memory size equals the batch size. The main evaluation was run with diverse AR values: 0.01, 0.03, 0.05, 0.1, 0.3, and 0.5. We report the mean accuracy and standard deviation over three random seeds. Latency was measured on three representative edge devices: Raspberry Pi 4 [38], Zero 2W [39], and Jetson Nano [32].

Dataset and model. We used three standard TTA benchmarks: **CIFAR10-C**, **CIFAR100-C** and **ImageNet-C** [10] for main evaluation. These datasets include 15 different types of corruption with five levels of severity, and we used the highest one. We employed **ResNet18** [8] as the backbone network, utilizing models pre-trained on CIFAR10 and CIFAR100 [18]. We also use **ResNet50** [8] and **Vit-Base** [4] pre-trained on ImageNet [3] from the TorchVision [25] library.

Baselines. SNAP is designed to integrate with existing TTA algorithms. Therefore, testing existing **TTA algorithms under different ARs** serves as our baseline (implementation details, including hyperparameters, are in Appendix A.1). We selected five SOTA TTA algorithms: (i) **Tent** [48] updates only BN affine parameters, (ii) **CoTTA** [50] updates the entire model parameters using a teacher-student framework, (iii) **EATA** [30], (iv) **SAR** [31], and (v) **RoTTA**[53].

Overall performance across various adaptation rates. Table 1 and Appendix C provide a performance comparison of baseline state-of-the-art (SOTA) TTA methods and SNAP integration across adaptation rates from 0.01 to 0.5 on CIFAR10/100-C and ImageNet-C. The results reveal that while STTA reduces adaptation latency by up to 93.38%, conventional SOTA algorithms suffer significant accuracy degradation in STTA settings. In contrast, SNAP effectively mitigates this performance drop. By utilizing minimal updates with only a fraction of the samples, SNAP consistently outperforms baseline methods and achieves accuracy comparable to fully adapted models. These findings highlight SNAP's ability to balance efficiency and performance, preserving or even improving classification accuracy in sparse adaptation scenarios.

Figure 5 further illustrates that SNAP maintains STTA performance even at adaptation rates as low as 0.01 while significantly reducing latency. In contrast, naïve STTA suffers substantial performance degradation as the adaptation rate decreases. Notably, computationally complex and latency-intensive method CoTTA benefits more from SNAP. This is because CoTTA updates all model parameters, making it highly dependent on an effective sampling strategy, underscoring the effectiveness of Cn-DRM. At higher adaptation rates (0.5

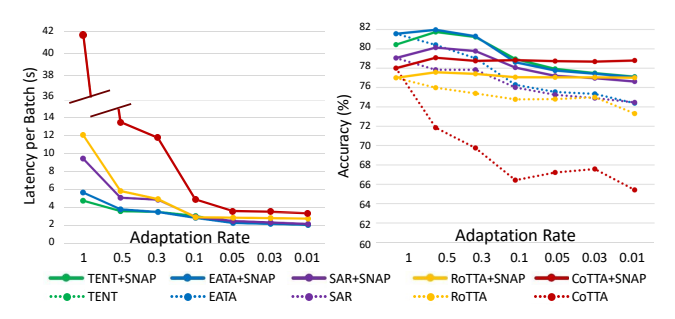


Figure 5: Latency on Raspberry Pi 4 and CIFAR10-C accuracy across adaptation rates. Due to SNAP's negligible overhead, solid and dotted lines overlap in the latency plot. Marker size indicates standard deviation.

or 0.3), SNAP can even surpass fully adapted methods by selectively utilizing the most informative samples, similar to existing sampling-based TTA methods [30, 31, 6, 7]. With sufficient samples and update frequency, SNAP's class-domain representative sampling filters harmful data points, further improving performance. Overall, these results confirm that SNAP significantly reduces per-batch latency while preserving accuracy, demonstrating its effectiveness in resource-constrained environments. Extended results on various adaptation rates and datasets (CIFAR10/100-C and ImageNet-C) are reported in Appendix C.

Contribution of SNAP's individual components. We conducted an ablative evaluation to understand the effects of the individual components of SNAP (Table 2; more results on various adaptation rates and datasets are in Appendix C.4). CRM denotes prediction-balanced sampling with a confidence threshold, and CnDRM denotes both Class and Domain Representative sampling (the first component of SNAP). For inference, the default uses test batch normalization statistics, EMA uses the exponential moving average of the test batch, and IoBMN uses memory samples' statistics corrected to match that of the test batch (the second component of SNAP).

Contrary to the belief that low-entropy samples benefit TTA [30, 31], LowEntropy performed worse than Rand for STTA, due to limited updates causing poor or slow convergence. CRM, originally for data-efficient supervised learning [2, 51], outperformed Rand but remained inferior to CnDRM due to reliance on uncertain pseudo-labels instead of ground truth. The highest accuracy was achieved with IoBMN, which mainly leverages memory

Table 2: Classification accuracy (%) comparison of ablative settings on the STTA (AR=0.1). Performance averaged over all 15 CIFAR10-C corruptions.

Methods	Tent	CoTTA	EATA	SAR	RoTTA
Naïve Random LowEntropy CRM	$\begin{array}{c} 76.81 \pm 0.18 \\ 77.08 \pm 0.14 \\ 75.66 \pm 0.09 \\ 77.77 \pm 0.05 \end{array}$	$\begin{array}{c} 66.42 \pm 0.12 \\ 65.61 \pm 0.08 \\ 63.19 \pm 0.14 \\ 65.71 \pm 0.19 \end{array}$	$\begin{array}{c} 76.29 \pm 0.11 \\ 76.59 \pm 0.10 \\ 74.89 \pm 0.12 \\ 77.18 \pm 0.08 \end{array}$	$ 76.01 \pm 0.07 \\ 76.33 \pm 0.13 \\ 74.41 \pm 0.18 \\ 74.36 \pm 0.11 $	$\begin{array}{c} 74.78 \pm 0.15 \\ 75.01 \pm 0.16 \\ 72.60 \pm 0.10 \\ 75.27 \pm 0.17 \end{array}$
CnDRM CnDRM+EMA CnDRM+IoBMN	77.46 ±0.07 78.02 ±0.12 78.95 ±0.09	77.69 ±0.10 72.19 ±0.15 78.83 ±0.06	77.17 ±0.06 77.05 ±0.11 78.61 ±0.13	76.85 ±0.09 76.84 ±0.13 78.06 ±0.07	75.64 ±0.08 76.18 ±0.05 77.07 ±0.10

statistics and adapts minimally to each test batch. These indicate that combining CnDRM and IoBMN in SNAP enhances performance in low-latency STTA.

Performance validation across diverse edge-devices. SNAP significantly reduces adaptation latency across a range of edge devices. At an adaptation rate of 0.05, latency was reduced by up to 91.3% on Raspberry Pi 4 [38], 86.2% on Jetson Nano [32], and 93.7% on Raspberry Pi Zero 2 W [39]. This consistent trend across varying hardware confirms SNAP's effectiveness in latency-sensitive edge deployments. Complete results across all adaptation rates and devices are provided in Appendix B.6.

Memory overhead and compatibility with memory-efficient TTA. SNAP's memory overhead primarily comes from the memory buffer in CnDRM and statistics stored for IoBMN. Empirical results confirm that this overhead is minimal, accounting for only 0.02% to 1.74% of the original memory usage across all algorithms. Additionally, SNAP improves average memory efficiency by reducing backpropagation frequency. Further theoretical and experimental analyses of memory usage are provided in Appendix B.7. SNAP is also compatible with memory-efficient TTA modules like MECTA [12]. Integrating MECTA with Tent + SNAP reduces peak memory usage by 32.08%, showcasing its effectiveness in meeting both latency and memory constraints (Appendix B.8).

SNAP on vision transformer. We validate SNAP on ViT-Base [4] by adapting CnDRM and IoBMN to instance-level layer normalization (LN), replacing batch statistics. This confirms that our core strategies, class-domain sample selection and normalization shift mitigation, generalize to LN. SNAP achieves up to 2.9× latency reduction while preserving or improving full adaptation accuracy across all five baselines (Figure 6).

Details are in Appendix B.9.

Robustness under continuous and persistent distribution shifts. SNAP adapts efficiently to evolving domains by smoothly moving its domain centroid with minimal overhead. In a continuous stream of corruptions from ImageNet-C, it outperforms naïve STTA by over 2.5% on average. We further assess long-term

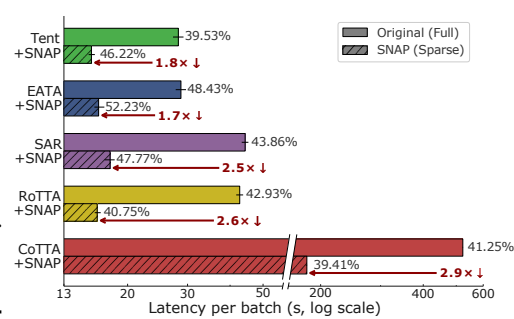


Figure 6: Latency comparison of full (original) and sparse (SNAP) TTA on ViT-Base [4], ImageNet-C. Accuracy values are annotated to the right of each bar.

robustness under temporally correlated and recurring shifts [11]. Combined with SNAP, accuracy remains consistently above 50% over 10 adaptation rounds, whereas naive STTA alone degrades sharply, dropping to 16.97%. These results highlight SNAP's ability to maintain stable performance across both continuous and persistent distribution changes. Details are in Appendices B.13 and B.14.

Robustness in single-sample (BS=1) adaptation scenario. In highly constrained environments where the batch size is limited to one, SNAP maintains strong performance. It achieves 51.80% accuracy with an adaptation rate of 0.1, closely matching the full SAR [31] baseline at 52.21% and performing over 5× better than naïve STTA. CnDRM continues to effectively select informative samples, while IoBMN leverages memory-based statistics to adaptively normalize each input under this extreme regime. Further details are provided in Appendix B.15.

Impact of memory size and learning rate. SNAP demonstrates robustness to both memory sizes and learning rates. It adapts effectively with a memory size equal to the batch size, as larger sizes offer only $1\sim2\%$ marginal gains before saturation. Likewise, it outperforms all baselines across learning rates, showing up to $5\sim10\%$ absolute gains under sparse adaptation. These results underscore SNAP's efficiency and stability under constrained adaptation. Full analyses are in Appendices B.16 and B.17.

6 Discussion and conclusion

Limitations and societal impacts. SNAP uses a fixed adaptation rate, but dynamically adjusting it based on distribution shifts or system load could improve responsiveness. The confidence threshold in CnDRM is also fixed as a simple safeguard, which may limit adaptability. Dynamically tuning this threshold based on data characteristics could further enhance sampling efficiency. In addition, our implementation reduces average latency by adapting sparsely across batches, rather than explicitly optimizing backpropagation delay, due to PyTorch [33] constraints that require backpropagation to run as a single block. Future work could explore distributing the backpropagation step allocation across batches to further enhance applicability. Furthermore, deploying deep learning on edge devices at scale can raise societal concerns, such as carbon emissions [41]. By lowering computational overhead, SNAP helps mitigate these environmental impacts. It also reduces the need to transmit user data to the server, supporting stronger privacy in real-world applications.

Conclusion. We highlight the often-overlooked issue of TTA latency, a critical factor for resource-constrained edge devices. To address this, we propose SNAP, a lightweight STTA framework that significantly reduces latency while preserving accuracy. SNAP leverages class-domain representative memory for adaptation and optimizes inference by adapting normalization layers using memory to account for domain shifts. Extensive experiments and ablation studies validate its effectiveness.

Acknowledgments and Disclosure of Funding

This work was partly supported by the Institute of Information & communications Technology Planning & Evaluation (IITP) grant funded by the Korea government (MSIT) (No.2024-00444862, Non-invasive near-infrared based AI technology for the diagnosis and treatment of brain diseases), the National Research Foundation of Korea (NRF) grant funded by the Korea government (MSIT) (RS-2024-00337007), and the Institute of Information & Communications Technology Planning & Evaluation (IITP) grant funded by the Korea government (MSIT) (RS-2025-25442824, AI Star Fellowship Program (Ulsan National Institute of Science and Technology)). * MSIT: Ministry of Science and ICT

References

- [1] Motasem Alfarra, Hani Itani, Alejandro Pardo, Shyma Yaser Alhuwaider, Merey Ramazanova, Juan Camilo Perez, Zhipeng Cai, Matthias Müller, and Bernard Ghanem. Evaluation of test-time adaptation under computational time constraints. In *Proceedings of the 41st International Conference on Machine Learning*, volume 235 of *Proceedings of Machine Learning Research*, pages 976–991. PMLR, 21–27 Jul 2024.
- [2] Hoyong Choi, Nohyun Ki, and Hye Won Chung. Bws: best window selection based on sample scores for data pruning across broad ranges. In *Proceedings of the 41st International Conference on Machine Learning*. JMLR.org, 2024.
- [3] Jia Deng, Wei Dong, Richard Socher, Li-Jia Li, Kai Li, and Li Fei-Fei. Imagenet: A large-scale hierarchical image database. In 2009 IEEE Conference on Computer Vision and Pattern Recognition, pages 248–255, 2009.
- [4] Alexey Dosovitskiy, Lucas Beyer, Alexander Kolesnikov, Dirk Weissenborn, Xiaohua Zhai, Thomas Unterthiner, Mostafa Dehghani, Matthias Minderer, G Heigold, S Gelly, et al. An image is worth 16x16 words: Transformers for image recognition at scale. In *International Conference on Learning Representations*, 2020.
- [5] Pierre Foret, Ariel Kleiner, Hossein Mobahi, and Behnam Neyshabur. Sharpness-aware minimization for efficiently improving generalization. In *International Conference on Learning Representations*, 2021.
- [6] Taesik Gong, Jongheon Jeong, Taewon Kim, Yewon Kim, Jinwoo Shin, and Sung-Ju Lee. NOTE: Robust continual test-time adaptation against temporal correlation. In *Advances in Neural Information Processing Systems*, 2022.
- [7] Taesik Gong, Yewon Kim, Taeckyung Lee, Sorn Chottananurak, and Sung-Ju Lee. SoTTA: Robust test-time adaptation on noisy data streams. In *Thirty-seventh Conference on Neural Information Processing Systems*, 2023.
- [8] Kaiming He, Xiangyu Zhang, Shaoqing Ren, and Jian Sun. Deep residual learning for image recognition. In *Proceedings of the IEEE Conference on Computer Vision and Pattern Recognition*, June 2016.
- [9] Dan Hendrycks, Steven Basart, Norman Mu, Saurav Kadavath, Frank Wang, Evan Dorundo, Rahul Desai, Tyler Zhu, Samyak Parajuli, Mike Guo, Dawn Song, Jacob Steinhardt, and Justin Gilmer. The many faces of robustness: A critical analysis of out-of-distribution generalization. *ICCV*, 2021.
- [10] Dan Hendrycks and Thomas Dietterich. Benchmarking neural network robustness to common corruptions and perturbations. In *International Conference on Learning Representations*, 2019.
- [11] Trung-Hieu Hoang, Duc Minh Vo, and Minh N. Do. Persistent test-time adaptation in recurring testing scenarios. In *Thirty-eighth Conference on Neural Information Processing Systems*, 2024.
- [12] Junyuan Hong, Lingjuan Lyu, Jiayu Zhou, and Michael Spranger. Mecta: Memory-economic continual test-time model adaptation. In *International Conference on Learning Representations*, 2023.

- [13] Yusuke Iwasawa and Yutaka Matsuo. Test-time classifier adjustment module for model-agnostic domain generalization. In *Advances in Neural Information Processing Systems*, volume 34, pages 2427–2440. Curran Associates, Inc., 2021.
- [14] Ziheng Jiang, Chiyuan Zhang, Kunal Talwar, and Michael C Mozer. Characterizing structural regularities of labeled data in overparameterized models. In *Proceedings of the 38th International Conference on Machine Learning*, volume 139 of *Proceedings of Machine Learning Research*, pages 5034–5044. PMLR, 18–24 Jul 2021.
- [15] Diederick P Kingma and Jimmy Ba. Adam: A method for stochastic optimization. In *International Conference on Learning Representations*, 2015.
- [16] Pang Wei Koh and Percy Liang. Understanding black-box predictions via influence functions. In *Proceedings of the 34th International Conference on Machine Learning*, volume 70 of *Proceedings of Machine Learning Research*, pages 1885–1894. PMLR, 06–11 Aug 2017.
- [17] Germain Kolossov, Andrea Montanari, and Pulkit Tandon. Towards a statistical theory of data selection under weak supervision. In *The Twelfth International Conference on Learning Representations*, 2024.
- [18] A. Krizhevsky and G. Hinton. Learning multiple layers of features from tiny images. *Master's thesis, Department of Computer Science, University of Toronto*, 2009.
- [19] Kimin Lee, Kibok Lee, Honglak Lee, and Jinwoo Shin. A simple unified framework for detecting out-of-distribution samples and adversarial attacks. *Advances in neural information processing systems*, 31, 2018.
- [20] Yanghao Li, Naiyan Wang, Jianping Shi, Jiaying Liu, and Xiaodi Hou. Revisiting batch normalization for practical domain adaptation. *Pattern Recognition*, 80, 03 2016.
- [21] Ji Lin, Wei-Ming Chen, Yujun Lin, John Cohn, Chuang Gan, and Song Han. Mcunet: Tiny deep learning on iot devices. In *In Advances in Neural Information Processing Systems*, volume 33, pages 11711–11722. Curran Associates, Inc., 2020.
- [22] Haolan Liu, Zixuan Wang, and Jishen Zhao. Cola: characterizing and optimizing the tail latency for safe level-4 autonomous vehicle systems. In 2025 IEEE International Conference on Robotics and Automation (ICRA), pages 3709–3719. IEEE, 2025.
- [23] Aleksej Logacjov, Kerstin Bach, Atle Kongsvold, Hilde Bremseth Bårdstu, and Paul Jarle Mork. Harth: A human activity recognition dataset for machine learning. *Sensors*, 21(23):7853, 2021.
- [24] Ilya Loshchilov and Frank Hutter. SGDR: Stochastic gradient descent with warm restarts. In *International Conference on Learning Representations*, 2017.
- [25] TorchVision maintainers and contributors. Torchvision: Pytorch's computer vision library. https://github.com/pytorch/vision, 2016.
- [26] Baharan Mirzasoleiman, Jeff Bilmes, and Jure Leskovec. Coresets for data-efficient training of machine learning models. In *Proceedings of the 37th International Conference on Machine Learning*, volume 119 of *Proceedings of Machine Learning Research*, pages 6950–6960. PMLR, 13–18 Jul 2020.
- [27] Eduardo Fernandes Montesuma, Fred Maurice NGOLE MBOULA, and Antoine Souloumiac. Optimal transport for domain adaptation through gaussian mixture models. *Transactions on Machine Learning Research*, 2025.
- [28] Zachary Nado, Shreyas Padhy, D Sculley, Alexander D'Amour, Balaji Lakshminarayanan, and Jasper Snoek. Evaluating prediction-time batch normalization for robustness under covariate shift. *arXiv preprint arXiv:2006.10963*, 2020.
- [29] Shuaicheng Niu, Chunyan Miao, Guohao Chen, Pengcheng Wu, and Peilin Zhao. Test-time model adaptation with only forward passes. In *The International Conference on Machine Learning*, 2024.

- [30] Shuaicheng Niu, Jiaxiang Wu, Yifan Zhang, Yaofo Chen, Shijian Zheng, Peilin Zhao, and Mingkui Tan. Efficient test-time model adaptation without forgetting. In *Proceedings of the 39th International Conference on Machine Learning*, volume 162 of *Proceedings of Machine Learning Research*, pages 16888–16905. PMLR, 17–23 Jul 2022.
- [31] Shuaicheng Niu, Jiaxiang Wu, Yifan Zhang, Zhiquan Wen, Yaofo Chen, Peilin Zhao, and Mingkui Tan. Towards stable test-time adaptation in dynamic wild world. In *The Eleventh International Conference on Learning Representations*, 2023.
- [32] NVIDIA Corporation. NVIDIA Jetson Nano, 2019. Accessed: 2024-11-20.
- [33] Adam Paszke, Sam Gross, Francisco Massa, Adam Lerer, James Bradbury, Gregory Chanan, Trevor Killeen, Zeming Lin, Natalia Gimelshein, Luca Antiga, Alban Desmaison, Andreas Kopf, Edward Yang, Zachary DeVito, Martin Raison, Alykhan Tejani, Sasank Chilamkurthy, Benoit Steiner, Lu Fang, Junjie Bai, and Soumith Chintala. Pytorch: An imperative style, high-performance deep learning library. In *Thirty-second Advances in Neural Information Processing Systems*, pages 8024–8035. Curran Associates, Inc., 2019.
- [34] Mansheej Paul, Surya Ganguli, and Gintare Karolina Dziugaite. Deep learning on a data diet: Finding important examples early in training. In *Advances in Neural Information Processing Systems*, 2021.
- [35] Geoff Pleiss, Tianyi Zhang, Ethan Elenberg, and Kilian Q Weinberger. Identifying mislabeled data using the area under the margin ranking. In *Advances in Neural Information Processing Systems*, volume 33, pages 17044–17056. Curran Associates, Inc., 2020.
- [36] Omead Pooladzandi, David Davini, and Baharan Mirzasoleiman. Adaptive second order coresets for data-efficient machine learning. In *Proceedings of the 39th International Conference on Machine Learning*, volume 162 of *Proceedings of Machine Learning Research*, pages 17848–17869. PMLR, 17–23 Jul 2022.
- [37] Joaquin Quiñonero-Candela, Masashi Sugiyama, Anton Schwaighofer, and Neil D Lawrence. *Dataset shift in machine learning*. Mit Press, 2008.
- [38] Raspberry Pi Foundation. Raspberry Pi 4 Model B, 2019. Accessed: 2024-11-20.
- [39] Raspberry Pi Foundation. Raspberry Pi Zero 2 W, 2021. Accessed: 2024-11-20.
- [40] Steffen Schneider, Evgenia Rusak, Luisa Eck, Oliver Bringmann, Wieland Brendel, and Matthias Bethge. Improving robustness against common corruptions by covariate shift adaptation. In *Advances in Neural Information Processing Systems*, volume 33, pages 11539–11551. Curran Associates, Inc., 2020.
- [41] Roy Schwartz, Jesse Dodge, Noah A. Smith, and Oren Etzioni. Green ai. *Commun. ACM*, 63(12):54–63, November 2020.
- [42] Mattia Segu, Alessio Tonioni, and Federico Tombari. Batch normalization embeddings for deep domain generalization. *Pattern Recognition*, 135:109115, 2023.
- [43] Junha Song, Jungsoo Lee, In So Kweon, and Sungha Choi. Ecotta: Memory-efficient continual test-time adaptation via self-distilled regularization. In *Proceedings of the IEEE/CVF Conference on Computer Vision and Pattern Recognition*, pages 11920–11929, 2023.
- [44] Ben Sorscher, Robert Geirhos, Shashank Shekhar, Surya Ganguli, and Ari S. Morcos. Beyond neural scaling laws: beating power law scaling via data pruning. In *Proceedings of the 36th International Conference on Neural Information Processing Systems*, NIPS '22, Red Hook, NY, USA, 2022. Curran Associates Inc.
- [45] Ardi Tampuu, Kristjan Roosild, and Ilmar Uduste. The effects of speed and delays on test-time performance of end-to-end self-driving. *Sensors*, 24(6):1963, 2024.
- [46] Mariya Toneva, Alessandro Sordoni, Remi Tachet des Combes, Adam Trischler, Yoshua Bengio, and Geoffrey J. Gordon. An empirical study of example forgetting during deep neural network learning. In *International Conference on Learning Representations*, 2019.

- [47] Cédric Villani. *The Wasserstein distances*, pages 93–111. Springer Berlin Heidelberg, Berlin, Heidelberg, 2009.
- [48] Dequan Wang, Evan Shelhamer, Shaoteng Liu, Bruno Olshausen, and Trevor Darrell. Tent: Fully test-time adaptation by entropy minimization. In *International Conference on Learning Representations*, 2021.
- [49] Haohan Wang, Songwei Ge, Zachary Lipton, and Eric P Xing. Learning robust global representations by penalizing local predictive power. In *Advances in Neural Information Processing Systems*, pages 10506–10518, 2019.
- [50] Qin Wang, Olga Fink, Luc Van Gool, and Dengxin Dai. Continual test-time domain adaptation. In Proceedings of the IEEE/CVF Conference on Computer Vision and Pattern Recognition, pages 7201–7211, June 2022.
- [51] Xiaobo Xia, Jiale Liu, Jun Yu, Xu Shen, Bo Han, and Tongliang Liu. Moderate coreset: A universal method of data selection for real-world data-efficient deep learning. In *The Eleventh International Conference on Learning Representations*, 2022.
- [52] Shuo Yang, Zeke Xie, Hanyu Peng, Min Xu, Mingming Sun, and Ping Li. Dataset pruning: Reducing training data by examining generalization influence. In *The Eleventh International Conference on Learning Representations*, 2023.
- [53] Longhui Yuan, Binhui Xie, and Shuang Li. Robust test-time adaptation in dynamic scenarios. In *Proceedings of the IEEE/CVF Conference on Computer Vision and Pattern Recognition*, pages 15922–15932, June 2023.
- [54] Matthew D Zeiler and Rob Fergus. Visualizing and understanding convolutional networks. In *Computer Vision–ECCV 2014: 13th European Conference, Zurich, Switzerland, September 6-12, 2014, Proceedings, Part I 13*, pages 818–833. Springer, 2014.
- [55] Marvin Zhang, Sergey Levine, and Chelsea Finn. Memo: Test time robustness via adaptation and augmentation. In *Advances in Neural Information Processing Systems*, volume 35, pages 38629–38642. Curran Associates, Inc., 2022.

A Experiment details

All experiments presented in this paper were conducted using three random seeds (0, 1, 2), and we report the average accuracies along with their corresponding standard deviations. To ensure efficiency in experimentation, accuracy measurements were obtained using NVIDIA GeForce RTX 3090 GPUs, as the performance differences attributable to the random seed are negligible. Latency measurements were mainly conducted on a Raspberry Pi 4 [38], equipped with a Quad-core Cortex-A72 (ARM v8) 64-bit SoC @ 1.8GHz CPU and 4GB RAM. In addition, two more edge-devices: NVIDIA Jetson Nano [32] and Raspberry Zero 2 W [39] are also utilized for latency measurements.

A.1 Baseline implementation details

In this study, we utilized the official implementations of the baseline methods. To ensure consistency, we adopted the reported best hyperparameters documented in the respective papers or source code repositories as much as possible. Also, we present information about the implementation specifics of the baseline methods and provide a comprehensive overview of our experimental setup, including detailed descriptions of the employed hyperparameters.

We adopt hyperparameters from the original papers or the official code of the baselines for consistency. To assess the generality of SNAP, the test batch sizes were set to 16 for all baseline methods to ensure a fair comparison. To minimize overhead and maintain consistency with inference batches, we set the size of CnDRM equal to the batch size. TTA is conducted in an online manner, with adaptation or inference performed per batch. When there was a conflict between the implementation of SNAP and certain components of the existing baseline methods, we prioritized SNAP's features for fair evaluation at the STTA setting.

Tent [48] We update the BN affine parameters using the SGD optimizer [24] with a learning rate of l=1e-3 for CIFAR10/100C and l=1e-4 for ImageNet-C. For separate experimentation on the ViT, we used a learning rate of l=2e-4.

CoTTA [50] We update all model parameters using the Adam optimizer [15] with a learning rate of l=1e-4. Furthermore, we set CoTTA's teacher model EMA factor to $\alpha=0.99$, the restoration factor to p=0.1, and the anchor probability to $p_{\rm th}=0.9$.

EATA [30] We use the SGD optimizer with a learning rate of l = 1e - 4. We set the entropy threshold as $E_0 = 0.4 \times \ln |N|$, where N is the total number of classes.

SAR [31] We use SAM [5] with the base optimizer as SGD with a learning rate of l = 1e - 3. For fair evaluation, we replaced the sample filtering scheme with SNAP's CnDRM.

RoTTA [53] We use the SGD optimizer with a learning rate of l=1e-3. For fair evaluation, we replaced RoTTA's RBN and CSTU with SNAP's CnDRM and IoBMN. For the teacher-student structure, we set the teacher model's exponential moving average update rate as v=1e-3.

Finally, we list the hyperparameters specific to the components of SNAP. The confidence threshold for CnDRM τ_{conf} is set to 0.4 for CIFAR10-C, 0.45 for CIFAR100-C, and 0.5 for ImageNet-C. The entropy threshold for our ablation study τ_{entr} is set to $\log(10) \times 0.40$ for CIFAR10-C and $\log(100) \times 0.40$ for CIFAR100-C, as referenced in a previous work using entropy-based filtering [30]. Additionally, the parameters for the soft shrinkage function in IoBMN are fixed with $\alpha=4$ for Tent, CoTTA, SAR, RoTTA, and $\alpha=2$ for EATA.

B Additional discussions

B.1 Theoretical analysis on class and domain representative sampling criteria

The sampling strategy in SNAP's CnDRM module is grounded in theoretical insights from dataefficient learning and generalization under constrained adaptation settings. Under latency-constrained scenarios, models can only adapt intermittently. This raises the following question: Which subset of streaming samples yields the greatest adaptation gain when only a fraction $\rho = n/N$ of them can be used for weight updates?

Selection ratio and phase transition. Let $\rho = n/N \in (0,1]$ denote the adaptation ratio, where n is the number of selected samples for model update out of N total seen test samples. Theoretical and empirical studies [2, 44, 17] show that the optimal selection strategy varies significantly depending on the value of ρ :

- When $\rho>0.6$ (high adaptation rate), selecting low-confidence samples near decision boundaries provides maximal information gain.
- When $\rho \le 0.5$ (sparse adaptation), selecting high-confidence, representative samples near class or domain centroids leads to better generalization.

This dichotomy is supported analytically in [2], which shows that in underparameterized regimes, boundary samples may inject noisy gradients and destabilize learning.

Illustrative example. Consider a binary classification task where inputs $x_i \sim \mathcal{N}(0, \frac{1}{\sqrt{d}}I_d)$, and labels are assigned by $y_i = \mathrm{sign}(x_{i1})$. The Bayes-optimal classifier aligns with e_1 , the first basis vector. Suppose we select a subset $(X_S, y_S) \in \mathbb{R}^{d \times n} \times \{-1, 1\}^n$ and compute the ridge regression solution:

$$w_S = \arg\min_{w \in \mathbb{R}^d} \|y_S - X_S^{\top} w\|^2.$$
 (7)

As shown in prior work [2], in the *sample-deficient regime* $(n \ll d)$, the solution w_S aligns best with the true decision direction when trained on high-confidence samples. In contrast, in the *sample-sufficient regime* $(n \gg d)$, boundary samples become more beneficial for refining decision boundaries.

Sampling criterion under sparse adaptation. Based on this, the optimal update subset $S^* \subset \mathcal{D}_{test}$ under $\rho \ll 1$ can be defined as:

$$S^* = \arg\max_{S} \sum_{x_i \in S} \|f(x_i) - \mu_{c_i}\|_2^2 \quad \text{s.t.} \quad c_i = \arg\max_{j} f_j(x_i),$$
 (8)

where μ_{c_i} is the estimated feature-space class centroid. This motivates our use of class- and domain-representative memory (CnDRM), which prioritizes confident, centroid-aligned samples for parameter updates under low-frequency adaptation.

Under sparse adaptation ($\rho \ll 1$), selecting the most informative subset of test samples becomes critical. Our method prioritizes samples that are both semantically reliable (class-representative) and statistically aligned (domain-representative).

For the class-representative criterion, we follow insights from [2], which show that in the sample-deficient regime, high-confidence samples, those far from the decision boundary, yield better generalization than boundary samples. Rather than explicitly computing class centroids, we approximate class-representative samples by selecting those with the highest prediction confidence:

$$S_{\text{class}}^* = \{ x_i \in \mathcal{D}_{test} \mid \text{Conf}(x_i) \ge \tau \}, \tag{9}$$

where $Conf(x_i) = \max_i f_i(x_i)$ is the softmax confidence score and τ is a confidence threshold.

To additionally enforce domain-level representativeness, we compute the Wasserstein-2 distance between each candidate sample and the estimated domain distribution. Specifically, each domain d is modeled as a Gaussian $\mathcal{N}(\nu_d, \Sigma_d)$, where:

$$\nu_d = \frac{1}{|\mathcal{D}_d|} \sum_{x_i \in \mathcal{D}_d} f(x_i), \qquad \Sigma_d = \frac{1}{|\mathcal{D}_d|} \sum_{x_i \in \mathcal{D}_d} (f(x_i) - \nu_d) (f(x_i) - \nu_d)^\top.$$
 (10)

Each sample x_i is treated as an empirical distribution $\mathcal{N}(\mu_i, \Sigma_i)$ using a local batch of neighboring features. The closed-form squared 2-Wasserstein distance between two Gaussians is given by:

$$W_2^2\left(\mathcal{N}(\mu_i, \Sigma_i), \mathcal{N}(\nu_d, \Sigma_d)\right) = \|\mu_i - \nu_d\|_2^2 + \text{Tr}\left(\Sigma_i + \Sigma_d - 2(\Sigma_d^{1/2} \Sigma_i \Sigma_d^{1/2})^{1/2}\right). \tag{11}$$

Combining both criteria, our final selection strategy becomes:

$$S^* = \arg\min_{S \subset S_{\text{class}}^*} \sum_{x_i \in S} W_2^2(\mathcal{N}(\mu_i, \Sigma_i), \mathcal{N}(\nu_d, \Sigma_d)), \tag{12}$$

i.e., we select a subset of high-confidence samples that are also distributionally aligned with the estimated domain centroid. This ensures that parameter updates occur on samples that are both semantically stable and statistically representative under test-time domain shift.

Practical implementation. In our system, we operate with $\rho < 0.5$ (e.g., update every two test batches). While this reduces update opportunities, the degradation in performance is mitigated via CnDRM's informed sample selection. In addition, SNAP integrates IoBMN (Inference-only Batch-aware Memory Normalization), which updates batch norm statistics from all incoming samples, even if they are not used for weight updates. This reduces covariate shift and maintains normalization stability across domains.

B.2 Assumptions and derivation of the Wasserstein formulation

The closed-form expression in Equation 1 assumes that feature distributions are Gaussian with diagonal covariance. This section clarifies the underlying assumptions and derivation.

Distribution definition. The distribution in Equation 1 refers to the empirical distribution of scalar *feature activations per channel*, rather than the input data distribution. We consider each channel's activation statistics (mean and variance) in a deep layer's feature map.

Wasserstein approximation and assumptions. To compute the Wasserstein distance efficiently, the feature distributions are approximated as *univariate Gaussian distributions* for each channel. These distributions are assumed to be independent, corresponding to a *diagonal covariance* assumption. The detailed assumptions are as follows:

- Gaussian assumption: Each channel's activations are assumed to follow a Gaussian distribution $\mathcal{N}(\mu, \sigma^2)$, which simplifies the formulation since Gaussian distributions are fully determined by their mean μ and variance σ^2 . This approximation is commonly adopted in deep learning, where normalized feature activations tend to exhibit near-Gaussian behavior in high-dimensional feature spaces.
- Diagonal covariance: The covariance matrix for each Gaussian is assumed to be diagonal, implying independence across channels. This assumption is widely used in domain adaptation and transport-based methods, as it reduces the computational complexity of full covariance estimation while focusing on per-channel variance shifts.
- 2-Wasserstein distance for Gaussian distributions: Under these assumptions (independent Gaussian distributions), the squared 2-Wasserstein distance between two univariate Gaussian distributions $\mathcal{N}(\mu_1, \sigma_1^2)$ and $\mathcal{N}(\mu_2, \sigma_2^2)$ is given by:

$$W_2^2 = (\mu_1 - \mu_2)^2 + (\sigma_1 - \sigma_2)^2.$$

This closed-form expression enables efficient computation of the Wasserstein distance without estimating full covariance matrices, which is computationally expensive.

Such approximations are widely adopted in the domain adaptation literature [20, 27], as they balance computational efficiency and empirical performance while providing a meaningful measure of domain-level similarity.

B.3 Comparison with prior TTAs under sparse update constraints

While prior TTA studies have partially explored using memory banks and the correction of Batch Normalization (BN) statistics at inference time, our key contribution lies in systematically redesigning these components for sparse-update regimes in resource-constrained environments, which impose fundamentally different computational and statistical constraints.

CnDRM vs. Prior memory-based sampling (RoTTA [53], NOTE [6], SAR [31], and EATA [30]) Previous methods assume frequent adaptation, updating every batch and using more than 50% of test samples. They typically select temporally balanced or low-entropy samples for updates. In contrast, our goal is *Sparse TTA* (e.g., 10% adaptation rate), where such filtering leaves too few useful samples for effective adaptation. To address this, CnDRM avoids low-entropy filtering and instead selects *representative samples* based on domain centroids and class confidence. This approach enables efficient adaptation with minimal latency. Theoretical analysis (Appendix B.1) and ablation results (Table 2, Appendix C.4) show that prior entropy-based filtering performs worse than even random selection under sparse-update settings.

IoBMN vs. Instance-wise BN correction (NOTE [6]) NOTE corrects BN statistics per instance, which introduces latency proportional to the number of test samples. In contrast, IoBMN leverages domain-class statistics from CnDRM's memory to correct batch BN statistics efficiently while remaining compatible with batch inference. The memory statistics are adaptively shifted toward batch statistics to mitigate skew from sparse updates. This design enhances computational efficiency and normalizes using adaptation-involved samples, yielding consistent performance gains (Table 2, Appendix C.4).

B.4 Domain influence in early layer representations

In deep learning models, early layers capture low-level features such as textures, edges, and frequency components [54]. These features are inherently domain-specific, making these layers more sensitive to shifts in input data distribution—a critical challenge for tasks requiring domain adaptation and generalization [19, 42]. This sensitivity arises because early layers encapsulate domain-specific patterns that may not generalize to new distributions. Under the covariate shift assumption [37], while input distributions differ between source and target domains, the conditional distribution of labels remains the same. This discrepancy between input distributions makes early layers particularly vulnerable to domain shifts.

Visualizing early layer feature embeddings using 2D PCA on CIFAR-10C domains reveals distinct domain-specific patterns, highlighting

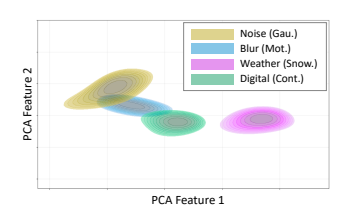


Figure 7: PCA embedding of early layer features for one domain from each of the four main CIFAR10-C corruption categories, showing clear separation between domains.

the significant influence of domain information in these representations (Figure 7). Our preliminary experiments further confirm that sparse TTA, using the Wasserstein distance between moving batch normalization statistics and instance-specific statistics derived from early layer hidden features, can significantly improve performance. Selecting instances closer to the target domain distribution center using this distance metric yields better adaptation results, as demonstrated by performance comparisons between the top 20% and bottom 20% of samples (Figure 4). These findings emphasize the crucial role of domain-sensitive early layers in achieving effective adaptation.

B.5 Analysis on confidence threshold on pseudo-label accuracy

We analyzed the impact of using a confidence threshold for pseudo-label selection by comparing random sampling with high-confidence sampling across three benchmarks: CIFAR10-C, CIFAR100-C, and ImageNet-C. Table 3 shows that high-confidence sampling consistently outperformed random sampling, achieving significantly higher pseudo-label accuracy in all datasets. This result demonstrates the effectiveness of selecting high-confidence samples to improve the quality of pseudo-labels, thereby enhancing model adaptation under domain shift conditions.

Table 3: Pseudo-label accuracy comparison between random and high-confidence sampling on three benchmakrs: CIFAR10-C, CIFAR100-C, and ImageNet-C. **Bold** numbers are the highest accuracy.

	CIFAR10-C	CIFAR100-C	ImageNet-C
Random	69.91 ± 0.31	45.30 ± 0.20	23.90±0.19
HighConf	74.80 ±0.15	59.38 ±0.26	59.40 ±0.04

B.6 Latency tracking of SNAP on diverse edge-devices

To evaluate the latency efficiency of SNAP on resource-constrained edge devices, we measured the adaptation latency across three devices: NVIDIA Jetson Nano [32], Raspberry Pi 4 [38], and Raspberry Pi Zero 2 W [39]. These experiments compared the latency of SNAP with the Original TTA framework, specifically focusing on five state-of-the-art TTA algorithms: Tent [48], EATA [30], SAR [31], RoTTA [53], and CoTTA [50]. The experiments were conducted at an adaptation rate of 0.1, demonstrating the effectiveness of SNAP in reducing adaptation latency while maintaining competitive accuracy. Figure 8 illustrates the latency performance for each device. It is evident

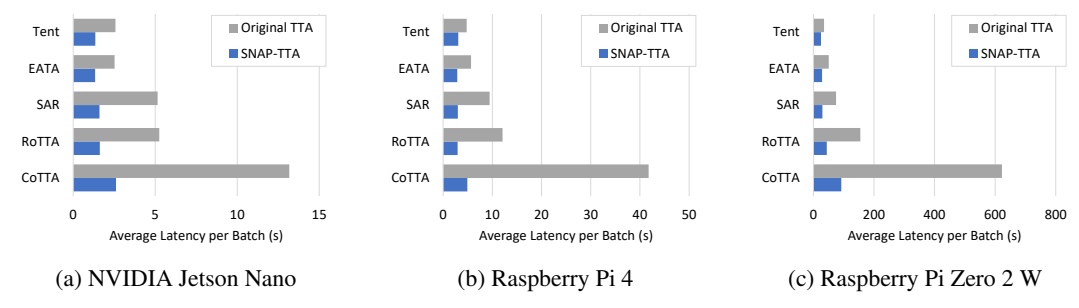


Figure 8: Latency comparison between SNAP-TTA and Original TTA across five state-of-the-art TTA algorithms (Tent, EATA, SAR, RoTTA, CoTTA) on three edge devices: (a) NVIDIA Jetson Nano, (b) Raspberry Pi 4, and (c) Raspberry Pi Zero 2 W. SNAP-TTA demonstrates significant latency reductions while maintaining competitive adaptation performance. The experiments were conducted at an adaptation rate of 0.1.

that SNAP achieves a significant reduction in adaptation latency compared to the Original TTA framework. Notably, the latency reduction was proportional to the adaptation rate, validating the efficiency of SNAP in sparse adaptation scenarios. For instance, the latency for CoTTA was reduced by up to 87.5% on the Raspberry Pi 4, emphasizing the practical benefits of SNAP in latency-sensitive environments. Additionally, similar trends were observed across other devices, including the resource-limited Raspberry Pi Zero 2 W. Since SNAP is hardware-agnostic, accuracy was not measured separately for each device, and no accuracy differences are expected. The results confirm that SNAP not only ensures substantial latency reductions but also adapts effectively to real-world conditions on diverse edge devices, proving its suitability for deployment in latency-sensitive applications.

Table 4: Latency Measurements (AR=1, 0.3, 0.1, 0.05) on Jetson Nano [32].

Methods	AR=1	AR=0.3	AR=0.1	AR=0.05
Tent	2.57	1.97 (-23.51%)	1.35 (-47.62%)	1.19 (-53.75%)
EATA	2.52	1.90 (-24.70%)	1.33 (-47.22%)	1.19 (-52.79%)
SAR	5.15	2.87 (-44.29%)	1.60 (-68.94%)	1.32 (-74.28%)
RoTTA	5.24	2.91 (-44.46%)	1.62 (-69.13%)	1.32 (-74.81%)
CoTTA	13.18	6.13 (-53.46%)	2.61 (-80.22%)	1.82 (-86.19%)

Table 5: Latency Measurements (AR=1, 0.3, 0.1, 0.05) on Raspberry Pi 4 [38].

Methods	AR=1	AR=0.3	AR=0.1	AR=0.05
Tent	4.78	3.54 (-26.09%)	3.09 (-35.45%)	2.35 (-50.87%)
EATA SAR	5.68 9.45	3.52 (-38.00%) 4.88 (-48.34%)	2.87 (-49.45%) 2.98 (-68.41%)	2.31 (-59.28%) 2.54 (-73.16%)
RoTTA	12.07	4.95 (-58.97%)	2.94 (-75.62%)	2.91 (-75.91%)
CoTTA	41.77	11.80 (-71.76%)	4.93 (-88.19%)	3.64 (-91.29%)

Table 6: Latency Measurements (AR=1, 0.3, 0.1, 0.05) on Raspberry Pi Zero 2 W [39].

Methods	AR=1	AR=0.3	AR=0.1	AR=0.05
Tent	34.96	24.67 (-29.42%)	25.06 (-28.32%)	17.07 (-51.16%)
EATA	50.72	27.01 (-46.75%)	28.43 (-43.93%)	17.00 (-66.48%)
SAR	74.64	47.79 (-35.96%)	29.56 (-60.40%)	18.64 (-75.02%)
RoTTA	154.88	86.54 (-44.13%)	44.08 (-71.54%)	22.44 (-85.51%)
CoTTA	622.28	228.03 (-63.36%)	92.01 (-85.21%)	39.22 (-93.70%)

B.7 Memory overhead of SNAP

The SNAP framework achieves substantial latency reduction and accuracy improvements with minimal memory overhead, even under resource-constrained scenarios like edge devices. In this section, we present both a theoretical analysis of the memory requirements and empirical results obtained from evaluations on a Raspberry Pi 4[38] (CPU-only edge device).

The memory overhead of SNAP arises from two main components: (1) the memory buffer in Class and Domain Representative Memory (CnDRM) for storing representative samples, including both feature statistics (mean and variance) and the raw image samples, and (2) the statistics required for Inference-only Batch-aware Memory Normalization (IoBMN). For a batch size B, the total theoretical memory overhead can be expressed as: Memory Overhead $= B \times (\text{Image Size} + 2 \times \text{Feature Dimension} \times \text{Bytes per Value}) + \text{Feature Dimension} \times \text{Bytes per Value} \times 2$. The last term accounts for the storage of IoBMN statistics (mean and variance for each feature channel). The image size is calculated based on the dataset resolution and data type.

For ResNet18 on CIFAR10-C, CIFAR10 images have a resolution of $32 \times 32 \times 3$ with each value stored as 1 byte. For a feature dimension of 512 and batch size B=16, the total overhead is: Image Overhead = $16 \times (32 \times 32 \times 3 \times 1) = 49,152$ bytes (48 KB), Feature Overhead (CnDRM) = $16 \times (512 \times 2 \times 4) = 65,536$ bytes (64 KB), Feature Overhead (IoBMN) = $512 \times 2 \times 4 = 4,096$ bytes (4 KB). Thus, the total memory overhead is: Total Overhead = 48 KB + 64 KB + 4 KB = 116 KB.

For ResNet50 on ImageNet-C, ImageNet images have a resolution of $224 \times 224 \times 3$, stored as 1 byte per value. For a feature dimension of 2048 and batch size B=16, the total overhead is: Image Overhead $=16 \times (224 \times 224 \times 3 \times 1)=12,044,928$ bytes (11.5 MB), Feature Overhead (CnDRM) $=16 \times (2048 \times 2 \times 4)=262,144$ bytes (256 KB), Feature Overhead (IoBMN) $=2048 \times 2 \times 4=16,384$ bytes (16 KB). Thus, the total memory overhead is: Total Overhead =11.5 MB +256 KB +16 KB ≈ 11.77 MB.

Table 7 shows the empirical memory usage of SNAP compared to Original TTA methods (Tent, EATA, CoTTA, SAR, and RoTTA). The results were averaged across three seeds of experiments and represent the memory footprint observed in a CPU-only edge device, Raspberry Pi 4. While minor variations in measurements are expected due to the nature of CPU memory footprint tracking, the results robustly indicate that the actual memory overhead of SNAP on edge devices is extremely low across all algorithms, ranging from 0.02% to 1.74%. Furthermore, while peak memory usage is either slightly increased or remains comparable to Original TTA methods, the average memory usage of SNAP is consistently lower. This is because SNAP performs backpropagation infrequently, which is the most memory-intensive operation in TTA.

Table 7: Comparison of memory usage (Average Memory, Peak Memory, and Memory Overhead) between Original TTA and SNAP (adaptation rate 0.3) across various methods (Tent, EATA, CoTTA, SAR, and RoTTA) tested on Raspberry Pi 4. **Bold** numbers are the lowest memory usage.

27.1.1	Average Mei	n (MB)	Peak Mem	(MB)	Mem Overhead (MB)				
Methods	Original TTA	SNAP	Original TTA	SNAP	SNAP - Original				
Tent	764.24	751.35	822.93	828.46	5.52 (0.67%)				
CoTTA	1133.52	1099.64	1211.21	1227.99	16.78 (1.13%)				
EATA	816.69	749.95	847.73	862.51	14.78 (1.74%)				
SAR	786.65	753.69	863.77	865.18	1.41 (0.02%)				
RoTTA	933.23	871.64	972.23	983.94	11.71 (1.20%)				

These findings demonstrate that **SNAP's memory overhead is negligible compared to its benefits** in latency reduction and accuracy improvements. By leveraging a small memory buffer for representative samples and minimizing backpropagation operations, SNAP not only achieves a lightweight memory profile but also becomes more efficient in terms of average memory usage compared to Original TTA. This lightweight design, combined with its advantages in latency and accuracy, underscores the practicality of SNAP for deployment in latency-sensitive applications on edge devices.

B.8 Integration of SNAP with memory-efficient TTA algorithm

This section evaluates the integration of SNAP with MECTA [12], a memory-efficient TTA algorithm, to demonstrate its applicability for resource-constrained edge devices. The experimental setup follows the evaluation settings presented in the MECTA paper to ensure a fair and consistent comparison. Specifically, we analyze the performance of Tent and EATA, enhanced with MECTA and further integrated with SNAP, using the ResNet50 model with a batch size of 64 on the ImageNet-C dataset.

Table 8 presents the classification accuracy and peak memory usage for Tent+MECTA and EATA+MECTA configurations with and without SNAP. Integrating SNAP with Tent+MECTA improves accuracy from 35.21% to 39.52%, while reducing peak memory usage by approximately 30% compared to the Tent baseline. Similarly, SNAP boosts the accuracy of EATA+MECTA from 35.55% to 42.86% while maintaining an efficient memory footprint.

Table 8: Comparison of classification (%) and memory peak (MB) in STTA with an adaptation rate of 0.1. MECTA significantly reduces memory consumption, and SNAP is applied alongside it to boost the performance of sparse adaptation. The accuracy is the average over 15 corruptions in ImageNet-C. **Bold** numbers indicate either the lowest memory usage or the highest accuracy.

Methods	Accuracy (%)	Max Memory (MB)
Tent	35.21±0.09	6805.26
+MECTA	37.62 ± 0.16	4620.25 (-32.10%)
+ SNAP	39.52 ±0.13	4622.12 (-32.08%)
EATA	35.55±0.19	6541.02
+MECTA	41.41 ± 0.37	4512.38 (-31.01%)
+ SNAP	42.86 ± 0.20	4535.44 (-30.66%)

Further details are provided in Table 9, which evaluates the combination of SNAP with MECTA across various corruption types and adaptation rates (AR = 0.3, 0.1, and 0.05). These results show that SNAP consistently outperforms baseline configurations across all adaptation rates and corruption types. This demonstrates the robustness of SNAP when integrated with MECTA and its suitability for real-world applications.

By adhering to the evaluation settings of the MECTA paper, this study ensures high reliability and comparability of results. The findings confirm that SNAP is highly compatible with MECTA, significantly improving both accuracy and memory efficiency. This synergy highlights the potential of combining SNAP and MECTA for deployment in resource-constrained environments such as edge devices.

Table 9: Evaluation of SNAP with MECTA on ImageNet-C through Adaptation Rates(AR) (0.3, 0.1, and 0.05). **Bold** numbers are the highest accuracy.

AR	Methods	Gau.	Shot	Imp.	Def.	Gla.	Mot.	Zoom	Snow	Fro.	Fog	Brit.	Cont.	Elas.	Pix.	JPEG	Avg.
	Tent + MECTA	28.20 ±0.30	30.13 ±0.41	29.58 ±0.08	23.07 ±0.22	23.35 ±0.47	34.49 ±0.13	45.95 ±0.13	40.97 ±0.15	35.68 ±0.41	55.66 ±0.04	66.56 ±0.06	14.72 ±0.47	53.09 ±0.18	57.16 ±0.05	50.74 ±0.15	39.29 ±0.22
0.3	+ SNAP	30.49 ±0.26	31.98 ±0.14	31.66 ±0.21	26.29 ±0.32	26.19 ±0.02	38.47 ±0.30	47.38 ±0.11	43.79 ±0.11	40.12 ±0.12	56.38 ±0.05	66.81 ±0.07	28.87 ±0.28	53.53 ±0.09	57.61 ±0.10	50.86 ±0.08	42.03 ±0.15
0.3	EATA + MECTA	32.18 ±0.60	34.85 ±0.49	33.06 ±0.31	28.80 ±0.22	29.18 ±0.18	41.02 ±0.26	49.24 ±0.08	47.10 ±0.20	41.56 ±0.25	57.35 ±0.12	66.27 ±0.05	34.56 ±0.12	55.38 ±0.10	58.19 ±0.04	52.87 ±0.26	44.11 ±0.22
	+ SNAP	33.67 ±0.19	35.76 ±0.24	34.86 ±0.10	30.35 ±0.11	30.29 ±0.04	42.78 ±0.06	49.55 ±0.10	47.46 ±0.10	42.32 ±0.05	57.50 ±0.15	66.18 ±0.06	39.08 ±0.81	55.38 ±0.16	58.35 ±0.12	52.72 ±0.02	45.08 ±0.15
	Tent + MECTA	24.94 ±0.15	26.73 ±0.20	25.63 ±0.07	21.11 ±0.22	21.46 ±0.18	32.11 ±0.02	44.05 ±0.19	38.22 ±0.27	36.36 ±0.09	53.92 ±0.12	66.48 ±0.02	18.50 ±0.45	50.80 ±0.12	55.67 ±0.18	48.33 ±0.11	37.62 ±0.16
0.1	+ SNAP	27.49 ±0.08	28.90 ±0.14	28.26 ±0.16	23.49 ±0.17	23.76 ±0.12	34.92 ±0.06	45.18 ±0.13	40.21 ±0.09	38.40 ±0.18	53.78 ±0.14	66.54 ±0.03	27.72 ±0.20	51.00 ±0.20	55.48 ±0.13	47.61 ±0.17	39.52 ±0.13
0.1	EATA + MECTA	29.42 ±0.67	31.72 ±0.30	29.44 ±0.32	24.41 ±0.74	25.48 ±0.45	37.04 ±0.18	47.10 ±0.15	43.60 ±0.19	39.43 ±0.38	55.95 ±0.13	66.42 ±0.14	28.85 ±1.18	53.70 ±0.15	57.34 ±0.15	51.20 ±0.36	41.41 ±0.37
	+ SNAP	31.26 ±0.11	32.71 ±0.17	32.22 ±0.17	27.31 ±0.46	27.61 ±0.28	38.88 ±0.28	47.83 ±0.09	44.52 ±0.14	40.58 ±0.05	56.42 ±0.06	66.24 ±0.21	35.38 ±0.63	53.67 ±0.17	57.39 ±0.13	50.83 ±0.12	42.86 ±0.20
	Tent + MECTA	21.22 ±0.13	23.19 ±0.22	21.90 ±0.13	18.69 ±0.18	19.39 ±0.20	29.89 ±0.13	42.02 ±0.10	36.53 ±0.22	35.23 ±0.05	51.75 ±0.15	66.23 ±0.04	19.64 ±0.27	48.43 ±0.03	53.54 ±0.13	45.43 ±0.11	35.54 ±0.14
0.05	+ SNAP	23.93 ±0.27	25.37 ±0.22	24.10 ±0.15	20.42 ±0.18	21.14 ±0.07	31.83 ±0.06	42.68 ±0.04	37.53 ±0.16	36.31 ±0.20	51.42 ±0.17	66.19 ±0.04	23.84 ±0.24	48.62 ±0.05	53.20 ±0.17	44.57 ±0.17	36.74 ±0.15
0.05	EATA + MECTA	24.97 ±0.42	26.95 ±0.27	21.87 ±3.29	21.19 ±0.90	21.94 ±0.45	33.61 ±0.08	45.11 ±0.11	40.92 ±0.19	37.73 ±0.42	54.64 ±0.10	66.60 ±0.07	23.03 ±0.59	51.87 ±0.35	56.60 ±0.25	49.15 ±0.23	38.41 ±0.51
	+ SNAP	28.39 ±0.57	30.10 ±0.38	29.45 ±0.22	24.32 ±0.20	25.12 ±0.07	35.54 ±0.20	46.04 ±0.27	41.87 ±0.07	39.16 ±0.15	55.12 ±0.01	66.61 ±0.09	30.34 ±0.34	52.06 ±0.24	56.42 ±0.11	49.11 ±0.07	40.64 ±0.20

Table 10: Classification accuracy (%) on ImageNet-C through SNAP (AR=0.1) using ViT-Base [4].

Method	Gau.	Shot	Imp.	Def.	Gla.	Mot.	Zoom	Snow	Fro.	Fog	Brit.	Cont.	Elas.	Pix.	JPEG	Avg.
Tent	40.56	41.30	41.69	35.76	31.81	42.01	38.02	44.33	53.53	20.69	72.41	30.42	45.87	51.95	56.11	43.10
Tent	± 0.11	± 0.28	± 0.22	± 0.15	± 0.07	± 0.26	± 0.13	± 0.18	± 0.06	± 0.25	± 0.14	± 0.21	± 0.17	± 0.12	± 0.29	± 0.19
+ SNAP	40.98	41.72	42.18	37.16	32.30	42.89	38.44	46.19	52.50	53.11	72.25	39.25	46.77	51.53	55.99	46.22
TOMAI	± 0.08	± 0.24	± 0.19	± 0.06	± 0.27	± 0.15	± 0.13	± 0.23	± 0.29	± 0.18	± 0.12	± 0.26	± 0.14	± 0.11	± 0.22	± 0.09
CoTTA	20.05	17.12	20.43	20.06	16.62	12.87	14.50	9.68	28.31	16.01	35.79	1.96	15.60	12.09	15.99	17.14
COLIA	± 0.16	± 0.20	± 0.21	± 0.14	± 0.25	± 0.13	± 0.12	± 0.23	± 0.27	± 0.19	± 0.20	± 0.11	± 0.22	± 0.29	± 0.17	± 0.18
+ SNAP	34.85	33.35	36.21	31.54	25.77	35.57	32.96	42.23	55.10	51.63	71.72	5.86	42.18	39.96	52.27	39.41
+ SNAF	± 0.13	± 0.22	± 0.28	± 0.18	± 0.06	± 0.24	± 0.11	± 0.25	± 0.07	± 0.27	± 0.16	± 0.29	± 0.08	± 0.19	± 0.21	± 0.13
EATA	20.12	21.52	21.40	20.90	23.42	15.71	18.00	16.12	28.35	22.24	35.97	11.33	19.78	20.22	19.99	21.00
EAIA	± 0.14	± 0.17	± 0.21	± 0.09	± 0.20	± 0.10	± 0.27	± 0.11	± 0.24	± 0.16	± 0.22	± 0.15	± 0.29	± 0.18	± 0.23	± 0.12
+ SNAP	40.74	43.22	43.11	40.63	44.59	51.58	50.63	54.77	58.32	61.50	73.91	33.85	60.19	63.35	63.01	52.23
+ SNAF	± 0.15	± 0.19	± 0.13	± 0.27	± 0.11	± 0.21	± 0.18	± 0.12	± 0.25	± 0.20	± 0.14	± 0.29	± 0.10	± 0.17	± 0.23	± 0.13
RoTTA	21.44	18.64	22.08	19.97	16.87	13.70	14.42	15.73	28.57	17.71	35.05	8.52	15.80	13.03	13.27	18.32
KOTTA	± 0.14	± 0.21	± 0.13	± 0.18	± 0.22	± 0.09	± 0.27	± 0.15	± 0.19	± 0.24	± 0.26	± 0.13	± 0.20	± 0.11	± 0.25	± 0.10
+ SNAP	35.68	34.60	36.86	31.20	25.81	36.24	33.47	42.72	55.50	51.74	71.84	17.84	42.86	42.24	52.67	40.75
+ SNAP	± 0.16	± 0.17	± 0.21	± 0.13	± 0.23	± 0.09	± 0.26	± 0.12	± 0.27	± 0.18	± 0.15	± 0.29	± 0.14	± 0.10	± 0.24	± 0.11

Table 11: SNAP accuracy and latency per batch, using Vit-Base [4]. Performance averaged over ImageNet-C. Values in parentheses show the performance difference from full adaptation.

Methods	Acc	curacy (%)	Latency per batch (s)						
Methods	Original TTA	SNAP (AR=0.1)	Original TTA	SNAP (AR=0.1)					
Tent	39.53 ±0.14	46.22 ±0.13 (+6.69)	28.19 ± 0.08	15.66 ±0.06 (-44.43%)					
CoTTA	41.25 ± 0.12	$39.41 \pm 0.15 (-1.83)$	523.26 ± 0.27	$182.20 \pm 0.18 (-65.18\%)$					
EATA	48.43 ± 0.11	52.23 ±0.13 (+3.79)	28.69 ± 0.07	$16.44 \pm 0.06 (-42.71\%)$					
SAR	43.86 ± 0.13	47.77 ±0.12 (+3.91)	44.28 ± 0.09	$17.76 \pm 0.07 (-59.90\%)$					
RoTTA	42.93 ± 0.15	$40.75 \pm 0.14 \; (\text{-}2.18)$	42.70 ± 0.10	$16.28 \pm 0.08 \; (\text{-}61.88\%)$					

B.9 Modification for layer normalization of Vision Transformer

The main text describes the use of Batch Normalization (BN) statistics for calculating domain centroids and centroid-instance distances, with subsequent adjustment of memory statistics to match the target test batch using the Inference-only Batch-aware Memory Normalization (IoBMN) method. Specifically, these calculations leverage the mean and variance across batches as follows:

$$\bar{\mu}_c = \frac{1}{B \times L} \sum_{b=1}^{B} \sum_{l=1}^{L} f_{b,c,l}, \quad \bar{\sigma}_c^2 = \frac{1}{B \times L} \sum_{b=1}^{B} \sum_{l=1}^{L} (f_{b,c,l} - \mu_{b,c})^2, \tag{13}$$

where B represents the batch size, L the number of spatial locations, and c the channel index.

However, modern models like Vision Transformer (ViT) utilize Layer Normalization (LN) instead of BN. Unlike BN, which calculates statistics across the entire batch, LN normalizes each instance independently by using the statistics calculated over individual feature dimensions. Specifically, for a feature vector \mathbf{f}_b belonging to the b-th instance, LN computes:

$$\mu_b = \frac{1}{C} \sum_{c=1}^{C} f_{b,c}, \quad \sigma_b^2 = \frac{1}{C} \sum_{c=1}^{C} (f_{b,c} - \mu_b)^2,$$
 (14)

where C is the number of channels. This difference implies that LN operates without batch-level interactions, focusing solely on within-instance normalization, which makes the method inherently more suitable for handling variable batch sizes, particularly in latency-sensitive applications like those considered in our Test-Time Adaptation (TTA) setting.

Despite the differences between BN and LN, the fundamental mechanism of using feature statistics to capture domain information remains valid. The key domain characteristics in early layer features are preserved in both normalization types, enabling the construction of a domain centroid that reflects the distributional characteristics of the test data. For LN, this centroid can be computed by aggregating across instances instead of across batches:

$$\bar{\mu}_c^{\text{LN}} = \frac{1}{M} \sum_{b=1}^{M} \mu_b, \quad \bar{\sigma}_c^{2\text{LN}} = \frac{1}{M} \sum_{b=1}^{M} \sigma_b^2,$$
 (15)

where M is memory capacity. This modified approach allows the domain centroid to still represent the overall domain-specific characteristics effectively, despite the lack of direct batch-level statistics.

Furthermore, this methodology extends seamlessly to other normalization layers, such as Group Normalization (GN). In GN, the statistics are computed across smaller groups of channels within

each instance, but the procedure for aggregating these statistics to form a domain centroid remains the same—by averaging the group-level statistics across instances.

To maintain the core concept of selecting domain-representative samples with minimal modifications, we continue to use the memory of high-confidence domain-representative samples in the Inference-only Batch-aware Memory Normalization (IoBMN) strategy. The adjustment for LN requires: 1. Calculating LN-specific centroids as described in Equation 15. 2. Replacing BN statistics with LN statistics in the IoBMN module, thereby aligning the feature normalization during inference with the domain-representative information derived from memory.

The effectiveness of this modification was validated experimentally, as shown in Table 10, 11, where ViT models using LN showed improved performance even under sparse TTA conditions. This indicates that, with minimal adjustments, SNAP remains effective for ViT with LN. The core principle of utilizing domain-representative statistics for aligning test-time feature distributions continues to provide significant benefits, ensuring robust adaptation in shifting domains with limited latency and computational overhead.

B.10 Comparison with forward-only TTA methods

Forward-only TTA methods, such as T3A [13] and FOA [29], aim to reduce computational burden by removing gradient-based updates. Instead, they update lightweight components: class prototypes in T3A and learned prompts in FOA. While these methods improve runtime efficiency, they exhibit structural limitations that hinder their robustness under dynamic distribution shifts.

Table 12: Performance comparison between T3A [13] and FOA [29] against Tent [48] + SNAP (adaptation rate 0.1) on ImageNet-C (i.i.d and non-i.i.d). Latency is measured on Raspberry Pi 4.

` I				_							•							
Dataset	Method	Gau.	Shot	Imp.	Def.	Gla.	Mot.	Zoom	Snow	Fro.	Fog	Brit.	Cont.	Elas.	Pix.	JPEG	Avg.	Lat.(s)
									ResNet5	0								
	T3A	14.03	14.21	14.56	12.97	13.07	23.02	34.67	30.79	27.84	43.95	61.51	12.57	39.79	44.50	36.11	28.24	18.35
	13A	±0.09	±0.43	±0.07	±0.18	±0.06	±0.21	±1.17	±0.15	±0.29	±0.06	±0.22	±0.91	±0.19	±1.46	±0.51	±0.39	±0.59
	Tent+SNAP	26.21	27.85	27.50	23.62	22.73	36.01	44.11	42.19	38.15	52.95	64.57	30.23	48.56	53.71	47.09	39.03	18.76
	Tellersival	±0.14	±0.19	±0.16	±0.10	±0.15	±0.23	±0.17	±0.12	±0.21	±0.18	±0.11	±0.27	±0.15	±0.13	±0.26	±0.19	±0.30
ImageNet-C									ViT-Bas									
(i.i.d)	FOA (K=28)	41.34	40.96	42.68	36.27	29.94	40.34	40.89	47.20	59.07	63.71	72.95	46.98	44.75	45.40	55.87	47.22	694.8
		±0.21	±0.39	±0.20	±0.06	±0.27	±0.34	±0.35	±2.03	±1.56	±0.14	±0.07	±0.12	±0.14	±0.38	±0.38	±0.51	±8.41
	FOA (K=2)	37.53	35.84	39.36	34.25	27.45	37.85	34.43	43.65	56.10	62.84	71.79	39.38	44.29	41.33	53.06	43.94	81.43
	/	±0.30	±0.12	±0.03	±0.27	±0.16	±0.10	±0.12	±0.06	±0.11	±0.19	±0.04	±0.68	±0.18	±0.09	±0.05	±0.37	±4.12
	Tent+SNAP	41.98 ±0.12	42.72 ±0.22	43.18 ±0.13	38.16 ±0.11	33.30 ±0.13	43.89 ±0.21	39.44 ±0.18	47.19 ±0.09	53.50 ±0.18	54.11 ±0.20	73.25 ±0.08	40.25 ±0.25	47.77 ±0.17	52.53 ±0.12	56.99 ±0.24	47.23	83.51 ±0.32
		±0.12	±0.22	±0.13	±0.11	±0.13	±0.21	±0.18	±0.09	±0.18	±0.20	±0.08	±0.23	±0.17	±0.12	±0.24	±0.16	±0.32
									ResNet5	0								
	T3A	11.75	11.94	11.44	11.30	10.98	19.98	31.30	27.16	24.51	38.35	56.31	10.89	37.41	42.95	32.52	25.25	18.82
	13/4	±0.10	±0.38	±0.06	±0.22	±0.05	±0.17	±1.34	±0.12	±0.27	±0.07	±0.18	±1.02	±0.23	±1.39	±0.49	±0.42	±0.57
	Tent+SNAP	24.00	24.69	24.78	21.37	21.15	32.20	42.83	39.26	35.41	51.17	62.89	21.25	46.95	52.31	45.60	36.39	18.98
	10111011111	±0.11	±0.25	±0.14	±0.13	±0.12	±0.19	±0.22	±0.10	±0.16	±0.24	±0.09	±0.28	±0.18	±0.15	±0.23	±0.14	±0.29
ImageNet-C									ViT-Bas									
(non-i.i.d)	FOA (K=28)	38.36	36.23	39.47	33.07	25.35	36.44	35.80	42.86	55.45	61.67	70.60	39.87	41.81	43.05	52.42	43.50	710.2
		±0.11	±0.41	±0.05	±0.20	±0.04	±0.19	±1.26	±0.14	±0.24	±0.08	±0.19	±0.96	±0.20	±1.43	±0.54	±0.40	±7.33
	FOA (K=2)	35.84	33.74	36.03	30.48	23.24	34.34	32.03	40.98	53.98	59.78	68.24	29.79	39.50	39.50	50.80	40.62	85.19
		±0.17 38.02	±0.00	±0.81	±0.09	±0.04	±0.04 40.17	±0.06	±0.06	±0.07	±0.09 52.01	±0.04 73.19	±0.22 24.68	±0.03 45.64	±0.07	±0.10	±0.13 43.81	±5.84
	Tent+SNAP		38.31	40.22	35.37	30.20		37.20	44.57	54.78					47.08	55.66		87.54
		±0.73	±0.50	±0.83	±0.11	±0.60	±0.48	±0.35	±0.54	±0.27	±0.77	±0.22	±0.32	±0.47	±0.81	±0.83	±0.52	±0.51

Prototype-based. T3A maintains a fixed feature extractor and updates per-class prototypes using pseudo-labels from incoming samples. Although it avoids backpropagation, T3A accumulates a growing support set of query features per pseudo-label to refine class-wise prototypes. This not only increases memory usage, but also incurs non-negligible latency during inference, especially when the number of classes is large (e.g., 1000-way classification in ImageNet) or when operating on edge devices. Matching a test sample against all stored support features becomes increasingly costly in such settings. As shown in Table 12, T3A achieves latency comparable to Tent+SNAP but consistently performs worse in accuracy, especially under non-i.i.d. ImageNet-C streams. This illustrates the limitation of relying solely on forward-only label-space correction without feature-level adaptation.

Prompt-based. FOA [29] introduces learnable prompts to adapt ViT encoders without backpropagation. However, it suffers from a trade-off between latency and accuracy, which is determined by the number of forward passes (K) required per test sample. While FOA theoretically avoids gradients, it performs K repeated forward steps to refine prompts, still incurring notable cost on edge devices. As shown in Table 12, FOA with its default configuration (K = 28) incurs significantly higher latency than Tent+SNAP, while achieving similar accuracy. Reducing K to 2 reduces latency to a comparable level, but results in substantial performance degradation, showing strong sensitivity to prompt update

depth. Moreover, FOA fails to generalize to CNNs, where the original paper [29] reports lower performance than Tent due to structural misalignment with the ViT-specific prompt.

Conclusion. In contrast, SNAP with Tent performs sparse backpropagation on confidently selected samples, striking a balance between low latency and high robustness. Despite using gradients, our latency profiling shows that Tent+SNAP remains within the latency range of forward-only methods, while outperforming them in accuracy across both i.i.d. and non-i.i.d. domains. This demonstrates the efficacy of targeted feature-level adaptation over purely forward-only correction.

B.11 Robustness in challenging out-of-distribution domains

To validate SNAP under more visually challenging and abstract domain shifts, we additionally apply SNAP to two nontrivial out-of-distribution datasets: **ImageNet-R** and **ImageNet-Sketch**. These datasets feature semantic deformation (R), sketch-style abstraction (Sketch), and both differ significantly from typical texture- and structure-rich natural images seen in ImageNet.

We test SNAP with an adaptation rate (AR) of AR=0.1 on five representative TTA backbones (Tent, CoTTA, EATA, SAR, and RoTTA) and compare results with full adaptation (AR=1.0). As summarized in Table 13, SNAP consistently maintains competitive performance with considerably reduced latency, demonstrating its suitability for low-overhead deployment under difficult real-world shifts.

Table 13: Performance of SNAP (AR=0.1) on ImageNet-R and ImageNet-Sketch. Accuracy and latency are reported as the mean \pm standard deviation over 3 seeds (0, 1, 2). Latency is measured by Raspberry Pi 4.

Method	Image	eNet-R	ImageNet-Sketch					
Wiethou	Accuracy (%)	Latency (s)	Accuracy (%)	Latency (s)				
Tent (Full)	40.53 ± 0.22	34.30 ± 0.06	28.43 ± 0.18	38.12 ± 0.05				
+ SNAP (AR=0.1)	38.26 ± 0.20	17.73 ± 0.05	28.42 ± 0.16	18.50 ± 0.11				
CoTTA (Full)	37.53 ± 0.25	295.19 ± 0.07	24.07 ± 0.19	302.80 ± 0.12				
+ SNAP (AR=0.1)	36.73 ± 0.21	150.40 ± 0.06	23.01 ± 0.19	158.32 ± 0.21				
EATA (Full)	42.88 ± 0.18	29.22 ± 0.02	30.52 ± 0.20	32.99 ± 0.08				
+ SNAP (AR=0.1)	39.45 ± 0.17	15.50 ± 0.08	27.43 ± 0.18	17.53 ± 0.23				
SAR (Full)	40.37 ± 0.22	72.51 ± 0.05	27.03 ± 0.19	76.37 ± 0.05				
+ SNAP (AR=0.1)	37.32 ± 0.20	19.59 ± 0.06	27.95 ± 0.17	22.52 ± 0.06				
RoTTA (Full)	39.08 ± 0.21	78.05 ± 0.09	26.05 ± 0.16	84.98 ± 0.06				
+ SNAP (AR=0.1)	36.79 ± 0.19	41.15 ± 0.06	24.08 ± 0.15	49.33 ± 0.16				

B.12 Efficient strategy for re-calculation of sample's distance

The domain centroid in our framework is updated using a momentum-based approach to effectively capture recent shifts in the target domain. This ensures that the centroid remains adaptive to evolving distributions without being overly influenced by temporary fluctuations. However, during sparse adaptation (SA), where model updates occur at extended intervals, the data distribution can shift substantially between updates. Consequently, distances calculated for older samples may become outdated, leading to inconsistencies when comparing them to more recently added samples that are evaluated based on the updated centroid.

To address this issue efficiently, our Class and Domain Representative Memory (CnDRM) recalculates the distance of samples only when the shift in the domain centroid exceeds a predefined significance threshold. Specifically, if the change in the domain centroid Δc_{domain} surpasses a threshold τ_{Δ} , the distances of all samples in memory are updated to reflect the new domain conditions. This threshold-based approach ensures that recalculations occur only when necessary, thereby minimizing computational costs while maintaining the representativeness of the memory.

In practice, we observed that the performance was not significantly affected as long as the threshold τ_{Δ} was not set too high, indicating robustness to the choice of threshold. Based on these observations, we set $\tau_{\Delta}=0.1$ and used this value consistently for all evaluations. By focusing recalculations on significant shifts, this strategy preserves consistency in sample selection, ensuring that both older and newer samples are compared fairly in the context of the current domain characteristics without excessive computational overhead.

B.13 Strategy for continuous domain shift setting

In our proposed framework, the centroid used for selecting domain-representative samples naturally adapts to changes in the domain as new data is encountered. This mechanism inherently ensures that the centroid evolves to reflect the characteristics of the current domain, allowing for effective performance even under continual Test-Time Adaptation (TTA) scenarios, where the domain may gradually or abruptly shift during adaptation.

Instead of employing additional mechanisms like z-score evaluation to detect domain shifts, we rely on the natural adaptability of the centroid to adjust to the incoming data. This simplifies the design and avoids unnecessary overhead while maintaining robustness. As the domain characteristics evolve, the centroid continuously aligns with the new domain without requiring explicit detection of changes or manual intervention.

To validate the effectiveness of SNAP under continual domain shift scenarios, we conducted experiments across various benchmark datasets with incremental and abrupt domain shifts. Table 14 summarizes the results, demonstrating that SNAP maintains strong performance across evolving domains without requiring additional computational overhead for explicit domain shift detection.

These results indicate that SNAP effectively handles both incremental and abrupt domain shifts, consistently outperforming baseline methods. By leveraging the natural adaptability of the centroid, SNAP provides a robust solution for continual domain adaptation in real-world scenarios. Notably, SNAP mitigates catastrophic forgetting not only through its sparse adaptation strategy but also by leveraging domain centroid-based sampling, allowing performance to be sustained longer in continual shift scenarios. Unlike Tent, CoTTA is specifically designed for continual domain shift environments, which highlights its superior performance under such conditions.

Future work could explore augmenting this adaptive mechanism by incorporating techniques like z-score evaluation to enable even more responsive adjustments. For instance, a z-score-based approach could further refine the centroid's responsiveness to subtle, gradual domain shifts by monitoring discrepancies between incoming data statistics and the current centroid. Such enhancements could make the system even more effective at handling continual domain evolution, particularly in scenarios with complex or noisy data streams.

Table 14: Performance of SNAP under continual domain shift scenarios. The table reports the accuracy (%) for different datasets with incremental and abrupt shifts. **Bold** numbers are the highest accuracy.

AR	Method	Gau.	Shot	Imp.	Def.	Gla.	Mot.	Zoom	Snow	Fro.	Fog	Brit.	Cont.	Elas.	Pix.	JPEG	Avg.
	Tent	24.68	19.65	5.12	0.63	0.43	0.40	0.44	0.41	0.30	0.33	0.42	0.24	0.32	0.31	0.31	3.60
	Tent	± 0.45	± 1.27	± 1.22	± 0.05	± 0.02	± 0.04	± 0.06	± 0.03	± 0.03	± 0.04	± 0.05	± 0.04	± 0.02	± 0.05	± 0.04	± 0.23
	+ SNAP	28.71	30.60	22.91	6.13	1.62	0.87	0.88	0.64	0.64	0.66	0.75	0.44	0.60	0.63	0.61	6.45
0.1	+ SNAF	±0.66	±1.82	±2.25	±0.90	± 0.20	±0.13	± 0.07	±0.08	± 0.06	±0.05	± 0.01	±0.05	±0.08	± 0.07	± 0.07	±0.43
0.1	CoTTA	10.99	12.21	11.54	11.28	11.13	22.08	34.80	30.69	29.45	43.87	61.92	12.76	40.03	44.99	36.43	27.61
	COLIA	± 0.40	±0.04	±0.30	±0.13	± 0.15	±0.07	± 0.18	±0.10	± 0.04	±0.19	±0.09	±0.16	± 0.13	± 0.14	±0.16	±0.15
	CNIAD	15.19	15.97	15.91	13.94	14.18	24.76	36.50	32.61	31.76	46.14	63.60	15.60	42.17	46.77	38.08	30.21
	+ SNAP	±0.17	±0.11	±0.02	±0.04	±0.03	±0.07	±0.23	±0.04	±0.06	±0.10	±0.14	±0.04	±0.02	±0.06	±0.12	±0.08
	Tent	23.31	27.08	22.71	9.72	4.14	2.03	1.16	0.66	0.45	0.47	0.61	0.33	0.47	0.47	0.46	6.27
	Tent	± 0.37	± 1.13	± 2.50	± 3.35	± 3.00	±1.53	± 0.75	± 0.22	± 0.12	± 0.09	± 0.16	±0.09	± 0.08	± 0.08	± 0.07	± 0.90
	+ SNAP	27.10	33.41	31.78	19.85	16.94	14.75	12.46	5.53	2.69	1.47	1.52	0.67	0.88	0.89	0.84	11.39
0.05	+ SNAP	±0.23	±0.10	±0.62	±0.79	±1.50	±2.53	±4.27	±2.30	±1.18	±0.49	± 0.40	±0.09	±0.10	± 0.10	± 0.07	±0.98
0.05	C TTL	11.04	12.25	11.73	11.62	11.25	22.05	34.89	30.73	29.50	44.09	61.87	12.87	40.15	45.06	36.53	27.71
	CoTTA	± 0.38	±0.39	± 0.42	±0.10	±0.59	±0.13	± 0.13	±0.20	± 0.17	± 0.18	±0.09	±0.18	±0.17	±0.19	± 0.14	±0.23
	+ SNAP	15.20	15.89	15.93	13.81	14.15	24.74	36.68	32.51	31.71	46.11	63.48	15.73	42.20	46.69	38.05	30.19
	TONAL	±0.15	± 0.02	± 0.10	± 0.04	±0.03	±0.16	± 0.27	± 0.04	± 0.20	±0.05	±0.09	±0.19	± 0.12	± 0.10	± 0.04	±0.10

B.14 Robustness under persistent distribution shifts

To evaluate the long-term stability of SNAP under temporally correlated and recurring domain shifts, we adopt the evaluation setup (persist-TTA) of work [11], which repeatedly cycles through non-i.i.d. CIFAR10-C corruptions across 10 rounds. This scenario emulates continual adaptation in environments where domain drift is both persistent and revisited.

We apply SNAP on top of CoTTA [50], a method specifically designed for continual test-time adaptation. While CoTTA alone initially performs well, we observe a steady degradation across rounds as it accumulates shift-induced bias and overfits to recent domains. In contrast, combining

CoTTA with SNAP enables the model to preserve robust performance even after multiple adaptation cycles.

The key to this stability lies in SNAP's architecture: (1) class-balanced memory to prevent label bias, (2) sparse but confident updates to mitigate overfitting, (3) IoBMN for adapting normalization statistics to each incoming sample, and (4) exponential moving average (EMA) domain centroids to smooth domain shift tracking. These collectively stabilize long-term adaptation dynamics without the need for explicit shift detection.

Table 15: Long-term TTA accuracy, cycling through all CIFAR10-C corruptions each round (R).

Method	$R1 \Longrightarrow$	$R2 \Longrightarrow$	R3 ⇒	R4>	R5 ⇒	R6 ⇒	R7 ⇒	R8 ⇒	R9 ⇒	R10
CoTTA (Full adapt)	58.49 ±0.12	50.32 ±0.09	48.71 ± 0.15	44.92 ±0.10	31.86 ±0.17	29.81 ±0.13	25.39 ±0.16	21.43 ±0.11	28.46 ± 0.18	16.97 ±0.14
+ SNAP (AR=0.1)	50.50 ± 0.10	49.32 ± 0.08	52.57 ±0.11	49.90 ±0.09	50.17 ±0.12	50.58 ±0.14	49.01 ±0.07	49.56 ±0.13	54.16 ±0.10	52.89 ± 0.09

Experimental results. Table 15 and Figure 9 shows adaptation accuracy over 10 rounds. While CoTTA gradually collapses after the 5th round, integration with SNAP maintains accuracy above 50%, showing clear stability under persistent shifts.

These results confirm that SNAP enhances long-term TTA robustness by stabilizing both parameter and feature statistics over time. This makes it a reliable plug-in module for continual test-time adaptation pipelines.

B.15 Robustness in single-sample (BS=1) adaptation scenario

To investigate the robustness of SNAP when adaptation is performed on a per-sample basis, we evaluate its performance in a single-sample adaptation setting, where the adaptation batch size is limited to 1. This scenario reflects highly constrained edge environments with limited memory or streaming inputs, where adaptation must occur with minimal latency and granularity.

To support this setup, we adopt the SAR [31] architecture, which natively supports a batch size of 1 and sparse update routines. SAR allows us to test SNAP with an adaptation rate of 0.1, meaning only one in every ten test samples is used for weight updates, using a single memory sample.

Table 16: Evaluation of SNAP (AR=0.1) with SAR on a single-sample (BS=1) adaptation scenario on ImageNet-C. Results are averaged over 3 random seeds (0, 1, 2).

Method	Accuracy (%)
SAR (single-sample)	52.21 ± 0.28
+ STTA	8.06 ± 0.12
+ SNAP	51.80 ± 0.25

SNAP achieves strong gains even when adapting from just one memory sample. When only one sample is used for adaptation, our method still selects the representative sample with high prediction confidence and low Wasserstein distance to the domain centroid, enabling stable model updates.

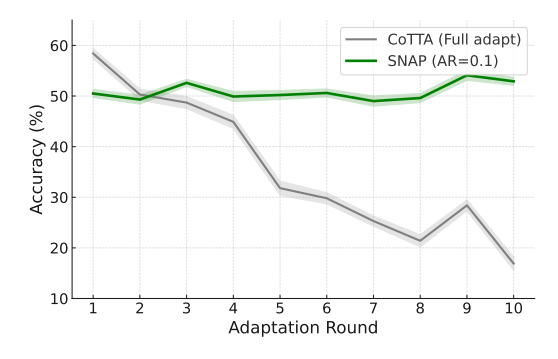


Figure 9: Long-term TTA accuracy over 10 adaptation rounds. Shaded regions indicate std over 3 seeds. SNAP maintains stable performance, while original CoTTA alone degrades over time.

Meanwhile, IoBMN continues to apply adaptive normalization to every incoming test sample, mitigating covariate shift even when parameter updates are sparse. Although small batches can slow the class distribution balancing process and moving domain centroid updates under skewed domains, we found that this effect has limited influence on overall adaptation performance and stability.

Evaluation protocol. We average performance over three random seeds (0, 1, 2) to ensure stability across different data orderings. Table 16 reports both the mean and standard deviation of accuracy.

These results demonstrate that SNAP preserves its robustness and sample-wise adaptability even under minimal adaptation frequency and granularity. CnDRM identifies meaningful memory samples, while IoBMN provides per-sample normalization, together enabling consistent performance in BS=1 settings.

B.16 Impact of memory size on SNAP performance

The memory size of the Class and Domain Representative Memory (CnDRM) in SNAP has implications for both performance and privacy. Increasing memory size allows storing more samples, which intuitively could improve adaptation. However, such an approach raises privacy concerns and needs additional memory and latency when storing sensitive samples. To evaluate the trade-off, we conducted experiments on ImageNet-C under Gaussian noise corruption, using Tent + SNAP(adaptation rate 0.3) with a batch size of 16 and varying the memory size.

As shown in Table 17, increasing the memory size beyond the base configuration of 16 does not lead to significant performance gains. This observation highlights the efficiency of SNAP's representative sampling strategy, which prioritizes storing samples based on proximity to class and domain centroids. The saturation in accuracy suggests that a carefully aligned memory size to the batch size is sufficient to balance computational efficiency, performance, and privacy considerations.

Table 17: Performance comparison with varying memory sizes on ImageNet-C.

Memory Size	Accuracy (%)
16 (Base)	26.60 ± 0.11
32	28.44 ± 0.17
64	28.89 ± 0.06
128	28.60 ± 0.09

In conclusion, to minimize computational overhead while ensuring robust test-time adaptation, the memory size in SNAP is designed to align with the batch size. This configuration addresses privacy and memory overhead risks by limiting the number of stored samples without compromising adaptation effectiveness.

B.17 Effect of learning rate on sparse and full adaptation

To investigate the impact of learning rates on the performance of SNAP and baseline methods, we conducted experiments under sparse adaptation settings. Initially, the same learning rate was applied for each SOTA TTA algorithms across all adaptation rates to ensure fair comparisons (Table 26, 27, 22, 23, 24,and 25). However, as sparse adaptation inherently limits the number of updates, the updates might be insufficient at lower adaptation rates and explored the effect of increasing the learning rate.

The results, summarized in Table 18, 19, and 20, reveal that higher learning rates improve the accuracy of both the naive baseline and SNAP under sparse settings. Notably, while the naive TTA baseline benefits from a higher learning rate, its performance still falls short of that achieved with full adaptation. In contrast, SNAP surpasses the performance of full adaptation at optimal learning rates, demonstrating its ability to leverage sparse adaptation effectively. At the same time, applying these higher learning rates to full adaptation results in model instability and collapse, underscoring the need to carefully tune learning rates based on adaptation frequency. Therefore, we selected a stable learning rate of 1×10^{-4} for the evaluations in our work that balances model convergence and performance across all adaptation rates. These findings suggest that SNAP not only adapts effectively under sparse settings but also maintains robustness under optimized learning rates.

Table 18: Accuracy with varying learning rates on ImageNet-C Gaussian noise adaptation rate 0.5. **Bold** numbers are the highest accuracy.

		Tent			CoTTA			EATA	
Learning rate	Full	naïve STTA	SNAP	Full	naïve STTA	SNAP	Full	naïve STTA	SNAP
2×10^{-3}	2.31 ±0.08	4.16 ±0.12	6.68 ±0.14	13.31 ±0.10	12.03 ±0.09	14.58 ±0.11	0.36 ±0.05	0.48 ±0.07	0.69 ±0.06
1×10^{-3}	4.54 ± 0.11	10.19 ± 0.14	16.37 ± 0.09	13.18 ±0.13	11.98 ± 0.08	14.63 ± 0.12	1.31 ± 0.06	1.36 ± 0.05	22.11 ± 0.15
5×10^{-4}	10.22 ± 0.12	18.43 ± 0.13	28.36 ±0.10	13.15 ±0.09	11.95 ± 0.07	15.17 ±0.11	21.96 ± 0.14	13.97 ± 0.12	25.42 ± 0.13
1×10^{-4}	27.03 ± 0.13	25.24 ± 0.10	28.05 ± 0.09	13.12 ±0.10	11.99 ± 0.08	15.16 ± 0.07	29.42 ±0.11	28.62 ± 0.13	30.00 ±0.12
5×10^{-5}	26.34 ± 0.09	22.62 ± 0.10	26.32 ± 0.11	13.34 ±0.10	12.10 ± 0.07	14.93 ± 0.09	29.37 ± 0.13	27.30 ± 0.11	28.76 ± 0.12

Table 19: Accuracy with varying learning rates on ImageNet-C Gaussian noise adaptation rate 0.3. **Bold** numbers are the highest accuracy.

		Tent			CoTTA			EATA	
Learning rate	Full	naïve STTA	SNAP	Full	naïve STTA	SNAP	Full	naïve STTA	SNAP
2×10^{-3}	2.31 ±0.09	7.04 ±0.13	13.69 ±0.15	13.31 ±0.10	11.88 ±0.08	14.67 ±0.11	0.36 ±0.04	0.59 ±0.05	0.75 ±0.06
1×10^{-3}	4.54 ± 0.12	16.13 ± 0.14	27.63 ± 0.13	13.18 ± 0.09	11.86 ± 0.07	14.68 ± 0.10	1.31 ± 0.06	0.95 ± 0.05	24.35 ± 0.14
5×10^{-4}	10.22 ± 0.13	24.96 ±0.15	29.95 ±0.12	13.15 ± 0.08	11.85 ± 0.06	15.11 ± 0.10	21.96 ± 0.13	20.96 ± 0.12	27.72 ± 0.11
1×10^{-4}	27.03 ± 0.10	23.63 ± 0.11	26.60 ± 0.12	13.12 ± 0.07	11.74 ± 0.06	15.26 ± 0.08	29.42 ± 0.10	27.35 ± 0.09	29.48 ±0.10
5×10^{-5}	26.34 ± 0.09	20.94 ± 0.12	24.87 ± 0.13	13.34 ±0.07	11.92 ± 0.06	14.85 ± 0.09	29.37 ± 0.11	26.07 ± 0.10	27.90 ± 0.11

Table 20: Accuracy with varying learning rates on ImageNet-C Gaussian noise adaptation rate 0.1. **Bold** numbers are the highest accuracy.

		Tent			CoTTA			EATA	
Learning rate	Full	naïve STTA	SNAP	Full	naïve STTA	SNAP	Full	naïve STTA	SNAP
2×10^{-3}	2.31 ± 0.10	18.06 ± 0.14	27.41 ±0.12	13.31 ±0.08	10.93 ± 0.07	14.80 ±0.11	0.36 ± 0.03	1.86 ± 0.06	9.59 ± 0.15
1×10^{-3}	4.54 ± 0.11	25.46 ± 0.13	31.12 ± 0.14	13.18 ± 0.09	10.93 ± 0.07	14.73 ± 0.10	1.31 ± 0.05	2.86 ± 0.08	24.95 ± 0.13
5×10^{-4}	10.22 ± 0.12	24.71 ± 0.14	28.01 ± 0.11	13.15 ± 0.07	10.92 ± 0.06	15.18 ± 0.09	21.96 ± 0.12	18.76 ± 0.10	28.09 ±0.11
1×10^{-4}	27.03 ± 0.10	22.00 ± 0.12	26.21 ± 0.13	13.12 ± 0.08	11.74 ± 0.06	15.13 ± 0.09	29.42 ±0.11	22.43 ± 0.10	26.10 ± 0.12
5×10^{-5}	26.34 ± 0.09	16.72 ± 0.13	19.31 ± 0.12	$\textbf{13.34} \pm 0.08$	10.92 ± 0.07	14.76 ± 0.09	$29.37 \pm \scriptstyle{0.11}$	20.32 ± 0.10	23.28 ± 0.10

In conclusion, selecting an appropriately high learning rate for sparse adaptation significantly enhances performance while ensuring model stability. This strategy is particularly useful for real-world deployment of SNAP, where computational efficiency and robust performance are paramount.

B.18 Evaluation on real-world sensor data

To validate SNAP's generalizability to other real-world domains, we further test SNAP on HARTH [23], a human activity recognition dataset that collects data from two three-axial accelerometers attached to participants' thigh and lower back. Unlike our main evaluations, which focus on 2D vision and corruption-based domain shifts, HARTH introduces a distinct domain shift caused by sensor positioning and user variation.

We evaluate SNAP with an adaptation rate (AR) of 0.1 on Tent [48] and SAR [31]. The base model is composed of four one-dimensional convolutional layers followed by a fully-connected layer, and is trained on the source domain, composing of data collected from the back of 15 participants. The target domain is the data collected from the thigh of the remaining 7 participants. As shown in Table 21, SNAP improves accuracy even with sparse updates, demonstrating its effectiveness under realistic shifts

Table 21: Performance of SNAP (AR=0.1) on HARTH. Accuracy is averaged over all target domain users.

Method	Average Accuracy (%)
Tent (Naïve STTA)	19.64
+ SNAP	30.67
SAR (Naïve STTA)	21.10
+ SNAP	26.63

C Detailed experiment results

In this section, we provide detailed experimental results for the performance comparison of SNAP across a wide range of adaptation rates. We evaluated the performance on CIFAR10-C, CIFAR100-C, and ImageNet-C datasets with adaptation rates of 0.01, 0.03, 0.05, 0.1, 0.3, and 0.5, and across five state-of-the-art (SOTA) TTA algorithms: Tent [48], EATA [30], SAR [31], CoTTA [50], and RoTTA [53]. This comprehensive evaluation resulted in a total of 150 combinations (3 datasets, 6 adaptation rates, 5 algorithms).

The results demonstrate that, regardless of the adaptation rate, dataset, or the TTA algorithm, integrating SNAP consistently outperforms the baseline methods. Specifically, SNAP achieved the highest accuracy across nearly all of these 150 combinations, effectively demonstrating its robustness in both high and low adaptation settings. For CIFAR10-C and CIFAR100-C, SNAP showed substantial performance improvements compared to the baseline, even at very low adaptation rates (e.g., 0.01 and 0.05). Similarly, for ImageNet-C, SNAP maintained superior accuracy across diverse corruption types.

These results highlight that SNAP effectively balances adaptation and latency, ensuring optimal performance even when the adaptation rate is sparse and regardless of the underlying TTA algorithm. This consistent superiority across all 150 combinations underscores SNAP's suitability for practical, real-world applications on resource-constrained devices.

C.1 CIFAR10-C

Table 22: STTA classification accuracy (%) comparing with and without SNAP on CIFAR10-C through Adaptation Rates(AR) (0.5, 0.3, and 0.1), including results for full adaptation (AR=1). **Bold** numbers are the highest accuracy.

AR	Methods	Gau.	Shot	Imp.	Def.	Gla.	Mot.	Zoom	Snow	Fro.	Fog	Brit.	Cont.	Elas.	Pix.	JPEG	Avg
	Source	22.13	29.25	22.53	54.54	55.10	67.45	64.37	78.25	69.93	74.26	91.29	35.45	77.20	46.56	73.38	57.4
	Bource	±0.00	±0.00	±0.00	±0.00	±0.00	±0.00	±0.00	±0.00	±0.00	±0.00	±0.00	±0.00	±0.00	±0.00	±0.00	±0.0
	BN stats	63.72 ±0.48	65.67 ±0.12	57.14 ±0.25	84.99 ±0.31	62.72 ±0.23	83.86 ±0.48	84.26 ±0.30	78.98 ±0.30	76.95 ±0.08	83.32 ±0.17	88.46 ±0.16	84.60 ±0.17	73.96 ±0.18	76.61 ±0.02	68.79 ±0.42	75.6 ±0.2
		73.66	76.18	68.04	86.61	67.12	85.73	86.24	82.34	81.56	86.02	89.99	87.16	76.40	82.95	76.45	80.4
	Tent	±0.88	±0.94	±1.32	±0.50	±0.76	±0.38	±0.09	±0.94	±0.64	±0.18	±0.16	±2.50	±0.82	±0.15	±0.46	±0.7
1	CoTTA	71.95	73.97	67.03	83.91	66.75	82.64	83.34	79.92	79.49	82.41	88.39	80.14	75.38	79.24	75.42	78.0
1	COLIA	±0.32	±0.48	±0.66	±0.20	±0.08	±0.34	±0.19	±0.09	±0.13	±0.23	±0.18	±0.17	±0.09	±0.07	±0.25	±0.2
	EATA	75.82 ±0.50	77.61 ±0.27	69.63 ±0.87	87.14 ±0.29	69.41 ±0.68	85.96 ±0.39	87.08	83.42 ±0.38	82.28 ±0.29	86.58 ±0.41	90.40 ±0.17	89.26 ±0.39	77.62 ±0.28	83.35 ±0.32	77.77 ±0.20	81.5 ±0.5
		73.52	74.03	65.45	£0.29 85.69	£0.08 65.01	±0.39 84.63	±0.27 85.01	±0.38 81.47	±0.29 80.91	±0.41 84.18	±0.17 88.70	±0.39 86.23	±0.28 74.94	\$1.20	74.84	±0
	SAR	±1.53	±0.46	±1.81	±0.37	±0.35	±0.53	±0.34	±0.37	±0.72	±0.09	±0.12	±0.16	±0.03	±0.28	±0.69	±0.
	RoTTA	66.54	68.60	60.27	85.73	64.84	84.68	85.01	80.15	78.02	84.13	89.00	84.91	75.06	77.96	70.12	77.
	KOTTA	±0.46	±0.23	±0.46	±0.35	±0.63	±0.36	±0.45	±0.56	±0.06	±0.09	±0.27	±0.19	±0.15	±0.16	±0.36	±0
	Tent	73.44	75.93	67.18	86.52	67.28	85.25	86.23	82.24	80.35	85.39	89.80	87.77	77.00	82.08	75.58	80.
		±0.61 75.17	±0.44 77.66	±0.78 68.78	±0.17 88.25	±1.78 69.18	±0.49 87.11	±0.42 88.19	±0.77 84.21	±0.14 82.72	±0.20 87.34	±0.28 91.63	±0.27 86.30	±0.65 78.76	±0.68 83.43	±0.60 77.28	±0.:
	+ SNAP	±0.00	±0.78	±1.26	±0.38	±0.51	±0.18	±0.13	±0.29	±0.45	±0.51	±0.12	±1.07	±0.28	±0.18	±0.50	±0.
	G mm.	65.08	66.67	61.30	77.50	61.36	77.70	77.37	74.05	72.86	77.43	82.69	72.44	70.52	70.94	69.79	71.
	CoTTA	±0.26	±0.21	±0.16	±0.48	±0.15	±0.37	±0.37	±0.22	±0.44	±0.19	±0.30	±0.72	±0.07	±0.27	±0.10	±0.
	+ SNAP	71.89	74.18	66.92	85.46	67.57	84.27	84.91	81.10	80.62	84.06	90.16	82.14	76.75	80.23	75.98	79.
	. 5	±0.45	±0.33	±0.19	±0.32	±0.26	±0.22	±0.18	±0.09	±0.46	±0.24	±0.17	±0.33	±0.16	±0.38	±0.50	±0.
	EATA	73.95 ±0.22	75.82 ±0.18	68.00 ±0.70	86.83 ±0.25	67.83 ±0.50	85.27 ±0.39	86.48 ±0.15	82.63 ±0.50	80.99 ±0.05	85.45 ±0.16	89.86 ±0.18	87.61 ±0.53	77.01 ±0.31	82.13 ±0.18	76.11 ±0.45	80. ±0.
0.5		74.85	77.63	68.43	88.53	69.70	87.19	88.16	83.87	82.84	87.18	91.54	89.62	78.91	83.76	77.36	81.
	+ SNAP	±0.51	±0.46	±0.43	±0.17	±0.69	±0.35	±0.18	±0.42	±0.33	±0.15	±0.12	±0.38	±0.48	±0.14	±0.22	±0.
	SAR	69.10	72.37	63.22	85.18	64.30	83.94	85.07	80.11	79.64	83.91	88.64	84.21	75.70	79.10	72.92	77.
	JAK	±1.63	±1.05	±0.44	±0.25	±1.02	±0.12	±0.45	±0.17	±0.60	±0.37	±0.10	±0.30	±0.34	±0.52	±0.09	±0.
	+ SNAP	73.98	75.48	66.41	86.63	68.15	85.50	86.53	81.62	80.20	85.06	91.46	87.04	77.22	81.16	75.53	80.
		±0.48 65.02	±0.65 66.84	±1.26 58.38	±0.15 85.26	±0.07 63.51	±0.15 83.81	±0.10 84.66	±0.39 79.26	±0.17 76.76	±0.27 83.46	±0.03 88.27	±0.11 83.47	±0.45 74.43	±0.27 77.39	±0.23 69.13	±0.
	RoTTA	±0.04	±0.52	±0.33	±0.42	±0.18	±0.15	±0.20	±0.29	±0.49	±0.21	±0.04	±0.05	±0.16	±0.29	±0.41	±0.
	CNIAD	66.03	68.09	58.88	87.09	64.55	85.70	86.48	80.97	78.87	85.29	90.28	86.22	76.05	78.76	70.51	77.
	+ SNAP	±0.14	±0.15	±0.06	±0.27	±0.07	±0.03	±0.02	±0.22	±0.20	±0.22	±0.13	±0.10	±0.22	±0.22	±0.35	±0.
	Tent	71.18	74.06	65.44	85.93	66.01	84.37	85.90	81.31	79.80	84.80	89.58	84.01	75.96	80.46	74.09	78.
	Tent	±0.99	±0.80	±1.17	±0.28	±0.97	±0.14	±0.17	±0.40	±0.09	±0.25	±0.23	±0.30	±0.30	±0.39	±0.54	±0.
	+ SNAP	74.95	77.29	67.59	88.27	67.46	86.97	87.64	83.46	82.45	86.72	91.22	87.79	78.26	82.61	75.79	81. ±0.
		±0.84 63.01	±0.55 64.38	±0.46 58.95	±0.27 75.43	±0.26 59.65	±0.21 76.08	±0.16 75.47	±0.40 71.75	±0.19 70.33	±0.19 75.52	±0.21 80.94	±0.98 70.53	±0.35 68.75	±0.38 67.87	±0.32 67.55	£0.
	CoTTA	±0.12	±0.64	±0.74	±0.61	±0.48	±0.58	±0.16	±0.55	±0.48	±0.32	±0.49	±0.51	±0.65	±0.30	±0.37	±0.
	+ SNAP	71.39	73.57	66.29	85.22	66.71	84.20	84.64	80.77	80.56	84.06	89.85	81.86	76.48	79.94	75.69	78.
	+ SNAP	±0.31	±0.27	±0.10	±0.22	±0.19	±0.18	±0.13	±0.21	±0.32	±0.15	± 0.17	±0.08	±0.07	±0.24	±0.27	±0.
	EATA	70.98	73.70	65.73	86.01	66.71	84.36	86.10	80.92	79.87	84.48	89.29	86.33	76.19	80.66	73.98	79.
0.3		±1.05	±0.28	±1.68	±0.35 87.93	±0.81 68.56	±0.23	±0.38	±0.47 83.56	±0.09 82.20	±0.04 86.60	±0.19	±0.31 88.94	±0.20	±0.58	±0.52	±0.
	+ SNAP	74.19 ±0.38	76.64 ±0.68	67.89 ±0.19	87.93 ±0.25	±0.20	87.08 ±0.05	87.89 ±0.34	±0.30	±0.25	±0.23	91.11 ±0.22	88.94 ±0.61	78.10 ±0.14	83.03 ±0.20	75.83 ±0.43	81. ±0.
		69.10	72.37	63.22	85.18	64.30	83.94	85.07	80.11	79.64	83.91	88.64	84.21	75.70	79.10	72.92	77.
	SAR	±1.63	±1.05	±0.44	±0.25	±1.02	±0.12	±0.45	±0.17	±0.60	±0.37	±0.10	±0.30	±0.34	±0.52	±0.09	±0.
	+ SNAP	72.72	75.25	65.78	86.53	66.19	85.53	86.40	81.61	80.53	85.08	91.41	86.74	77.23	81.00	74.52	79.
	1 51411	±0.94	±0.30	±1.06	±0.16	±0.60	±0.26	±0.27	±0.45	±0.64	±0.23	±0.14	±0.08	±0.41	±0.37	±1.04	±0.
	RoTTA	64.09	66.07	57.58	84.97	62.66	83.06	84.08	78.60	76.40	82.86	88.03	83.21	74.14	76.35	68.70	75.
		±0.44 65.83	±0.13 67.57	±0.63 58.39	±0.20 86.97	±0.15 64.22	±0.18 85.63	±0.17 86.39	±0.34 80.75	±0.36 78.90	±0.05 85.21	±0.22 90.19	±0.24 85.92	±0.58 75.92	±0.47 78.91	±0.17 70.42	±0.
	+ SNAP	±0.18	±0.19	±0.29	±0.33	±0.16	±0.18	±0.09	±0.15	±0.08	±0.17	±0.16	±0.21	±0.09	±0.05	±0.37	±0.
		67.32	69.39	60.69	85.34	63.82	83.52	84.70	79.68	77.79	83.75	88.53	83.12	75.18	77.82	71.47	76.
	Tent	±0.93	±0.96	±0.36	±0.24	± 0.41	± 0.13	±0.15	± 0.41	± 0.50	± 0.08	± 0.49	±0.66	± 0.68	±0.69	±0.44	±0
	+ SNAP	70.22	71.48	63.08	87.35	65.74	85.89	86.38	81.93	80.00	85.62	90.34	87.47	76.44	79.63	72.72	78.
	+ SIVAP	±0.44	±0.91	±0.04	±0.20	±0.26	±0.25	±0.32	±0.33	±0.21	±0.14	±0.22	±0.11	±0.12	± 0.14	±0.39	±0.
	CoTTA	59.11	60.26	56.07	72.23	56.77	73.55	72.20	68.05	66.68	72.88	77.66	65.95	65.67	64.12	65.16	66.
		±0.43 71.70	±0.56 73.54	±0.65 66.70	±0.69 85.16	±0.64 66.83	±0.68 84.30	±0.94 84.88	±0.63 81.02	±0.52 80.61	±0.56 84.20	±1.15 89.84	±1.17 81.71	±0.83 76.60	±0.95 79.66	±0.58 75.71	±0 78.
	+ SNAP	±0.40	±0.21	±0.02	85.16 ±0.19	±0.39	±0.08	54.88 ±0.20	\$1.02 ±0.25	±0.24	±0.23	59.84 ±0.08	81.71 ±0.20	±0.20	+0.14	±0.25	78 ±0
	EATA	66.65	68.96	59.73	84.93	63.26	83.10	84.53	79.28	77.46	83.48	88.12	82.46	74.49	77.48	70.43	76
0.1	EATA	±0.43	±0.47	±0.15	±0.27	± 0.36	±0.24	±0.15	±0.44	±0.42	± 0.13	±0.09	±0.24	±0.20	±0.69	±0.25	±0
0.1	+ SNAP	69.29	70.49	61.71	87.32	65.48	85.96	86.64	81.44	79.56	85.47	90.50	86.84	76.32	79.64	72.51	78
	· Divis	±0.39	±0.57	±0.37	±0.42	±0.38	±0.29	±0.21	±0.34	±0.47	±0.23	±0.38	±0.36	±0.21	±0.12	±0.32	±0
	SAR	66.11	68.18	59.15	84.91	62.87	82.33	84.27	79.23	77.58	83.21	88.29	82.60	74.65	75.92	70.79	76
		±0.59 67.76	±0.83 70.68	±0.72 60.82	±0.45 86.78	±0.27 64.73	±0.60 85.29	±0.13 86.22	±0.32 80.82	±0.43 79.30	±0.18 84.95	±0.09 91.33	±0.57 86.59	±0.46 75.72	±0.77 78.72	±0.40 71.24	±0 78
	+ SNAP	±0.22	±0.14	±1.08	±0.26	±0.43	±0.10	±0.11	±0.23	±0.48	±0.28	±0.17	±0.14	±0.26	±0.35	±0.46	±0
	DoTT4	63.12	64.84	56.72	84.49	62.15	82.53	83.84	78.03	76.13	82.88	87.48	81.49	73.75	76.04	68.24	74
	RoTTA	±0.33	±0.21	±0.30	±0.04	±0.17	±0.30	±0.02	±0.29	±0.71	±0.16	±0.08	±0.11	± 0.14	±0.29	±0.27	±0
	+ SNAP	65.35	66.99	58.09	86.77	63.63 ±0.18	85.47 ±0.13	86.01 ±0.21	80.54	78.38 ±0.24	84.99	90.00 ±0.23	85.99 ±0.03	75.67	78.14 ±0.06	70.09	77.
	+ SINAP	±0.20	±0.15	±0.18	±0.18				±0.11		± 0.43			±0.17		±0.23	±0

Table 23: STTA classification accuracy (%) comparing with and without SNAP on CIFAR10-C through Adaptation Rates(AR) (0.05, 0.03, and 0.01). **Bold** numbers are the highest accuracy.

AR	Methods	Gau.	Shot	Imp.	Def.	Gla.	Mot.	Zoom	Snow	Fro.	Fog	Brit.	Cont.	Elas.	Pix.	JPEG	Avg.
лк		64.65	67.08	58.48	85.00	62.61	82.76	84.63	79.01	77.66	83.32	88.00	82.34	74.16	77.11	69.40	75.75
	Tent	±0.55	±0.58	58.48 ±0.42	±0.60	±0.44	±0.70	±0.55	19.01 ±0.74	±0.91	±0.48	±0.56	82.34 ±0.93	±0.10	±0.60	±0.48	±0.57
	GNA D	67.71	69.84	59.53	87.10	64.66	85.73	86.35	80.68	78.92	85.60	90.19	86.72	76.16	78.86	70.95	77.93
	+ SNAP	±0.38	±0.82	±1.10	±0.15	±0.25	±0.20	±0.20	±0.23	±0.14	±0.08	±0.31	±0.20	±0.17	±0.42	±0.30	±0.33
	CoTTA	59.27	61.18	56.33	72.22	57.37	74.27	72.61	70.03	68.68	74.82	79.72	65.57	66.92	64.13	65.25	67.22
	COLIN	±0.66	±1.12	±0.06	±1.43	±1.10	±1.46	±1.11	±1.02	±0.92	±1.09	±1.07	±1.38	±1.14	±1.27	±0.98	±1.05
	+ SNAP	71.42	73.31	65.91	85.23	67.01	84.19	84.91	80.80	80.56	84.19	90.00	82.09	76.31	79.79	75.18	78.73
		±0.29 64.68	±0.12 67.01	±0.13 58.07	±0.11 84.90	±0.21 62.56	±0.20 82.64	±0.14 84.57	±0.19 78.77	±0.34 77.16	±0.14 83.09	±0.23 87.80	±0.35 81.62	±0.05 74.05	±0.29 76.99	±0.21 69.31	±0.20 75.55
	EATA	±0.31	±0.37	±0.24	±0.54	±0.33	±0.67	±0.61	±0.71	±0.92	±0.44	±0.47	±0.59	±0.28	±0.41	±0.71	±0.51
0.05	CNAD	67.36	68.73	59.35	87.05	64.36	85.62	86.48	81.31	78.73	85.33	90.03	86.31	76.04	78.79	70.90	77.76
	+ SNAP	±0.33	±0.26	±0.37	±0.22	±0.18	±0.18	±0.25	±0.24	±0.22	±0.15	±0.24	±0.07	±0.12	± 0.27	±0.38	±0.23
	SAR	64.79	66.32	57.58	84.66	62.46	81.42	84.13	78.87	77.20	82.62	88.10	82.12	74.04	75.38	69.13	75.25
		±0.13	±0.86	±0.69	±0.72	±0.26	±1.52	±0.34	±0.26	±0.81	±1.24	±0.41	±0.74	±0.05	±0.80	±0.52	±0.62
	+ SNAP	66.00 ±0.17	68.85 ±0.75	58.47 ±0.42	86.54 ±0.25	63.06 ±0.28	85.26 ±0.09	86.13 ±0.38	80.38 ±0.09	78.17 ±0.27	85.17 ±0.13	90.93 ±0.36	85.96 ±0.20	75.27 ±0.31	77.37 ±0.28	70.61 ±0.30	77.21 ±0.29
		63.21	64.87	56.60	84.64	62.16	82.31	84.13	78.16	76.39	82.90	87.44	81.47	73.59	76.02	68.09	74.80
	RoTTA	±0.37	±0.62	±0.28	±0.52	±0.31	±0.63	±0.56	±0.71	±0.95	±0.62	±0.46	±0.65	±0.42	±0.40	±0.33	±0.52
	+ SNAP	65.28	66.91	57.88	86.75	63.51	85.48	86.17	80.46	78.38	85.24	89.99	85.82	75.66	77.98	70.15	77.05
	+ SNAP	±0.32	±0.22	±0.06	±0.25	±0.13	±0.13	±0.10	±0.23	±0.26	±0.13	±0.23	±0.03	±0.16	±0.19	±0.29	±0.18
	Tent	64.36	66.21	57.65	84.73	62.95	83.07	84.50	78.46	76.99	83.00	88.07	82.62	73.93	76.50	68.82	75.46
	Tent	±0.43	±0.16	±1.01	±0.48	±0.52	±0.50	±0.32	±0.82	±0.32	±0.36	±0.43	±0.34	±0.23	±0.46	±0.48	±0.46
	+ SNAP	66.32	68.38	59.00	86.93	64.04	85.58	86.35	80.78	78.68	85.34	90.08	86.19	75.77	78.37	70.49	77.49
		±0.61 60.38	±0.71 61.26	±0.52 56.71	±0.19 72.44	±0.24 57.58	±0.34 74.64	±0.05 72.73	±0.10 69.68	±0.02 68.34	±0.05 74.64	±0.10 79.52	±0.31 67.28	±0.05 67.42	±0.06 64.89	±0.08 66.19	±0.23 67.58
	CoTTA	±1.71	±1.94	±2.47	±2.23	±1.85	±1.74	±2.61	±2.03	±2.02	±2.52	±2.37	±1.89	±1.77	±0.79	±1.73	±1.98
	GNA D	71.12	73.68	66.34	85.30	66.64	84.25	84.55	80.88	80.11	84.06	89.89	81.98	76.27	79.77	75.35	78.68
	+ SNAP	±0.47	±0.29	±0.24	±0.01	±0.12	±0.34	±0.13	±0.15	±0.15	±0.14	±0.14	±0.37	±0.19	±0.26	±0.08	±0.21
	ΕΔΤΔ	63.99	65.95	57.39	84.71	62.66	83.11	84.44	78.42	76.63	82.97	88.00	82.55	73.85	76.46	68.91	75.34
0.03	EATA 0.03	±0.87	±0.44	±1.05	±0.48	±0.62	±0.52	±0.33	±0.75	±0.26	±0.26	±0.47	±0.34	±0.33	±0.29	±0.56	±0.50
	+ SNAP	66.16 ±0.03	67.60 ±0.41	58.81 ±0.36	86.95 ±0.13	64.06 ±0.17	85.49 ±0.36	86.34 ±0.08	80.79 ±0.01	78.65 ±0.25	85.24 ±0.13	90.09 ±0.12	86.23 ±0.08	75.88 ±0.18	78.48 ±0.10	70.56 ±0.47	77.42 ±0.19
		63.72	65.75	57.89	84.37	62.45	81.47	82.46	78.32	76.79	81.93	88.60	82.72	73.89	74.55	68.79	74.91
	SAR	±0.46	±0.29	±0.65	±0.81	±0.69	±1.61	±2.95	±0.81	±0.24	±1.33	±0.68	±0.29	±0.43	±0.98	±0.61	±0.85
	+ SNAP	65.40	67.68	58.37	86.72	63.11	85.10	86.18	79.93	78.05	84.92	90.93	85.58	75.30	77.22	69.97	76.96
	+ SIVAF	±0.33	±0.60	±0.45	±0.18	±0.16	±0.16	±0.29	±0.17	±0.31	±0.22	±0.35	±0.14	±0.14	±0.30	±0.30	±0.27
	RoTTA	63.36	65.10	56.64	84.62	62.41	82.96	84.35	78.10	76.42	82.69	87.90	82.34	73.56	76.09	68.39	75.00
		±0.80 65.27	±0.55 67.05	±0.56 58.05	±0.49 86.79	±0.79	±0.67 85.46	±0.43 86.25	±0.80	±0.23 78.34	±0.25 85.19	±0.53 90.10	±0.32 85.94	±0.25 75.67	±0.44 78.04	±0.31 69.75	±0.50 77.05
	+ SNAP	±0.32	±0.19	±0.22	±0.21	63.48 ±0.18	±0.33	±0.09	80.39 ±0.08	±0.15	±0.19	±0.16	±0.08	±0.12	±0.09	±0.27	±0.17
	Tent	62.43 ±1.70	64.13 ±1.51	55.85 ±1.35	84.03 ±1.07	62.21 ±1.20	82.47 ±0.88	83.87 ±0.93	77.71 ±0.66	76.55 ±0.18	82.75 ±0.14	87.35 ±1.11	81.83 ±1.81	73.24 ±1.33	75.34 ±1.18	67.73 ±1.50	74.50 ±1.10
		65.51	67.26	58.05	86.89	63.53	85.44	85.97	80.58	78.35	85.12	90.09	85.86	75.66	78.38	70.12	77.12
	+ SNAP	±0.24	±0.31	±0.34	±0.28	±0.07	±0.33	±0.20	±0.12	±0.12	±0.16	±0.21	±0.11	±0.08	±0.21	±0.33	±0.21
	C-TTA	59.75	59.44	54.47	71.12	57.11	72.47	72.83	66.05	65.14	69.75	75.12	64.31	66.22	62.65	64.76	65.41
	CoTTA	±4.69	±6.21	±5.57	± 5.10	± 4.35	±4.52	± 4.80	±7.60	±7.65	±9.79	±6.79	±6.46	±4.50	±5.27	±5.36	±5.91
	+ SNAP	71.79	73.61	65.98	85.34	66.76	84.26	84.93	80.64	80.38	83.94	89.98	82.47	76.48	79.61	75.60	78.79
		±0.22	±0.29	±0.58	±0.36	±0.26	±0.12	±0.21	±0.45	±0.30	±0.42	±0.08	±0.64	±0.26	±0.24	±0.29	±0.31
	EATA	62.36 ±1.73	63.92 ±1.66	55.73 ±1.39	84.05 ±1.10	62.24 ±1.18	82.38 ±0.85	83.90 ±0.93	77.66 ±0.72	76.48 ±0.15	82.67 ±0.17	87.34 ±1.12	81.82 ±1.81	73.30 ±1.24	75.31 ±1.20	67.76 ±1.52	74.46 ±1.12
0.01		65.49	67.19	57.93	86.92	63.65	85.42	85.97	80.46	78.13	85.07	90.03	85.87	75.69	78.20	70.03	77.07
	+ SNAP	±0.29	±0.04	±0.40	±0.41	±0.18	±0.28	±0.24	±0.18	±0.27	±0.13	±0.10	±0.20	±0.11	±0.13	±0.46	±0.23
	SAR	62.50	64.13	55.65	82.30	62.22	77.21	80.11	77.66	76.75	79.12	89.45	81.97	73.39	69.39	67.83	73.31
	JAK	±1.69	±1.83	±1.38	±3.37	±1.21	±6.27	±6.19	±0.80	±0.34	±3.28	±1.79	±1.97	±1.21	±5.48	±1.65	±2.57
	+ SNAP	65.06	66.93	57.66	86.76	62.78	85.05	85.94	79.95	77.62	84.65	90.72	85.48	75.34	75.72	69.61	76.62
		±0.17	±0.11	±0.51	±0.29	±0.24	±0.21	±0.48	±0.18	±0.37	±0.21	±0.62	±0.35	±0.13	±1.35	±0.25	±0.36
	RoTTA	62.25 ±1.65	63.71 ±1.68	55.59 ±1.46	84.05 ±1.12	62.17 ±1.37	82.32 ±0.83	83.86 ±0.90	77.56 ±0.75	76.39 ±0.24	82.64 ±0.10	87.27 ±1.12	81.75 ±1.82	73.21 ±1.21	75.15 ±1.27	67.75 ±1.48	74.38 ±1.13
		65.32	66.94	57.85	86.91	63.44	85.32	85.98	80.49	78.22	85.04	90.01	85.77	75.75	78.15	70.06	77.02
	+ SNAP	±0.25	±0.12	±0.29	±0.31	±0.24	±0.22	±0.14	±0.24	±0.20	±0.15	±0.06	±0.24	±0.11	±0.07	±0.47	±0.21

C.2 CIFAR100-C

Table 24: STTA classification accuracy (%) comparing with and without SNAP on CIAFR100-C through Adaptation Rates(AR) (0.5, 0.3, and 0.1), including results for full adaptation (AR=1). **Bold** numbers are the highest accuracy.

AR	Methods	Gau.	Shot	Imp.	Def.	Gla.	Mot.	Zoom	Snow	Fro.	Fog	Brit.	Cont.	Elas.	Pix.	JPEG	Avg
	Source	10.26	11.87	6.48	35.16	20.33	44.42	42.13	45.99	34.84	41.12	66.37	19.54	50.59	22.68	45.48	33.1
	Bource	±0.00	±0.00	±0.00	±0.00	±0.00	±0.00	±0.00	±0.00	±0.00	±0.00	±0.00	±0.00	±0.00	±0.00	±0.00	±0.0
	BN stats	36.90 ±0.10	37.96 ±0.24	32.13 ±0.44	62.65 ±0.26	39.14 ±0.19	60.05 ±0.42	61.16 ±0.05	50.68 ±0.13	50.38 ±0.09	54.81 ±0.24	64.40 ±0.05	60.33 ±0.12	50.48 ±0.24	53.49 ±0.11	41.98 ±0.49	50.4 ±0.2
		46.71	48.06	40.98	65.19	44.10	62.78	63.95	55.43	55.46	59.32	67.43	63.83	53.89	59.40	49.91	55.7
	Tent	±0.29	±0.47	±0.13	±0.40	±0.41	±0.24	±0.23	±0.36	±0.49	±0.30	±0.17	±0.42	±0.15	±0.32	±0.66	±0.3
1	CoTTA	42.14	42.92	37.92	55.40	41.01	55.18	55.39	49.46	50.61	50.86	61.35	47.44	48.69	54.38	48.11	49.3
	COTIA	±0.34	±0.44	±0.18	±0.12	±0.39	±0.10	±0.58	±0.23	±0.63	±0.31	±0.27	±0.37	±0.18	±0.16	±0.65	±0.3
	EATA	38.42 ±0.41	39.96 ±0.47	32.64 ±0.71	62.35 ±0.41	38.73 ±0.33	59.93 ±0.17	61.07 ±0.19	50.50 ±0.36	50.79 ±0.34	55.30 ±0.23	64.38 ±0.12	60.63 ±0.13	49.66 ±0.32	53.63 ±0.41	43.02 ±0.20	50.1 ±0.1
		±0.41 50.75	52.00	43.87	65.44	±0.33 46.30	63.60	£0.19 64.68	58.41	±0.34 58.26	£0.23 61.34	68.03	67.68	±0.32 54.53	61.52	±0.20 52.72	±0
	SAR	±0.44	±0.22	±0.40	±0.39	±0.22	±0.17	±0.09	±0.48	±0.09	±0.40	±0.15	±0.31	±0.25	±0.21	±0.21	±0.2
	RoTTA	38.54	39.85	33.73	63.45	40.74	60.54	62.03	51.61	51.75	56.20	65.14	61.55	51.22	54.42	42.50	51.:
	KOTTA	±0.22	±0.24	±0.37	±0.17	±0.32	±0.19	±0.26	±0.09	±0.14	±0.31	±0.10	±0.14	±0.14	±0.22	±0.35	±0.
	Tent	43.96	45.42	36.57	62.28	36.57	59.96	61.90	53.25	53.14	57.36	65.20	60.14	49.72	57.62	46.83	52.
		±0.85 49.06	±1.34 50.43	±1.57 41.49	±0.13 65.55	±2.97 44.09	±0.59 63.31	±0.48 65.62	±0.72 57.62	±1.70 56.81	±0.22 60.75	±0.20 68.72	±2.77 67.52	±0.08 54.08	±0.61 61.15	±0.52 51.54	±0.
	+ SNAP	±0.00	±0.13	±0.80	±0.24	±0.06	±0.53	±0.37	±0.09	±0.31	±0.48	±0.31	±0.64	±0.19	±0.14	±0.11	±0.
	C. TTTA	34.31	35.16	31.42	47.78	34.99	48.91	47.79	41.27	41.42	43.77	52.16	38.30	42.25	44.12	41.58	41.0
	CoTTA	±0.09	±0.46	±0.28	±0.45	±0.40	± 0.48	±0.46	±0.86	±0.37	±0.57	±0.27	±0.46	±0.49	±0.41	±0.22	±0.4
	+ SNAP	41.28	42.23	37.17	58.29	40.70	57.32	57.78	49.85	50.82	52.21	63.69	51.30	49.41	55.15	47.92	50
		±0.46 38.02	±0.16 39.48	±0.19	±0.21 61.68	±0.08	±0.12	±0.09	±0.38 50.15	±0.11 49.92	±0.28	±0.18 63.43	±0.23 58.70	±0.14 49.42	±0.09 53.08	±0.25 42.62	±0.:
	EATA	±0.22	±0.15	32.77 ±0.17	±0.38	38.42 ±0.07	59.11 ±0.09	60.63 ±0.18	±0.25	±0.67	54.60 ±0.13	±0.21	±0.44	±0.22	±0.20	±0.21	±0.:
0.5	+ SNAP	39.75	41.14	34.15	63.75	40.55	61.09	62.81	52.12	52.12	56.47	65.73	61.85	51.14	55.75	44.86	52.
	+ SNAP	±0.11	±0.26	±0.10	±0.23	±0.21	± 0.08	±0.19	±0.08	±0.30	±0.18	±0.23	±0.34	±0.28	±0.15	±0.51	±0.
	SAR	49.00	50.00	42.99	65.10	45.21	62.51	64.43	55.78	56.59	60.21	67.33	65.17	53.90	60.22	51.28	56.
		±0.61	±0.42 52.79	±0.30	±0.44 66.59	±0.41 47.84	±0.20	±0.43	±0.27 59.02	±0.46 59.12	±0.48	±0.44	±0.46	±0.50	±0.29	±0.23	±0.
	+ SNAP	51.71 ±0.46	±0.08	44.95 ±0.54	±0.10	±0.01	64.40 ±0.18	66.15 ±0.28	±0.20	±0.37	62.62 ±0.16	69.15 ±0.06	68.20 ±0.16	55.89 ±0.26	62.66 ±0.31	53.77 ±0.23	58. ±0.
	D. TETTA	37.12	38.34	32.54	62.25	38.91	59.52	61.19	50.22	49.91	54.69	63.74	59.40	50.32	53.29	41.94	50.
	RoTTA	±0.09	±0.20	±0.22	±0.09	± 0.13	±0.19	±0.21	±0.23	± 0.56	± 0.15	±0.19	±0.47	±0.29	±0.29	±0.15	±0.
	+ SNAP	38.33 ±0.30	39.12 ±0.24	32.93 ±0.28	64.01 ±0.15	40.36 ±0.44	61.30 ±0.38	62.96 ±0.16	51.77 ±0.22	51.54 ±0.19	56.15 ±0.28	66.13	61.67	51.60	54.90 ±0.23	43.14	51.
												±0.05	±0.17	±0.24		±0.36	±0.
	Tent	44.41 ±0.80	46.79 ±0.72	38.72 ±1.17	62.98 ±0.28	39.79 ±0.92	60.38 ±0.53	62.25 ±0.33	52.47 ±0.76	53.69 ±0.65	57.47 ±0.63	65.80 ±0.28	60.13 ±2.70	50.03 ±0.60	58.21 ±0.81	47.23 ±0.43	53.1 ±0.1
		49.23	50.15	42.19	65.85	45.12	63.39	64.91	57.45	57.13	60.72	68.86	66.65	54.25	61.38	51.80	57.
	+ SNAP	±0.04	±0.48	±0.75	±0.15	±1.15	±0.28	±0.26	±0.51	±0.37	±0.17	±0.31	±1.52	±0.41	±0.54	±0.68	±0.
	CoTTA	31.74	32.66	29.28	44.98	32.96	46.51	44.96	38.57	38.16	41.91	49.38	35.53	40.04	40.77	39.12	39.
	COTIA	±0.43	±0.38	±0.15	±0.45	±0.56	±0.48	±0.37	±0.90	±0.78	±0.39	±0.86	±0.33	±0.61	±0.67	±0.43	±0.
	+ SNAP	41.44 ±0.38	42.49 ±0.09	37.08 ±0.13	58.27 ±0.24	40.99 ±0.37	57.24 ±0.37	57.68 ±0.17	50.36 ±0.22	51.09 ±0.18	51.66 ±0.22	63.50 ±0.13	50.90 ±0.52	49.49 ±0.26	54.75 ±0.42	47.81 ±0.13	50. ±0.
		37.97	39.47	32.69	61.45	37.96	59.02	60.79	49.73	49.55	54.63	63.38	58.16	49.07	53.17	42.49	49.
	EATA	±0.04	±0.34	±0.12	±0.19	±0.17	±0.28	±0.12	±0.05	±0.38	±0.41	±0.07	±0.21	±0.24	±0.41	±0.44	±0.
0.3	+ SNAP	40.03	41.39	34.91	63.58	40.29	61.58	62.56	51.85	51.78	56.13	65.70	61.68	51.25	55.28	44.80	52.
	+ SIVAF	±0.26	±0.29	±0.58	±0.15	±0.28	±0.12	±0.25	±0.25	±0.21	±0.01	±0.22	±0.29	±0.35	±0.23	±0.17	±0.
	SAR	49.00	50.00	42.99	65.10	45.21	62.51	64.43	55.78	56.59	60.21	67.33	65.17	53.90	60.22	51.28	56.
		±0.61 50.63	±0.42 52.03	±0.30 44.89	±0.44 66.28	±0.41 47.08	±0.20 64.32	±0.43 65.90	±0.27 57.98	±0.46 58.09	±0.48 61.88	±0.44 69.17	±0.46 67.82	±0.50 55.47	±0.29 62.02	±0.23 53.09	±0.
	+ SNAP	±0.31	±0.32	±0.54	±0.13	±0.26	64.32 ±0.09	±0.21	57.98 ±0.27	58.09 ±0.49	±0.24	69.17 ±0.42	±0.29	±0.29	62.02 ±0.31	±0.15	58. ±0.
	DoTT4	36.83	37.94	32.00	61.90	38.67	59.15	60.97	49.92	49.32	54.62	63.71	58.31	49.79	52.88	41.59	49.
	RoTTA	±0.18	±0.22	±0.05	± 0.20	±0.10	±0.14	±0.24	±0.23	± 0.38	± 0.21	±0.18	±0.11	±0.22	±0.34	±0.27	±0.
	+ SNAP	38.11	39.21	32.80	63.72	40.01	61.51	62.74	51.37	51.49	55.68	65.90	61.56	51.50	54.67	43.01	51.
		±0.13	±0.23	±0.14	±0.13	±0.23	±0.13	±0.16	±0.15	±0.30	±0.25	±0.13	±0.29	±0.08	±0.13	±0.19	±0.
	Tent	43.55	44.25	37.95	62.56	41.80	59.45	62.13	53.04	51.60	56.76	64.60	61.19	51.01	56.42	46.28	52.
		±0.66	±0.54	±0.72 39.92	±0.47	±0.04	±0.20	±0.21	±0.84	±0.39	±0.15	±0.56	±1.68	±0.39	±0.27	±0.49	±0.
	+ SNAP	46.51 ±0.35	47.68 ±0.23	39.92 ±0.48	65.39 ±0.11	44.14 ±0.60	63.29 ±0.18	64.53 ±0.38	55.20 ±0.47	55.55 ±0.11	59.71 ±0.33	68.05 ±0.17	64.90 ±0.90	53.91 ±0.30	59.28 ±0.16	49.58 ±0.75	55. ±0.
	C TTT:	28.53	29.53	26.45	42.19	30.34	44.69	41.88	34.44	33.93	39.03	45.49	31.17	37.25	36.17	36.84	35
	CoTTA	±0.90	±0.86	± 0.60	±1.19	±0.77	±1.07	±0.62	± 0.84	± 1.07	±0.89	±1.36	± 0.60	± 0.80	±1.20	±0.71	±0.
	+ SNAP	41.72	42.62	37.46	58.43	41.24	57.33	57.96	50.34	51.17	52.29	63.59	51.32	49.68	54.78	47.89	50.
	DIVAL	±0.25	±0.60	±0.13	±0.13	±0.21	±0.07	±0.30	±0.38	±0.18	±0.16	±0.20	±0.36	±0.21	±0.28	±0.35	±0.
	EATA	38.41	39.03	32.29	61.07	38.45	58.21 ±0.47	60.62	49.59	49.19	54.23	62.88	57.39	49.00	53.01	42.05	49
0.1		±0.53 40.62	±0.45 41.53	±0.32 34.31	±0.36 64.08	±0.29 40.29	±0.47 61.32	±0.36 63.04	±0.30 52.00	±0.34 51.77	±0.50 56.85	±0.28 65.98	±0.62 61.96	±0.65 51.05	±0.60 55.67	±0.15 44.80	±0.
	+ SNAP	±0.26	±0.49	±0.24	±0.30	±0.21	±0.24	±0.16	±0.53	±0.40	±0.43	±0.09	±0.34	±0.09	±0.28	±0.15	±0.
	SAR	43.92	45.28	38.64	63.36	42.58	60.36	62.78	53.39	52.23	57.54	65.41	60.88	52.07	56.80	47.16	53.
	SAK	±0.52	±0.55	±0.28	±0.25	±0.44	±0.42	±0.23	±0.86	±0.28	±0.32	±0.41	±0.88	±0.59	±0.13	±0.20	±0
	+ SNAP	46.29	47.60	39.95	65.26	44.00	63.09	64.97	55.08	55.17	59.73	68.13	64.72	53.84	58.98	49.54	55.
		±0.68 36.28	±0.06 37.12	±0.21 31.38	±0.18 61.20	±0.22 38.36	±0.25 58.26	±0.36 60.30	±0.24 49.20	±0.17 48.21	±0.24 53.54	±0.09 62.80	±0.44 56.78	±0.31 49.61	±0.35 52.28	±0.65 41.26	±0.
		30.28				±0.15	±0.24	±0.47	±0.23	±0.14	±0.23	±0.40	±0.51	±0.24	±0.41	±0.11	±0.
	RoTTA	+0.15	+0.41	+0.27													
	ROTTA + SNAP	±0.15 37.83	±0.41 38.42	±0.27 32.38	±0.07 63.73	39.72	61.32	62.58 ±0.19	51.38	51.18	55.61	65.70 ±0.29	61.39 ±0.21	51.36	54.51	42.85	51.

Table 25: STTA classification accuracy (%) comparing with and without SNAP on CIFAR100-C through Adaptation Rates(AR) (0.05, 0.03, and 0.01). **Bold** numbers are the highest accuracy.

Tent	AR	Methods	Gau.	Shot	Imp.	Def.	Gla.	Mot.	Zoom	Snow	Fro.	Fog	Brit.	Cont.	Elas.	Pix.	JPEG	Avg.
+ SNAP		Tent			35.14							55.52						51.24
Cotta 20.37 20.70 20.81 20.01 20.		Tent																±0.54
CoTTA		+ SNAP																54.13 ±0.31
COLITA 4.060 40.32 40.44 40.71 40.76 41.14 40.85 40.65 41.15 41.65 40.65 41.15 40.82 40.																		33.20
+ SNAP 42.01 42.01 40.13 40.31 40.25 40.25 40.25 40.25 40.25 40.25 40.25 40.25 40.95 40.95 40.85 40.25 40.25 40.25 40.95 40.95 40.25 40.25 40.25 40.25 40.25 40.95 40.95 40.25 40		CoTTA						±0.76										±0.75
0.05 Act		CNIAD		42.70	37.67	58.30	41.57				51.31	52.34	63.63					50.63
Parison Pari		+ SIVAF																±0.22
10.15 10.16 10.		EATA																49.81
SNAP 40.21	0.05																	±0.50 52.43
SAR		+ SNAP																±0.29
SNAP* **SNAP**** **ANA**** **ANA		G + D																51.50
FSNAP 10.29		SAR																±0.43
ROTTA 36.8 37.38 37.38 37.38 37.38 37.38 34.39 35.30 50.89 48.30 53.50 62.29 56.52 49.37 52.19 41.60 4		+ SNAD																53.59
**************************************		TOMAI																±0.33
+ SNAP		RoTTA																49.12
Tent																		±0.34 51.41
Helit		+ SNAP																±0.23
+ SNAP		T	38.55	39.28	33.77	61.64	39.66	58.83	60.89	49.45	49.51	54.64	63.48	57.29	50.34	53.44	43.28	50.27
COTTA		rent																±0.37
COTTA 27.11 27.73 25.87 40.02 29.52 42.16 39.60 20.40		+ SNAP																52.99
Hand Hand Hand Hand Hand Hand Hand Hand		. 51.11																±0.28
+ SNAP		CoTTA																34.21 ±2.05
EATA		+ SNAP																50.70
EATA																		±0.26
+ SNAP		EATA	37.94	38.63	32.00		39.08					53.89	63.03			52.93		49.56
SNAP 49.89 ±0.20 ±0.08 ±0.09 ±0.00 ±0.08 ±0.09 ±0.00 ±0.08 ±0.04 ±0.19 ±0.09 ±0.00 ±0.08 ±0.09 ±0.00 ±0.08 ±0.09 ±0.00 ±0.08 ±0.09 ±0.00 ±0.09 ±0.00 ±0.09 ±0.00 ±0.09 ±0.00 ±0.09 ±0.00 ±0.09 ±0.00 ±0.09 ±0.00 ±0.09 ±0.00 ±0.09 ±0.00 ±0.09 ±0.00 ±0.09 ±0.00 ±0.09 ±0.00 ±0.09 ±0.00 ±0.09 ±0.00 ±0.09 ±	0.03																	±0.47
SAR																		52.36
+ SNAP																		±0.26 50.30
+ SNAP																		±0.35
RoTTA		CNIAD																52.41
Heat Hand Hand Hand Hand Hand Hand Hand Hand		+ SNAP																±0.28
+SNAP		RoTTA																48.87
Tent #0.20 ±0.20 ±0.31 ±0.24 ±0.17 ±0.16 ±0.52 ±0.27 ±0.28 ±0.37 ±0.20 ±0.13 ±0.19 ±0.26 ±0.33 ±0.19 ±0.26 ±0.33 ±0.19 ±0.26 ±0.33 ±0.19 ±0.26 ±0.33 ±0.19 ±0.26 ±0.33 ±0.19 ±0.26 ±0.33 ±0.19 ±0.29 ±																		±0.35
Tent 36.08 36.95 31.31 61.03 38.09 57.63 58.76 48.24 48.65 53.45 62.14 55.07 48.59 51.82 40.68 ±0.42 ±0.21 ±0.47 ±0.51 ±0.56 ±0.53 ±0.31 ±0.47 ±0.87 ±0.19 ±0.49 ±2.13 ±0.25 ±0.58 ±0.04 ±0.18 ±0.06 ±0.08 ±0.34 ±0.17 ±0.29 ±0.00 ±0.30 ±0.16 ±0.10 ±0.11 ±0.36 ±0.34 ±0.24 ±0.06 ±0.00 ±0.34 ±0.17 ±0.29 ±0.00 ±0.30 ±0.16 ±0.17 ±0.29 ±0.00 ±0.30 ±0.16 ±0.17 ±0.29 ±0.00 ±0.30 ±0.16 ±0.17 ±0.29 ±0.00 ±0.30 ±0.16 ±0.17 ±0.29 ±0.00 ±0.33 ±0.16 ±0.17 ±0.29 ±0.00 ±0.30 ±0.16 ±0.17 ±0.29 ±0.00 ±0.30 ±0.16 ±0.17 ±0.29 ±0.00 ±0.30 ±0.16 ±0.17 ±0.29 ±0.00 ±0.30 ±0.16 ±0.17 ±0.29 ±0.00 ±0.30 ±0.16 ±0.17 ±0.29 ±0.00 ±0.30 ±0.16 ±0.17 ±0.29 ±0.00 ±0.30 ±0.16 ±0.17 ±0.29 ±0.00 ±0.30 ±0.16 ±0.17 ±0.29 ±0.00 ±0.30 ±0.16 ±0.17 ±0.29 ±0.00 ±0.30 ±0.16 ±0.17 ±0.29 ±0.00 ±0.30 ±0.16 ±0.17 ±0.29 ±0.00 ±0.30 ±0.16 ±0.17 ±0.29 ±0.00 ±0.30 ±0.16 ±0.17 ±0.29 ±0.00 ±0.30 ±0.16 ±0.17 ±0.29 ±0.00 ±0.30 ±0.16 ±0.17 ±0.29 ±0.00 ±0.30 ±0.16 ±0.17 ±0.29 ±0.00 ±0.25 ±0.17 ±0.59 ±0.09 ±0.17 ±0.25 ±0.09 ±0.33 ±0.68 ±0.47 ±0.27 ±0.59 ±0.03 ±0.12 ±0.35 ±0.17 ±0.59 ±0.09 ±0.25 ±0.17 ±0.59 ±0.09 ±0.25 ±0.17 ±0.59 ±0.09 ±0.25 ±0.20 ±0.24 ±0.17 ±0.59 ±0.34 ±0.50 ±0.37 ±0.57 ±0.32 ±0.50 ±1.26 ±0.09 ±0.43 ±2.22 ±0.15 ±0.05 ±0.02 ±0.25 ±0.27 ±0.14 ±0.15 ±0.27 ±0.09 ±0.35 ±0.17 ±0.59 ±0.09 ±0.35 ±0.17 ±0.57 ±0.29 ±0.34 ±0.17 ±0.59 ±0.09 ±0.25 ±0.29 ±0.29 ±0.25 ±0.29 ±0.25 ±0.29 ±0.29 ±0.25 ±0.29 ±0.25 ±0.29 ±0.25 ±		+ SNAP																51.45 ±0.25
Hent																		
+ SNAP 38.40 39.40 33.26 63.85 40.36 61.23 62.79 51.92 51.73 56.20 65.83 60.95 51.82 54.75 43.53		Tent						57.63										48.57 ±0.54
COTTA																		51.73
Cotta		+ SNAP																±0.18
+SNAP		C-TTA																34.58
EATA		COTTA																±2.13
EATA		+ SNAP																50.62
0.01 + SNAP 80.72 + SNAP 80.73 + SNAP 80.74 + SNAP 80.75		. 51.11																±0.26
+ SNAP 38.54 39.78 33.11 63.82 39.98 61.33 62.53 51.76 51.50 56.03 65.94 61.16 51.47 54.52 43.67 51.50 56.03 65.94 61.16 51.47 54.52 43.67 51.50 56.03 65.94 61.16 51.47 54.52 43.67 51.50 56.03 65.94 61.16 51.47 54.52 43.67 51.50 56.03 65.94 61.16 51.47 54.52 43.67 51.50 56.03 65.94 61.16 51.47 54.52 43.67 51.50 56.03 65.94 61.16 51.47 54.52 43.67 51.50 56.03 65.94 61.16 51.47 54.52 51.50 56.03 65.94 61.16 51.47 54.52 51.50 56.03 65.94 61.16 51.47 54.52 51.50 56.03 65.94 61.16 51.47 54.52 51.50 56.03 65.94 61.16 51.47 54.52 51.50 56.03 65.94 61.16 51.47 54.52 51.50 56.03 65.94 61.16 51.17 51.04 51.50 51.17 51.17 51.04 51.50 51.17		EATA																48.51 ±0.55
SAR #0.14 ±0.15 ±0.22 ±0.10 ±0.53 ±0.20 ±0.24 ±0.12 ±0.32 ±0.44 ±0.19 ±0.11 ±0.04 ±0.27 ±0.04 ±0.17 ±0.06 ±0.27 ±0.04 ±0.19 ±0.11 ±0.04 ±0.27 ±0.04 ±0.07 ±0.06 ±0.26 ±0.30 ±0.35 ±0.44 ±0.59 ±0.36 ±0.47 ±0.92 ±0.16 ±0.50 ±2.20 ±0.15 ±0.57 ±0.19 ±0.19 ±0.14 ±0.59 ±0.36 ±0.17 ±0.06 ±0.27 ±0.19 ±0.18 ±0.19 ±0	0.01																	51.68
SAR ±0.00 ±0.26 ±0.30 ±0.35 ±0.44 ±0.59 ±0.36 ±0.47 ±0.92 ±0.16 ±0.50 ±2.20 ±0.15 ±0.57 ±0.19 +SNAP ±0.39 ±0.25 ±0.38 ±0.23 ±0.45 ±0.51 ±0.26 ±0.11 ±0.28 ±0.41 ±0.16 ±0.15 ±0.15 ±0.47 ±0.06 RoTTA ±0.33 ±0.31 ±0.45 ±0.50 ±0.50 ±0.56 ±0.50 ±0.56 ±0.30 ±0.28 ±0.97 ±0.23 ±0.28 ±0.91 ±0.18 ±0.1		+ SNAP																±0.21
+SNAP 37.82 38.72 32.60 63.53 39.80 61.00 62.27 51.42 51.43 52.71 65.67		SAR	36.04	37.02	31.38	61.13	38.07	58.00	59.08	48.44		53.52	62.57	55.19	48.87	52.01	40.71	48.72
RoTTA #0.39 #0.25 #0.38 #0.23 #0.45 #0.51 #0.26 #0.11 #0.28 #0.41 #0.16 #0.15 #0.15 #0.47 #0.06 RoTA #0.33 #0.31 #0.45 #0.50 #0.50 #0.50 #0.50 #0.50 #0.26 #0.30 #0.27 #0.23 #0.62 #0.97 #0.23 #0.62 #0.84		SAK																±0.50
RoTTA 35.55 36.34 30.55 60.76 37.42 57.50 58.57 47.87 48.31 53.11 61.90 54.70 48.25 51.37 40.29 40.33 ±0.31 ±0.45 ±0.50		+ SNAP																50.98
ENAP 37.82 38.72 32.60 63.53 39.80 61.00 62.27 51.42 51.33 55.71 65.64 60.89 51.50 54.27 42.92																		±0.28
+SNAP 37.82 38.72 32.60 63.53 39.80 61.00 62.27 51.42 51.33 55.71 65.64 60.89 51.50 54.27 42.92		RoTTA																48.16 ±0.52
																		51.30
		+ SNAP	±0.16	±0.05	±0.10	±0.01	±0.49	±0.37	±0.23	±0.06	±0.12	±0.42	±0.14	±0.18	±0.18	±0.19	±0.47	±0.21

C.3 ImageNet-C

Table 26: STTA classification accuracy (%) comparing with and without SNAP on ImageNet-C through Adaptation Rates(AR) (0.5, 0.3, and 0.1), including results for full adaptation (AR=1). **Bold** numbers are the highest accuracy.

AR	Methods	Gau.	Shot	Imp.	Def.	Gla.	Mot.	Zoom	Snow	Fro.	Fog	Brit.	Cont.	Elas.	Pix.	JPEG	Avg
	Source	3.00	3.70	2.64	17.90	9.74	14.72	22.45	16.60	23.06	24.00	59.11	5.37	16.50	20.88	32.63	18.13
	Source	± 0.00	±0.00	± 0.00	± 0.00	± 0.00	± 0.00	±0.00	±0.00	±0.00	± 0.00	± 0.00	± 0.00	± 0.00	± 0.00	±0.00	±0.00
	BN stats	14.29 ±0.05	15.06 ±0.02	14.89 ±0.08	13.30 ±0.08	13.38 ±0.08	23.78 ±0.05	35.22 ±0.06	31.78 ±0.04	30.26 ±0.07	44.40 ±0.14	62.39 ±0.11	15.14 ±0.05	40.42	45.25 ±0.04	36.53 ±0.16	29.0° ±0.0°
		27.03	28.98	28.64	24.66	23.63	±0.03 38.70	±0.06 45.77	±0.04 44.82	38.06	±0.14 54.59	64.61	±0.03 16.84	±0.10 51.64	55.54	49.38	39.5
	Tent	±0.05	±0.08	±0.29	±0.27	±0.25	±0.10	±0.12	±0.08	±0.35	±0.08	±0.10	±1.51	±0.10	±0.15	±0.07	±0.2
1	CoTTA	13.12	13.98	13.94	12.44	12.18	23.74	35.22	31.78	30.26	44.40	62.40	15.13	40.42	45.26	36.53	28.7
1	COLIA	± 0.08	±0.07	± 0.01	± 0.10	± 0.04	± 0.04	±0.06	±0.05	± 0.06	± 0.14	± 0.11	± 0.03	± 0.10	± 0.04	±0.16	±0.0
	EATA	29.62	31.79	31.17	26.89	26.30	40.65	47.44	46.29	40.78	55.57	64.97	38.02	52.66	56.03	50.26	42.5
		±0.02 29.23	±0.09 31.14	±0.19 29.88	±0.03 29.29	±0.15 27.39	±0.12 39.76	±0.06 44.13	±0.09 45.98	±0.05 29.39	±0.08 55.13	±0.08 63.71	±0.08 17.34	±0.20 52.31	±0.04 56.09	±0.16 49.35	±0.1
	SAR	±0.40	±1.44	±0.96	±0.72	±0.97	±0.63	±0.11	±0.23	±0.30	±0.20	±0.08	±0.61	±0.08	±0.18	±0.13	±0.4
	p. mm.	20.60	22.83	19.81	10.46	10.10	21.31	31.83	39.66	32.09	46.08	62.22	20.27	42.54	47.47	40.67	31.2
	RoTTA	±0.07	±0.09	±0.24	±0.04	±0.26	±0.27	±0.23	±0.18	±0.18	±0.23	±0.27	±0.49	±0.29	±0.23	±0.10	±0.2
	Tent	25.24	26.86	26.35	23.26	22.41	35.99	44.60	42.96	37.68	53.60	64.40	21.35	50.23	54.32	47.93	38.4
	TCIII	±0.10	±0.27	±0.08	±0.06	±0.05	±0.09	±0.10	±0.13	±0.17	±0.15	±0.12	±0.94	±0.12	±0.15	±0.04	±0.1
	+ SNAP	28.05 ±0.00	29.97 ±0.04	29.39 ±0.19	25.73 ±0.15	23.39 ±0.06	38.49 ±0.17	45.65 ±0.03	44.21 ±0.09	39.57 ±0.10	53.90 ±0.10	64.52 ±0.09	34.39 ±1.83	49.99 ±0.14	54.88 ±0.07	48.72 ±0.09	40.7 ±0.2
		11.99	13.04	12.86	11.90	11.64	22.92	35.06	31.20	29.97	44.28	62.16	14.02	40.39	45.29	36.58	28.2
	CoTTA	±0.13	±0.20	±0.10	±0.07	±0.07	±0.02	±0.06	±0.09	±0.06	±0.07	±0.07	±0.09	±0.05	±0.09	±0.12	±0.0
	+ SNAP	15.16	15.96	15.86	13.98	14.13	24.69	36.51	32.59	31.71	45.98	63.62	15.72	42.05	46.71	37.93	30.1
	T SIMI	±0.14	±0.02	±0.14	±0.04	±0.00	±0.09	±0.07	±0.16	±0.06	±0.09	±0.05	±0.04	±0.09	±0.24	±0.14	±0.0
	EATA	28.62 ±0.10	30.12	29.94 ±0.14	25.34 ±0.20	24.48 ±0.44	38.94 ±0.10	46.85 ±0.25	45.20 ±0.12	40.03 ±0.01	55.04 ±0.06	64.84 ±0.07	34.48 ±0.41	52.06 ±0.24	55.57 ±0.13	49.85 ±0.05	41.4 ±0.
0.5		±0.10 30.00	±0.10 31.88	±0.14 31.47	±0.20 26.93	±0.44 26.64	±0.10 39.16	±0.23	±0.12 45.36	±0.01 39.75	±0.06	±0.07	±0.41 33.75	±0.24 52.29	±0.13	±0.05	±0.
	+ SNAP	±0.29	±0.17	±0.13	±0.21	±0.28	±0.15	±0.07	±0.13	±0.14	±0.14	±0.10	±0.07	±0.09	±0.18	±0.08	±0.
	SAR	26.74	28.56	28.77	19.90	21.50	39.97	44.98	45.95	34.22	55.04	63.93	6.58	52.50	55.98	49.71	38.
	SAK	±0.25	±1.75	±0.13	±0.21	± 0.38	±0.10	±0.12	±0.17	± 0.80	±0.05	± 0.03	± 0.64	± 0.10	±0.19	±0.09	±0.3
	+ SNAP	31.58	33.22	33.77	26.47	26.26	44.01	47.94	48.77	42.51	56.96	64.86	28.31	54.23	57.55	51.90	43.
		±0.38 18.17	±2.44 19.59	±0.56 18.49	±1.69 12.32	±0.94 11.79	±0.10 23.56	±0.04 34.62	±0.12 37.84	±0.09 32.91	±0.13 47.86	±0.10 63.94	±10.99 18.68	±0.08 43.21	±0.16 48.54	±0.19 40.20	±1.3
	RoTTA	±0.05	±0.03	±0.10	±0.11	±0.13	±0.15	±0.14	±0.11	±0.06	±0.05	±0.16	±0.42	±0.08	±0.23	±0.23	±0.
	CNIAD	20.43	22.03	21.05	15.47	14.49	26.36	36.46	38.98	34.15	48.41	64.02	20.74	43.66	49.16	41.05	33.
	+ SNAP	±0.03	±0.08	±0.11	±0.11	±0.07	±0.06	±0.10	±0.09	±0.12	±0.13	±0.13	±0.23	±0.10	±0.10	±0.15	±0.1
	Tent	23.63	25.18	24.80	21.81	20.97	34.11	43.60	41.44	36.98	52.66	64.21	22.74	48.96	53.46	46.80	37.4
	Tent	±0.08	±0.37	±0.28	±0.02	±0.18	±0.07	±0.04	±0.05	±0.04	±0.15	±0.13	±0.04	±0.16	±0.07	±0.09	±0.1
	+ SNAP	26.60	28.21	27.94	24.37	22.39	36.45	44.36	42.64	38.54	52.91	64.26	33.47	48.58	53.90	47.41	39.4
		±0.20 11.74	±0.19 12.74	±0.33 12.68	±0.36 11.77	±0.12 11.62	±0.07 22.64	±0.13 34.97	±0.07 31.05	±0.15 29.81	±0.06 44.24	±0.10 62.12	±0.44 13.73	±0.10 40.31	±0.14 45.19	±0.11 36.71	±0.: 28.0
	CoTTA	±0.09	±0.06	±0.07	±0.17	±0.14	±0.14	±0.07	±0.01	±0.13	±0.05	±0.06	±0.02	±0.15	±0.08	±0.09	±0.0
	+ SNAP	15.26	16.00	15.83	13.81	14.13	24.84	36.46	32.58	31.73	46.04	63.52	15.69	42.18	46.74	38.00	30.
	+ SNAP	±0.16	±0.09	±0.06	±0.04	± 0.01	±0.03	±0.13	±0.03	±0.08	±0.21	±0.06	±0.08	±0.07	±0.05	±0.14	±0.
	EATA	27.35	29.03	28.62	23.94	23.45	37.21	46.18	44.05	39.19	54.52	64.54	32.20	51.22	55.00	49.27	40.3
0.3		±0.04	±0.15 31.20	±0.27 30.69	±0.06	±0.60 25.90	±0.30 38.24	±0.13	±0.20	±0.22 39.31	±0.01 54.82	±0.06	±0.62	±0.16	±0.10	±0.21	±0.2
	+ SNAP	29.48 ±0.14	±0.04	±0.11	26.68 ±0.14	±0.25	38.24 ±0.01	46.60 ±0.22	44.62 ±0.06	59.51 ±0.19	54.82 ±0.06	64.44 ±0.13	32.87 ±0.29	51.41 ±0.25	55.41 ±0.06	49.78 ±0.14	41.4 ±0.1
		28.12	29.30	29.63	22.37	23.88	39.34	45.36	45.69	36.73	54.91	64.11	10.96	52.22	55.76	49.60	39.2
	SAR	±0.13	±0.89	±0.17	±0.47	±0.33	±0.18	±0.11	±0.18	±0.79	±0.07	±0.02	±1.33	±0.19	±0.13	±0.08	±0.3
	+ SNAP	32.63	34.69	34.26	28.91	27.96	43.51	47.79	48.27	42.41	56.45	64.77	32.76	53.74	57.21	51.67	43.
	TOMAI	±0.11	±0.23	±0.18	±0.27	±0.29	±0.14	±0.03	±0.11	±0.13	±0.09	±0.07	±3.04	±0.13	±0.28	±0.12	±0.
	RoTTA	16.90	17.88	17.25	12.89	12.51	23.96	35.26	36.26	32.32	47.25 ±0.02	63.98	17.46	42.77	48.21	39.35	30.5
		±0.15 18.63	±0.11 19.94	±0.08 19.35	±0.17 14.88	±0.05 14.34	±0.03 25.88	±0.16 36.47	±0.01 37.13	±0.07 33.32	±0.02	±0.13 63.96	±0.18 19.08	±0.09 42.98	±0.24 48.73	±0.15 40.27	±0.
	+ SNAP	±0.07	±0.08	±0.06	±0.08	±0.05	±0.03	±0.03	±0.02	±0.11	±0.17	±0.06	±0.21	±0.07	±0.17	±0.20	±0.
		22.00	23.51	23.07	19.38	18.86	32.15	42.29	39.70	34.33	51.62	63.70	15.79	47.74	52.35	45.54	35.4
	Tent	± 3.47	±3.92	±3.85	± 2.30	± 2.06	± 3.40	±2.45	±3.27	± 0.60	± 2.30	±0.29	±4.61	± 2.84	±2.27	±2.98	±2.
	+ SNAP	26.21	27.85	27.50	23.62	22.73	36.01	44.11	42.19	38.15	52.95	64.57	30.23	48.56	53.71	47.09	39.
	T SIMI	±4.92	±5.36	±5.30	±4.23	±4.11	±5.57	±3.72	±4.49	±3.37	±3.47	±1.18	±5.15	±4.29	±3.31	±4.09	±4.
	CoTTA	10.97	11.92	11.98	11.45	11.38	22.39	34.96	30.88	29.89	44.09	61.96	13.08	40.20	45.27	36.71	27.5
		±0.32 15.13	±0.32 16.03	±0.18 15.91	±0.04 13.86	±0.34 14.02	±0.02 24.90	±0.15 36.51	±0.14 32.56	±0.09	±0.23 46.02	±0.05 63.60	±0.28 15.69	±0.18 41.94	±0.16 46.78	±0.10 38.03	±0.
	+ SNAP	±0.06	±0.09	±0.04	±0.00	±0.07	±0.05	±0.05	±0.06	±0.12	±0.06	±0.10	±0.04	±0.09	±0.09	58.05 ±0.12	50. ±0.
	EATA	22.43	23.78	23.26	19.38	19.42	32.18	43.22	40.65	36.64	52.38	63.87	24.59	48.13	52.89	46.33	36.
0.1	EATA	±0.05	±0.16	±0.43	±0.26	±0.51	±0.31	±0.19	±0.15	±0.16	±0.27	±0.05	±1.52	± 0.40	±0.12	±0.14	±0.
0.1	+ SNAP	26.10	27.29	27.13	22.38	22.15	33.45	43.92	40.96	36.68	52.71	63.77	27.93	48.47	53.23	47.46	38.
	DIVAL	±0.09	±0.13	±0.20	±0.32	±0.14	±0.27	±0.08	±0.16	±0.01	±0.09	±0.10	±0.18	±0.24	±0.10	±0.17	±0.
	SAR	26.12	27.56	26.93	22.51	23.35	36.03	44.48	43.19	37.26	53.82	64.15	19.87	50.78	54.78	48.43	38
		±0.17 30.28	±0.01 31.97	±0.11 31.30	±0.24 26.67	±0.21 26.31	±0.21 39.66	±0.09 46.08	±0.09 45.43	±0.32 40.26	±0.21 54.76	±0.11 64.62	±2.10 36.12	±0.12 51.26	±0.18 55.42	±0.07 49.63	±0.
	+ SNAP	±0.16	±0.24	±0.12	±0.34	±0.37	±0.25	±0.04	±0.09	±0.13	±0.23	±0.05	±0.67	±0.06	±0.20	±0.06	±0.
	D. TETTA	14.77	15.59	15.33	13.17	13.19	23.85	35.38	32.73	30.77	45.22	63.08	15.62	41.05	46.15	37.19	29.
	RoTTA	±0.04	±0.04	± 0.04	±0.07	±0.10	±0.05	±0.05	±0.03	±0.04	±0.15	±0.12	±0.02	±0.10	±0.07	±0.13	±0.
		15.35	16.20	16.01	13.67	13.66	24.27	35.62	33.04	31.02	45.38	62.95	15.96	41.06	46.17	37.44	29.
	+ SNAP	±0.03	± 0.01	± 0.07	±0.09	± 0.07	±0.03	±0.01	±0.07	±0.04	±0.11	±0.08	±0.08	±0.11	±0.07	±0.19	±0.

Table 27: STTA classification accuracy (%) comparing with and without SNAP on ImageNet-C through Adaptation Rates(AR) (0.05, 0.03, and 0.01). **Bold** numbers are the highest accuracy.

				` /	`												
AR	Methods	Gau.	Shot	Imp.	Def.	Gla.	Mot.	Zoom	Snow	Fro.	Fog	Brit.	Cont.	Elas.	Pix.	JPEG	Avg.
		23.77	24.65	24.44	20.54	20.27	32.73	43.57	40.82	35.92	52.78	63.82	15.95	49.33	53.46	47.19	36.62
	Tent	±0.40	±0.43	±0.58	±0.70	±0.69	±0.30	±0.14	±0.15	±0.33	±0.12	±0.02	±1.18	±0.18	±0.09	±0.03	±0.35
	+ SNAP	29.12	30.46	30.30	25.77	25.22	38.21	46.14	44.29	39.95	54.65	65.47	33.81	50.83	55.59	49.21	41.27
	TOTAL	±0.09	±0.22	±0.48	± 0.20	±0.23	±0.43	±0.00	±0.13	± 0.07	±0.15	±0.09	±1.10	±0.13	±0.10	±0.03	±0.23
	CoTTA	11.03	11.91	11.75	11.03	11.20	22.30	34.98	30.87	29.78	43.99	61.87	12.92	40.26	45.23	36.63	27.72
		±0.30 15.22	±0.57 15.97	±0.33 15.93	±0.24 13.91	±0.46 14.05	±0.18 24.87	±0.05 36.48	±0.08 32.60	±0.01 31.65	±0.11 46.09	±0.06 63.59	±0.36 15.67	±0.19 42.00	±0.17 46.71	±0.07 37.96	±0.21 30.18
	+ SNAP	±0.08	±0.11	±0.03	±0.06	±0.12	±0.04	±0.00	±0.07	±0.04	±0.03	±0.07	±0.05	±0.03	±0.09	±0.09	±0.06
		19.53	20.65	20.72	16.74	16.96	29.11	41.22	37.96	34.84	50.75	63.29	19.86	45.92	51.15	44.13	34.19
0.05	EATA	±0.31	±0.66	±0.75	±0.41	±0.58	±0.49	±0.27	±0.18	±0.23	±0.21	±0.13	±1.26	±0.35	±0.17	±0.09	±0.41
0.05	+ SNAP	22.83	23.95	23.62	19.43	19.70	30.34	41.59	38.06	35.06	50.98	63.30	23.72	46.26	51.52	45.46	35.72
	+ SNAP	±0.10	±0.34	±0.30	±0.09	±0.19	±0.56	±0.08	±0.11	±0.21	±0.18	±0.13	±0.30	±0.16	±0.16	±0.18	±0.21
	SAR	23.25	24.23	23.66	19.98	20.38	33.05	43.04	40.73	36.06	52.61	64.09	20.17	49.00	53.35	46.73	36.69
	5.11	±0.21	±0.34	±0.30	±0.09	±0.16	±0.30	±0.16	±0.02	±0.12	±0.09	±0.07	±0.84	±0.11	±0.10	±0.11	±0.20
	+ SNAP	27.54	29.03	28.66	24.05	23.42	36.28	44.12	42.89	38.54	53.24	64.25	31.83	48.79	54.04	47.80	39.63
		±0.16 14.42	±0.05 15.22	±0.04 15.02	±0.16 13.25	±0.08 13.31	±0.12 23.79	±0.10 35.27	±0.11 32.09	±0.07 30.43	±0.07 44.71	±0.05 62.64	±0.24 15.24	±0.23 40.63	±0.19 45.55	±0.08 36.75	±0.12 29.22
	RoTTA	±0.06	±0.05	±0.10	±0.11	±0.07	±0.03	±0.08	±0.05	±0.07	±0.13	±0.14	±0.09	±0.03	±0.07	±0.16	±0.09
		14.65	15.48	15.29	13.43	13.45	23.93	35.33	32.18	30.53	44.71	62.58	15.41	40.64	45.55	36.81	29.33
	+ SNAP	±0.06	±0.02	±0.08	±0.09	±0.09	±0.03	±0.05	±0.04	±0.05	±0.16	±0.10	±0.04	±0.09	±0.10	±0.14	±0.08
		21.76	22.76	22.58	19.06	18.90	30.85	42.34	38.94	35.53	51.58	63.42	18.61	47.96	52.41	45.56	35.48
	Tent	±0.17	±0.35	±0.17	±0.04	±0.12	±0.22	±0.12	±0.26	±0.31	±0.18	±0.11	±0.91	±0.26	±0.21	±0.08	±0.23
	CNIAD	26.42	28.20	27.81	23.79	22.82	35.77	44.80	42.37	38.81	53.34	64.95	30.05	49.28	54.16	47.57	39.34
	+ SNAP	±0.14	±0.26	±0.37	±0.46	±0.21	±0.11	±0.16	±0.34	±0.14	±0.06	±0.11	±0.62	±0.17	±0.09	±0.08	±0.22
	CoTTA	10.61	12.36	11.78	11.66	11.32	22.25	35.01	30.88	29.84	44.09	61.83	12.92	40.26	45.20	36.58	27.77
	COTIN	±0.18	±0.36	±0.57	±0.57	±0.26	±0.11	±0.18	±0.24	±0.07	±0.11	±0.16	±0.12	±0.19	±0.11	±0.09	±0.22
	+ SNAP	15.29	16.02	16.00	13.99	14.06	24.78	36.54	32.62	31.70	46.01	63.49	15.69	42.05	46.75	37.97	30.20
		±0.08	±0.07	±0.09	±0.07	±0.11	±0.05	±0.07	±0.06	±0.08	±0.01	±0.04	±0.04	±0.18	±0.19	±0.08	±0.08
	EATA	17.17 ±0.41	18.34 ±0.19	17.94 ±0.36	14.48 ±0.82	15.04 ±0.22	26.31 ±0.25	39.47 ±0.33	35.51 ±0.50	33.41 ±0.33	49.16 ±0.19	63.06 ±0.05	18.01 ±0.88	44.16	49.90 ±0.09	42.47 ±0.31	32.30 ±0.35
0.03		20.75	±0.19 21.87	±0.36	17.34	±0.22	28.08	39.84	36.27	33.54	49.50	63.04	20.86	±0.31 44.68	±0.09 49.97	43.53	33.90
	+ SNAP	±0.32	±0.41	±0.35	±0.30	±0.34	±0.34	±0.16	±0.13	±0.11	±0.12	±0.07	±0.33	±0.28	±0.13	±0.03	±0.23
		20.38	21.34	21.18	18.24	18.28	30.56	41.63	38.57	35.23	51.19	63.74	20.40	47.32	52.02	44.81	34.99
	SAR	±0.10	±0.14	±0.36	±0.18	±0.27	±0.08	±0.12	±0.17	±0.28	±0.22	±0.04	±0.20	±0.09	±0.09	±0.19	±0.17
	+ SNAP	25.11	26.27	26.00	22.02	21.25	33.51	42.86	40.83	37.09	51.87	63.83	28.36	47.19	52.63	45.80	37.64
	TOMAT	±0.23	±0.31	±0.10	±0.49	±0.56	±0.31	±0.14	±0.16	±0.21	±0.18	± 0.10	±0.29	±0.34	±0.06	± 0.30	±0.25
	RoTTA	14.36	15.12	14.95	13.30	13.34	23.78	35.23	31.89	30.33	44.52	62.48	15.20	40.50	45.36	36.63	29.13
	ROTIN	±0.04	±0.03	±0.08	±0.08	±0.08	±0.04	±0.05	±0.04	±0.07	±0.11	±0.12	±0.01	±0.11	±0.07	±0.17	±0.07
	+ SNAP	14.45	15.21	15.06	13.35	13.42	23.83	35.26	31.92	30.36	44.53	62.47	15.27	40.50	45.39	36.65	29.18
		±0.04	±0.02	±0.08	±0.08	±0.07	±0.04	±0.06	±0.02	±0.08	±0.10	±0.09	±0.04	±0.10	±0.08	±0.16	±0.07
	Tent	17.09	17.70	17.69	14.91	15.25	25.23	38.66	34.15	32.28	48.14	62.65	15.76	43.44	49.14	41.18	31.55
	10	±0.14	±0.10	±0.13	±0.23	±0.09	±0.25	±0.27	±0.27	±0.21	±0.21	±0.16	±0.48	±0.23	±0.04	±0.10	±0.19
	+ SNAP	20.66 ±0.02	21.73 ±0.12	21.55	18.46	18.28 ±0.33	29.88	40.63	36.97	34.89 ±0.10	49.85	64.29	22.64	45.13	50.77	43.17	34.59
		11.11	13.24	±0.18 11.86	±0.34 10.85	10.97	±0.12 22.18	±0.14 34.96	±0.21 30.88	29.63	±0.26 44.09	±0.10 61.71	±0.14 12.81	±0.29 40.16	±0.07 45.14	±0.51 36.73	±0.19 27.75
	CoTTA	±0.61	±0.12	±0.65	±0.59	±0.98	±0.05	±0.18	±0.14	±0.21	±0.21	±0.22	±0.53	±0.10	±0.22	±0.12	±0.34
		15.09	16.00	15.83	13.84	14.06	24.70	36.47	32.59	31.66	46.10	63.62	15.60	42.03	46.74	38.17	30.17
	+ SNAP	±0.04	±0.09	±0.14	±0.09	±0.02	±0.07	±0.02	±0.11	±0.03	±0.15	±0.07	±0.06	±0.10	±0.01	±0.20	±0.08
	F + F +	14.85	15.61	15.69	13.26	13.37	23.72	36.18	32.57	31.14	46.06	62.35	13.88	41.91	47.00	38.88	29.76
0.01	EATA	±0.13	±0.21	±0.21	±0.04	±0.06	±0.19	±0.13	±0.09	±0.06	±0.29	±0.09	±0.35	±0.17	±0.15	±0.09	±0.15
	+ SNAP	16.73	17.55	17.30	14.35	14.64	24.13	36.83	32.81	31.09	46.63	62.20	15.26	42.34	47.44	39.81	30.61
	TOMAT	±0.12	± 0.10	±0.19	±0.09	±0.10	±0.36	±0.23	±0.08	± 0.10	±0.19	±0.16	±0.54	±0.12	±0.18	±0.34	±0.19
	SAR	16.08	17.04	16.69	14.72	14.78	25.92	37.85	34.07	32.25	47.66	63.15	17.20	43.05	48.78	40.14	31.29
	57110	±0.08	±0.07	±0.10	±0.16	±0.12	±0.13	±0.05	±0.24	±0.11	±0.13	±0.05	±0.15	±0.20	±0.09	±0.20	±0.13
	+ SNAP	18.89	19.45	19.70	16.70	16.55	27.69	38.57	35.34	33.09	48.08	63.04	20.39	42.95	48.76	40.99	32.68
		±0.15	±0.15	±0.12	±0.14	±0.15	±0.16	±0.11	±0.22	±0.09	±0.31	±0.07	±0.12	±0.29	±0.26	±0.33	±0.18
	RoTTA	14.30 ±0.05	15.06 ±0.03	14.89	13.30	13.37 ±0.08	23.78 ±0.04	35.22 ±0.06	31.79	30.27	44.40 ±0.14	62.40 ±0.11	15.16	40.42	45.27 ±0.05	36.54	29.08
		±0.05 14.30	±0.03	±0.07 14.92	±0.07 13.30	±0.08	±0.04 23.78	35.22	±0.04 31.78	±0.06 30.26	±0.14 44.41	£0.11	±0.06 15.15	±0.10 40.43	±0.05 45.27	±0.16 36.54	±0.07 29.08
	+ SNAP	±0.06	±0.03	±0.08	±0.08	±0.07	±0.04	±0.06	±0.04	±0.07	±0.14	±0.11	±0.05	±0.43	±0.04	±0.15	±0.07
		±0.00	±0.03	±0.08	±0.08	EU.U/	±0.04	TU.00	±0.04	±0.07	IU.14	E0.11	±0.05	±0.09	±0.04	IU.13	IU.U/

C.4 Additional results on ablation study

In this section, we provide additional details on the ablation study to evaluate the contributions of the CnDRM and IoBMN components in SNAP. Specifically, we measured the average accuracy across 15 corruption types on CIFAR10-C and CIFAR100-C datasets under varying adaptation rates (0.3, 0.1, 0.05) to thoroughly assess the effectiveness of each component.

Tables 28 and 29 summarize the results for different combinations of CnDRM and IoBMN across these adaptation rates. The results indicate that the combination of CnDRM (Class and Domain Representative sampling) and IoBMN (inference using memory statistics corrected to match the test batch) consistently yields the highest accuracy. This trend is observed across all evaluated adaptation rates, suggesting that both components contribute significantly to enhancing adaptation performance.

Moreover, individual evaluations show that each component has a distinct positive effect, as evidenced by consistently higher accuracy compared to using no adaptation or only a single component. This emphasizes the complementary nature of CnDRM and IoBMN, which together provide robust adaptation capabilities for domain-shifted scenarios. These tables provide further insight into the benefits of each configuration and how the synergy of CnDRM and IoBMN results in improved robustness against various corruptions.

Table 28: STTA classification accuracy (%) of ablative settings on the CIFAR10-C, adaptation rate (AR) 0.3, 0.1, and 0.05. Averaged over all 15 corruptions. **Bold** numbers are the highest accuracy.

AR	Methods	Tent	CoTTA	EATA	SAR	RoTTA
	Naïve	78.86 ± 0.12	69.75 ± 0.08	79.02 ± 0.14	77.83 ± 0.11	75.39 ± 0.09
	Random	78.90 ± 0.15	66.04 ± 0.10	78.97 ± 0.13	77.77 ± 0.12	75.06 ± 0.07
	LowEntropy	78.68 ± 0.11	63.74 ± 0.16	78.42 ± 0.09	76.21 ± 0.10	72.83 ± 0.14
0.3	CRM	80.32 ± 0.07	66.50 ± 0.12	80.14 ± 0.08	75.78 ± 0.13	75.49 ± 0.06
	CnDRM	79.62 ±0.13	77.68 ±0.10	79.63 ±0.12	78.22 ±0.09	75.85 ±0.08
	CnDRM+EMA	80.96 ± 0.06	72.42 ± 0.14	80.27 ± 0.11	78.19 ± 0.13	76.73 ± 0.07
	CnDRM+IoBMN	81.23 ± 0.09	78.75 ± 0.10	81.30 ±0.07	79.77 ±0.08	77.41 ±0.06
	Naïve	76.81 ±0.18	66.42 ±0.12	76.29 ± 0.11	76.01 ±0.07	74.78 ±0.15
	Random	77.08 ± 0.14	65.61 ± 0.08	76.59 ± 0.10	76.33 ± 0.13	75.01 ± 0.16
	LowEntropy	75.66 ± 0.09	63.19 ± 0.14	74.89 ± 0.12	74.41 ± 0.18	72.60 ± 0.10
0.1	CRM	77.77 ± 0.05	65.71 ± 0.19	$77.18 \; {\pm} 0.08$	74.36 ± 0.11	75.27 ± 0.17
	CnDRM	77.46 ±0.07	77.69 ±0.10	77.17 ±0.06	76.85 ±0.09	75.64 ±0.08
	CnDRM+EMA	78.02 ± 0.12	72.19 ± 0.15	77.05 ± 0.11	76.84 ± 0.13	76.18 ± 0.05
	CnDRM+IoBMN	78.95 ± 0.09	78.83 ± 0.06	78.61 ±0.13	78.06 ±0.07	77.07 ± 0.10
	Naïve	75.75 ±0.18	67.22 ±0.12	75.55 ±0.14	75.25 ±0.17	74.80 ±0.11
	Random	75.82 ± 0.13	65.90 ± 0.21	75.56 ± 0.16	75.27 ± 0.15	74.91 ± 0.10
	LowEntropy	74.07 ± 0.20	64.08 ± 0.25	73.73 ± 0.19	73.58 ± 0.22	72.83 ± 0.14
0.05	CRM	76.55 ± 0.11	66.14 ± 0.17	76.06 ± 0.13	74.02 ± 0.15	75.23 ± 0.09
	CnDRM	76.53 ±0.14	77.67 ±0.16	76.29 ± 0.18	76.18 ±0.12	75.61 ±0.13
	CnDRM+EMA	76.86 ± 0.10	71.69 ± 0.19	75.98 ± 0.15	75.43 ± 0.14	75.95 ± 0.11
	CnDRM+IoBMN	77.93 ±0.09	78.73 \pm 0.13	77.76 ±0.12	77.21 ±0.11	77.05 ± 0.08

Table 29: STTA classification accuracy (%) of ablative settings on the CIFAR100-C, adaptation rate (AR) 0.3, 0.1, and 0.05. Averaged over all 15 corruptions. **Bold** numbers are the highest accuracy.

AR	Methods	Tent	CoTTA	EATA	SAR	RoTTA
0.3	Naïve Random LowEntropy CRM	53.36 ±0.22 53.00 ±0.24 53.53 ±0.20 54.21 ±0.18	$\begin{array}{c} 39.11 \pm 0.17 \\ 33.49 \pm 0.21 \\ 32.29 \pm 0.28 \\ 32.86 \pm 0.24 \end{array}$	49.97 ±0.19 49.24 ±0.17 45.51 ±0.23 47.42 ±0.20	56.65 ± 0.20 56.06 ± 0.26 55.84 ± 0.22 56.40 ± 0.19	49.84 ±0.18 49.00 ±0.16 44.77 ±0.19 46.68 ±0.17
	CnDRM CnDRM+EMA CnDRM+IoBMN	55.15 ± 0.21 55.39 ± 0.16 57.27 ± 0.13	50.02 ±0.14 41.34 ±0.20 50.32 ±0.15	51.36 ± 0.16 50.11 ± 0.19 52.19 ± 0.14	57.72 ±0.18 57.68 ±0.21 58.44 ±0.16	50.74 ± 0.15 49.88 ± 0.17 51.55 ± 0.12
0.1	Naïve Random LowEntropy CRM	$\begin{array}{c} 52.84 \pm 0.19 \\ 52.68 \pm 0.22 \\ 51.76 \pm 0.20 \\ 52.43 \pm 0.17 \end{array}$	$\begin{array}{c} 35.86 \pm 0.23 \\ 33.18 \pm 0.26 \\ 32.30 \pm 0.28 \\ 32.54 \pm 0.25 \end{array}$	$\begin{array}{c} 49.70 \pm 0.18 \\ 49.39 \pm 0.20 \\ 46.03 \pm 0.23 \\ 47.68 \pm 0.21 \end{array}$	$\begin{array}{c} 53.49 \pm 0.21 \\ 53.42 \pm 0.18 \\ 52.15 \pm 0.24 \\ 53.12 \pm 0.20 \end{array}$	$\begin{array}{c} 49.11 \pm 0.17 \\ 48.84 \pm 0.14 \\ 45.18 \pm 0.19 \\ 47.01 \pm 0.16 \end{array}$
	CnDRM CnDRM+EMA CnDRM+IoBMN	54.46 ±0.16 54.36 ±0.15 55.84 ±0.14	50.06 ± 0.13 41.63 ± 0.22 50.52 ± 0.11	51.41 ± 0.19 50.21 ± 0.18 52.35 ± 0.15	55.24 ±0.14 54.84 ±0.17 55.76 ±0.13	50.47 ± 0.12 49.95 ± 0.13 51.33 ± 0.10
0.05	Naïve Random LowEntropy CRM	$\begin{array}{c} 51.24 \pm 0.18 \\ 51.35 \pm 0.20 \\ 49.79 \pm 0.24 \\ 50.17 \pm 0.19 \end{array}$	$\begin{array}{c} 33.20 \pm 0.25 \\ 33.71 \pm 0.22 \\ 32.36 \pm 0.26 \\ 32.74 \pm 0.27 \end{array}$	$\begin{array}{c} 49.81\ \pm0.16\\ 49.57\ \pm0.17\\ 46.65\ \pm0.19\\ 47.47\ \pm0.20 \end{array}$	51.50 ±0.21 51.48 ±0.20 49.51 ±0.23 50.49 ±0.22	49.12 ±0.19 48.98 ±0.15 45.41 ±0.18 46.58 ±0.16
	CnDRM CnDRM+EMA CnDRM+IoBMN	52.86 ±0.14 52.68 ±0.13 54.13 ±0.11	50.08 ± 0.13 41.43 ± 0.21 50.63 ± 0.14	51.47 ± 0.17 50.32 ± 0.18 52.43 ± 0.16	53.09 ± 0.15 52.80 ± 0.17 53.59 ± 0.12	50.44 ±0.13 50.04 ±0.14 51.41 ±0.10

D License of assets

Datasets CIFAR10/CIFAR100 (MIT License), CIFAR10-C/CIFAR100-C (Creative Commons Attribution 4.0 International), ImageNet-C (Apache 2.0), and ImageNet-R/Scketch (MIT License).

Codes Torchvision for ResNet18, ResNet50, and VitBase-LN (Apache 2.0), the official repository of CoTTA (MIT License), the official repository of Tent (MIT License), the official repository of EATA (MIT License), the official repository of SAR (BSD 3-Clause License), the official repository of RoTTA (MIT License), the official repository of T3A (MIT License), the official repository of FOA (NTUITIVE License) and the official repository of MECTA (Sony AI).

NeurIPS Paper Checklist

1. Claims

Question: Do the main claims made in the abstract and introduction accurately reflect the paper's contributions and scope?

Answer: [Yes]

Justification: The claims in the abstract and introduction accurately reflect the paper's contributions and are supported by the presented results.

Guidelines:

- The answer NA means that the abstract and introduction do not include the claims made in the paper.
- The abstract and/or introduction should clearly state the claims made, including the contributions made in the paper and important assumptions and limitations. A No or NA answer to this question will not be perceived well by the reviewers.
- The claims made should match theoretical and experimental results, and reflect how much the results can be expected to generalize to other settings.
- It is fine to include aspirational goals as motivation as long as it is clear that these goals are not attained by the paper.

2. Limitations

Question: Does the paper discuss the limitations of the work performed by the authors?

Answer: [Yes]

Justification: Limitations are discussed in Section 6.

Guidelines:

- The answer NA means that the paper has no limitation while the answer No means that the paper has limitations, but those are not discussed in the paper.
- The authors are encouraged to create a separate "Limitations" section in their paper.
- The paper should point out any strong assumptions and how robust the results are to violations of these assumptions (e.g., independence assumptions, noiseless settings, model well-specification, asymptotic approximations only holding locally). The authors should reflect on how these assumptions might be violated in practice and what the implications would be.
- The authors should reflect on the scope of the claims made, e.g., if the approach was only tested on a few datasets or with a few runs. In general, empirical results often depend on implicit assumptions, which should be articulated.
- The authors should reflect on the factors that influence the performance of the approach. For example, a facial recognition algorithm may perform poorly when image resolution is low or images are taken in low lighting. Or a speech-to-text system might not be used reliably to provide closed captions for online lectures because it fails to handle technical jargon.
- The authors should discuss the computational efficiency of the proposed algorithms and how they scale with dataset size.
- If applicable, the authors should discuss possible limitations of their approach to address problems of privacy and fairness.
- While the authors might fear that complete honesty about limitations might be used by reviewers as grounds for rejection, a worse outcome might be that reviewers discover limitations that aren't acknowledged in the paper. The authors should use their best judgment and recognize that individual actions in favor of transparency play an important role in developing norms that preserve the integrity of the community. Reviewers will be specifically instructed to not penalize honesty concerning limitations.

3. Theory assumptions and proofs

Question: For each theoretical result, does the paper provide the full set of assumptions and a complete (and correct) proof?

Answer: [NA]

Justification: No theoretical result.

Guidelines:

- The answer NA means that the paper does not include theoretical results.
- All the theorems, formulas, and proofs in the paper should be numbered and crossreferenced.
- All assumptions should be clearly stated or referenced in the statement of any theorems.
- The proofs can either appear in the main paper or the supplemental material, but if they appear in the supplemental material, the authors are encouraged to provide a short proof sketch to provide intuition.
- Inversely, any informal proof provided in the core of the paper should be complemented by formal proofs provided in appendix or supplemental material.
- Theorems and Lemmas that the proof relies upon should be properly referenced.

4. Experimental result reproducibility

Question: Does the paper fully disclose all the information needed to reproduce the main experimental results of the paper to the extent that it affects the main claims and/or conclusions of the paper (regardless of whether the code and data are provided or not)?

Answer: [Yes]

Justification: Experimental details for reproducibility are provided in Section 5 and Appendix A. Also, we provided source code in the supplemental material.

Guidelines:

- The answer NA means that the paper does not include experiments.
- If the paper includes experiments, a No answer to this question will not be perceived well by the reviewers: Making the paper reproducible is important, regardless of whether the code and data are provided or not.
- If the contribution is a dataset and/or model, the authors should describe the steps taken to make their results reproducible or verifiable.
- Depending on the contribution, reproducibility can be accomplished in various ways. For example, if the contribution is a novel architecture, describing the architecture fully might suffice, or if the contribution is a specific model and empirical evaluation, it may be necessary to either make it possible for others to replicate the model with the same dataset, or provide access to the model. In general, releasing code and data is often one good way to accomplish this, but reproducibility can also be provided via detailed instructions for how to replicate the results, access to a hosted model (e.g., in the case of a large language model), releasing of a model checkpoint, or other means that are appropriate to the research performed.
- While NeurIPS does not require releasing code, the conference does require all submissions to provide some reasonable avenue for reproducibility, which may depend on the nature of the contribution. For example
- (a) If the contribution is primarily a new algorithm, the paper should make it clear how to reproduce that algorithm.
- (b) If the contribution is primarily a new model architecture, the paper should describe the architecture clearly and fully.
- (c) If the contribution is a new model (e.g., a large language model), then there should either be a way to access this model for reproducing the results or a way to reproduce the model (e.g., with an open-source dataset or instructions for how to construct the dataset).
- (d) We recognize that reproducibility may be tricky in some cases, in which case authors are welcome to describe the particular way they provide for reproducibility. In the case of closed-source models, it may be that access to the model is limited in some way (e.g., to registered users), but it should be possible for other researchers to have some path to reproducing or verifying the results.

5. Open access to data and code

Question: Does the paper provide open access to the data and code, with sufficient instructions to faithfully reproduce the main experimental results, as described in supplemental material?

Answer: [Yes]

Justification: Anonymized source code and instructions are provided in the supplementary material. The complete codebase and scripts will be made publicly available upon publication.

Guidelines:

- The answer NA means that paper does not include experiments requiring code.
- Please see the NeurIPS code and data submission guidelines (https://nips.cc/public/guides/CodeSubmissionPolicy) for more details.
- While we encourage the release of code and data, we understand that this might not be possible, so "No" is an acceptable answer. Papers cannot be rejected simply for not including code, unless this is central to the contribution (e.g., for a new open-source benchmark).
- The instructions should contain the exact command and environment needed to run to reproduce the results. See the NeurIPS code and data submission guidelines (https://nips.cc/public/guides/CodeSubmissionPolicy) for more details.
- The authors should provide instructions on data access and preparation, including how
 to access the raw data, preprocessed data, intermediate data, and generated data, etc.
- The authors should provide scripts to reproduce all experimental results for the new proposed method and baselines. If only a subset of experiments are reproducible, they should state which ones are omitted from the script and why.
- At submission time, to preserve anonymity, the authors should release anonymized versions (if applicable).
- Providing as much information as possible in supplemental material (appended to the paper) is recommended, but including URLs to data and code is permitted.

6. Experimental setting/details

Question: Does the paper specify all the training and test details (e.g., data splits, hyperparameters, how they were chosen, type of optimizer, etc.) necessary to understand the results?

Answer: [Yes]

Justification: Details are provided in Section 5 and Appendix A.

Guidelines:

- The answer NA means that the paper does not include experiments.
- The experimental setting should be presented in the core of the paper to a level of detail that is necessary to appreciate the results and make sense of them.
- The full details can be provided either with the code, in appendix, or as supplemental
 material.

7. Experiment statistical significance

Question: Does the paper report error bars suitably and correctly defined or other appropriate information about the statistical significance of the experiments?

Answer: [Yes]

Justification: All experiments were conducted using three random seeds (0, 1, and 2), and the corresponding standard deviations are reported and visualized as error bars. Note that standard deviations omitted from Table 1 are reported in Appendix C. Detailed descriptions are provided in Section 5 and Appendix A.

- The answer NA means that the paper does not include experiments.
- The authors should answer "Yes" if the results are accompanied by error bars, confidence intervals, or statistical significance tests, at least for the experiments that support the main claims of the paper.
- The factors of variability that the error bars are capturing should be clearly stated (for example, train/test split, initialization, random drawing of some parameter, or overall run with given experimental conditions).

- The method for calculating the error bars should be explained (closed form formula, call to a library function, bootstrap, etc.)
- The assumptions made should be given (e.g., Normally distributed errors).
- It should be clear whether the error bar is the standard deviation or the standard error
 of the mean.
- It is OK to report 1-sigma error bars, but one should state it. The authors should preferably report a 2-sigma error bar than state that they have a 96% CI, if the hypothesis of Normality of errors is not verified.
- For asymmetric distributions, the authors should be careful not to show in tables or figures symmetric error bars that would yield results that are out of range (e.g. negative error rates).
- If error bars are reported in tables or plots, The authors should explain in the text how they were calculated and reference the corresponding figures or tables in the text.

8. Experiments compute resources

Question: For each experiment, does the paper provide sufficient information on the computer resources (type of compute workers, memory, time of execution) needed to reproduce the experiments?

Answer: [Yes]

Justification: Details are provided in Section 5 and Appendix A.

Guidelines:

- The answer NA means that the paper does not include experiments.
- The paper should indicate the type of compute workers CPU or GPU, internal cluster, or cloud provider, including relevant memory and storage.
- The paper should provide the amount of compute required for each of the individual experimental runs as well as estimate the total compute.
- The paper should disclose whether the full research project required more compute than the experiments reported in the paper (e.g., preliminary or failed experiments that didn't make it into the paper).

9. Code of ethics

Question: Does the research conducted in the paper conform, in every respect, with the NeurIPS Code of Ethics https://neurips.cc/public/EthicsGuidelines?

Answer: [Yes]

Justification: Ensure that our work adheres to the NeurIPS Code of Ethics.

Guidelines:

- The answer NA means that the authors have not reviewed the NeurIPS Code of Ethics.
- If the authors answer No, they should explain the special circumstances that require a deviation from the Code of Ethics.
- The authors should make sure to preserve anonymity (e.g., if there is a special consideration due to laws or regulations in their jurisdiction).

10. Broader impacts

Question: Does the paper discuss both potential positive societal impacts and negative societal impacts of the work performed?

Answer: [Yes]

Justification: Potential societal impacts are described in Section 6.

- The answer NA means that there is no societal impact of the work performed.
- If the authors answer NA or No, they should explain why their work has no societal impact or why the paper does not address societal impact.
- Examples of negative societal impacts include potential malicious or unintended uses (e.g., disinformation, generating fake profiles, surveillance), fairness considerations (e.g., deployment of technologies that could make decisions that unfairly impact specific groups), privacy considerations, and security considerations.

- The conference expects that many papers will be foundational research and not tied to particular applications, let alone deployments. However, if there is a direct path to any negative applications, the authors should point it out. For example, it is legitimate to point out that an improvement in the quality of generative models could be used to generate deepfakes for disinformation. On the other hand, it is not needed to point out that a generic algorithm for optimizing neural networks could enable people to train models that generate Deepfakes faster.
- The authors should consider possible harms that could arise when the technology is being used as intended and functioning correctly, harms that could arise when the technology is being used as intended but gives incorrect results, and harms following from (intentional or unintentional) misuse of the technology.
- If there are negative societal impacts, the authors could also discuss possible mitigation strategies (e.g., gated release of models, providing defenses in addition to attacks, mechanisms for monitoring misuse, mechanisms to monitor how a system learns from feedback over time, improving the efficiency and accessibility of ML).

11. Safeguards

Question: Does the paper describe safeguards that have been put in place for responsible release of data or models that have a high risk for misuse (e.g., pretrained language models, image generators, or scraped datasets)?

Answer: [NA]

Justification: No such components.

Guidelines:

- The answer NA means that the paper poses no such risks.
- Released models that have a high risk for misuse or dual-use should be released with necessary safeguards to allow for controlled use of the model, for example by requiring that users adhere to usage guidelines or restrictions to access the model or implementing safety filters.
- Datasets that have been scraped from the Internet could pose safety risks. The authors should describe how they avoided releasing unsafe images.
- We recognize that providing effective safeguards is challenging, and many papers do not require this, but we encourage authors to take this into account and make a best faith effort.

12. Licenses for existing assets

Question: Are the creators or original owners of assets (e.g., code, data, models), used in the paper, properly credited and are the license and terms of use explicitly mentioned and properly respected?

Answer: [Yes]

Justification: All licenses and credits are described in Appendix D.

- The answer NA means that the paper does not use existing assets.
- The authors should cite the original paper that produced the code package or dataset.
- The authors should state which version of the asset is used and, if possible, include a URL.
- The name of the license (e.g., CC-BY 4.0) should be included for each asset.
- For scraped data from a particular source (e.g., website), the copyright and terms of service of that source should be provided.
- If assets are released, the license, copyright information, and terms of use in the package should be provided. For popular datasets, paperswithcode.com/datasets has curated licenses for some datasets. Their licensing guide can help determine the license of a dataset.
- For existing datasets that are re-packaged, both the original license and the license of the derived asset (if it has changed) should be provided.

 If this information is not available online, the authors are encouraged to reach out to the asset's creators.

13. New assets

Question: Are new assets introduced in the paper well documented and is the documentation provided alongside the assets?

Answer: [NA]

Justification: No new assets are introduced.

Guidelines:

- The answer NA means that the paper does not release new assets.
- Researchers should communicate the details of the dataset/code/model as part of their submissions via structured templates. This includes details about training, license, limitations, etc.
- The paper should discuss whether and how consent was obtained from people whose asset is used.
- At submission time, remember to anonymize your assets (if applicable). You can either create an anonymized URL or include an anonymized zip file.

14. Crowdsourcing and research with human subjects

Question: For crowdsourcing experiments and research with human subjects, does the paper include the full text of instructions given to participants and screenshots, if applicable, as well as details about compensation (if any)?

Answer: [NA]

Justification: No crowdsourcing or human-subject experiments were required.

Guidelines:

- The answer NA means that the paper does not involve crowdsourcing nor research with human subjects.
- Including this information in the supplemental material is fine, but if the main contribution of the paper involves human subjects, then as much detail as possible should be included in the main paper.
- According to the NeurIPS Code of Ethics, workers involved in data collection, curation, or other labor should be paid at least the minimum wage in the country of the data collector.

15. Institutional review board (IRB) approvals or equivalent for research with human subjects

Question: Does the paper describe potential risks incurred by study participants, whether such risks were disclosed to the subjects, and whether Institutional Review Board (IRB) approvals (or an equivalent approval/review based on the requirements of your country or institution) were obtained?

Answer: [NA]

Justification: No IRB approvals were required.

Guidelines:

- The answer NA means that the paper does not involve crowdsourcing nor research with human subjects.
- Depending on the country in which research is conducted, IRB approval (or equivalent) may be required for any human subjects research. If you obtained IRB approval, you should clearly state this in the paper.
- We recognize that the procedures for this may vary significantly between institutions and locations, and we expect authors to adhere to the NeurIPS Code of Ethics and the guidelines for their institution.
- For initial submissions, do not include any information that would break anonymity (if applicable), such as the institution conducting the review.

16. Declaration of LLM usage

Question: Does the paper describe the usage of LLMs if it is an important, original, or non-standard component of the core methods in this research? Note that if the LLM is used only for writing, editing, or formatting purposes and does not impact the core methodology, scientific rigorousness, or originality of the research, declaration is not required.

Answer: [NA]

Justification: No LLMs were used in this research components.

- The answer NA means that the core method development in this research does not involve LLMs as any important, original, or non-standard components.
- Please refer to our LLM policy (https://neurips.cc/Conferences/2025/LLM) for what should or should not be described.